

University of Groningen

Photodynamic therapy and fluorescence localisation of experimental oral dysplasia and squamous cell carcinoma : A study with aluminium phthalocyanine disulphonate.

Witjes, Max Johannes Hendrikus

IMPORTANT NOTE: You are advised to consult the publisher's version (publisher's PDF) if you wish to cite from it. Please check the document version below.

Document Version

Publisher's PDF, also known as Version of record

Publication date:

1997

[Link to publication in University of Groningen/UMCG research database](#)

Citation for published version (APA):

Witjes, M. J. H. (1997). *Photodynamic therapy and fluorescence localisation of experimental oral dysplasia and squamous cell carcinoma : A study with aluminium phthalocyanine disulphonate.* [S.n.].

Copyright

Other than for strictly personal use, it is not permitted to download or to forward/distribute the text or part of it without the consent of the author(s) and/or copyright holder(s), unless the work is under an open content license (like Creative Commons).

The publication may also be distributed here under the terms of Article 25fa of the Dutch Copyright Act, indicated by the "Taverne" license. More information can be found on the University of Groningen website: <https://www.rug.nl/library/open-access/self-archiving-pure/taverne-amendment>.

Take-down policy

If you believe that this document breaches copyright please contact us providing details, and we will remove access to the work immediately and investigate your claim.

Downloaded from the University of Groningen/UMCG research database (Pure): <http://www.rug.nl/research/portal>. For technical reasons the number of authors shown on this cover page is limited to 10 maximum.

SSC

M.J.H. Witjes

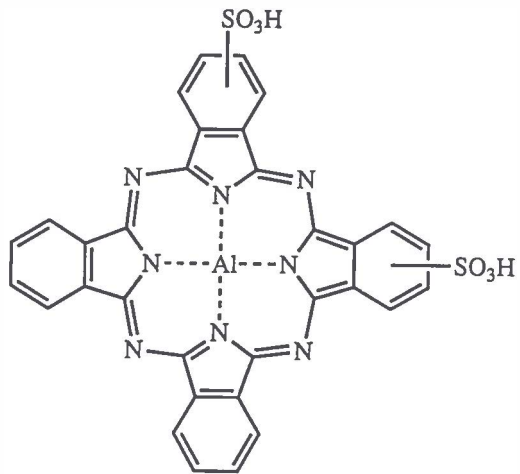
33

**PHOTODYNAMIC THERAPY AND FLUORESCENCE
LOCALISATION OF EXPERIMENTAL ORAL
DYSPLASIA AND SQUAMOUS CELL CARCINOMA**

A study with aluminium phthalocyanine disulphonate

PHOTODYNAMIC THERAPY AND FLUORESCENCE LOCALISATION OF
EXPERIMENTAL DYSPLASIA AND ORAL SQUAMOUS CELL CARCINOMA

A STUDY WITH ALUMINIUM PHTHALOCYANINE DISULPHONATE



aluminium phthalocyanine disulphonate

Ontwerp omslag door Pieter Duijser

STELLINGEN
BEHOREND BIJ HET PROEFSCHRIFT

PHOTODYNAMIC THERAPY AND FLUORESCENCE LOCALISATION OF
EXPERIMENTAL ORAL DYSPLASIA AND SQUAMOUS CELL CARCINOMA. A
STUDY WITH ALUMINIUM PHTHALOCYANINE DISULPHONATE

1. Fluorescence imaging of oral dysplasia or squamous cell carcinoma can provide detailed information during the diagnostic work-up and therefore its efficacy in clinical applications should be more investigated.
This thesis
2. Sufficient light delivery is of more importance for the success of PDT than a high aluminium phthalocyanine disulphonate (AlPcS₂) accumulation in oral dysplasia or squamous cell carcinoma.
This thesis
3. It is of vital importance that teeth are not irradiated during PDT with AlPcS₂.
This thesis
4. An equal concentration of AlPcS₂ in different tissues will not result in an equal or comparable amount of tissue damage by PDT.
This thesis
5. Autologous tumour models mimic the human situation more closely than transplanted tumour models and should therefore be preferred in cancer research.
6. The possibility of inducing osteoradionecrosis by PDT should be excluded by new investigations before applying PDT to previously therapeutically irradiated patients.

7. Life is a precancerous condition.
S.L. Thomsen
8. Deelnemen aan het verkeer in het gebied de Grote Markt/Waagstraat in Groningen vereist een avontuurlijk ingestelde geest.
9. De huidige ontwikkelingen in de techniek van het klonen geeft de vraag of je met jezelf overweg kunt een extra dimensie.
10. Kaal worden is erger dan kaal zijn.
11. Om het nut van dierproeven te bepalen zijn de statistieken van het U.S. General Accounting Office weinig behulpzaam. Een voorstander zal beweren dat 48 % van de medicijnen getest op dieren succesvol op de markt zijn gebracht terwijl een tegenstander zal volhouden dat 52 % van de met dierproeven geteste medicijnen bijwerkingen hebben die zich pas bij klinische toepassing openbaarden.
Barnard, S. Kaufman (1997), Sci. American, 276(2):64-66
12. De snelle ontwikkelingen van nieuwe opslagmedia van data voorzien niet in de mogelijkheid om na één of enkele decennia de data probleemloos terug te lezen.
13. Definitieve ruststand Ajax vak F - Feijenoord vak Z 0-1.

Groningen, 21 mei 1997

Max J.H. Witjes

RIJKSUNIVERSITEIT GRONINGEN

**PHOTODYNAMIC THERAPY AND FLUORESCENCE LOCALISATION OF
EXPERIMENTAL ORAL DYSPLASIA AND SQUAMOUS CELL CARCINOMA.**

A study with aluminium phthalocyanine disulphonate

PROEFSCHRIFT

ter verkrijging van het doctoraat in de Medische Wetenschappen

aan de Rijksuniversiteit Groningen

op gezag van de

Rector Magnificus, dr. F. van der Woude,

in het openbaar te verdedigen op

woensdag 21 mei 1997

des namiddags te 2.45 uur

door

MAX JOHANNES HENDRIKUS WITJES

geboren op 4 april 1965

te Katwijk

Drukkerij Ponsen & Looijen B.V.

Wageningen, 1997

Promotores: Prof. Dr. J.L.N. Roodenburg
Prof. Dr. A. Vermey, FACS

Referenten: Dr. W.M. Star
Dr. P.G.J. Nikkels

To my parents,
from whom I received

To Carmelita,
with whom I share

To Milan and Andra,
to whom we bequeath

Promotiecommissie: Prof. Dr. G. Boering
Prof. Dr. J.J. ten Bosch
Prof. Dr. P. Slootweg

Paranimfen: Drs. J.C. Coops
Drs. M. Rutten

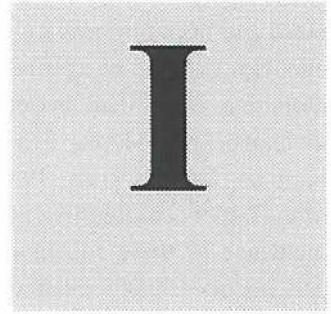
This study was supported by the Dutch Cancer Society (grant GUKC 91-04).

ISBN 90 367 0761 7

CONTENTS

Part I	Introduction and aim	
1.1	Malignant tumours of the upper aero-digestive tract	2
1.2	Aim of this thesis	4
1.3	Photodynamic therapy and fluorescence localisation	5
1.4	Characterization of an autologous tumour model for the investigation of fluorescence localisation and PDT of the oral mucosa	13
Part II	Fluorescence localisation of dysplasia and squamous cell carcinoma	
2.1	<i>In-vivo</i> fluorescence kinetics and localisation of aluminium phthalocyanine disulphonate in an autologous tumour model	20
2.2	Distribution of aluminium phthalocyanine disulphonate in an oral squamous cell carcinoma model. <i>In vivo</i> fluorescence imaging compared with <i>ex vivo</i> analytical methods	35
Part III	Effects of photodynamic therapy on normal oral mucosa, dysplasia and squamous cell carcinoma	
3.1	Photodynamic therapy of normal rat oral mucosa using aluminium phthalocyanine disulphonate. Analysis of the nature and recovery of injury	60
3.2	Photodynamic therapy of experimental dysplasia and squamous cell carcinoma of the oral mucosa using aluminium phthalocyanine disulphonate	79
3.3	Increase of aluminium phthalocyanine disulphonate mediated fluorescence during photodynamic therapy <i>in vivo</i>	95
Part IV	General discussion and summary	
4.1	General discussion	108
4.2	Summary	113
4.3	Samenvatting (Dutch summary)	119
4.4	Bibliography.....	126
	Addenda	141
	List of papers and co-authors	146
	Dankwoord	149
	Curriculum Vitae	152





INTRODUCTION AND AIM

1.1 MALIGNANT TUMOURS OF THE UPPER AERODIGESTIVE TRACT

INCIDENCE

Head and neck tumours are described as malignant tumours arising from the tissues above the clavicles with the exception of tumours of the brain and spinal cord (Zagars *et al.*, 1993). This definition is justified because of similarities in the aetiology, routes of metastatic spread, diagnostic procedures, treatment and rehabilitation after therapeutic intervention of these tumours (Vermey *et al.*, 1991; Zagars *et al.*, 1993). Squamous cell carcinomas of the mucosa of the upper aerodigestive tract constitute an important part of the head and neck tumours. The incidence of these squamous cell carcinomas in the Netherlands is approximately 13 new patients per 100.000 inhabitants which boils down to approximately 1950 new cases per year (Visser *et al.*, 1995; Otter and Schouten, 1995). Generally these cancers afflict persons in the fifth and sixth decades of their lives. The most common sites are the larynx, oral cavity (tongue, floor of mouth), lip and oropharynx .

DIAGNOSIS

Diagnosis of tumours of the upper aerodigestive tract is performed by physical examination, histological evaluation of biopsies and, if necessary, by using imaging techniques. Most squamous cell carcinomas present as ulcerations of the mucosa. Clinically, malignancy of a lesion can be suspected but not diagnosed. The premalignant stages (dysplasia) preceding squamous cell carcinoma can often be recognised as a whitish (leukoplakia) or reddish (erythroplakia) lesion. Histological examination of biopsies is usually conclusive for the type of lesion. A wide variety of radiographic diagnostic methods is available. These comprise plain films (including contrast techniques), computed tomography, magnetic resonance imaging, nuclear isotope scans and positron emission tomography. These imaging techniques are valuable tools for oncologists in the staging of the tumour and planning of treatment. The dimensions of a tumour, its relation to the surrounding normal structures and the presence of lymph node metastases can be evaluated. However, imaging techniques are not capable of determining the nature of a lesion. Furthermore, small superficial tumours or dysplasia cannot be detected by these imaging techniques. Currently this is performed by clinical inspection and histological analysis of biopsies. For clinicians, an additional tool for detecting early lesions (dysplasia and small invasive tumours) and determining their extension would be helpful.

TREATMENT MODALITIES

The major curative modalities for tumours of the upper aerodigestive tract are surgery and

radiotherapy or a planned combination of both. Small primary lesions (T1-T2, UICC classification, Hermanek and Sobin, 1992) can be treated by surgical resection or radiotherapy only. In case of surgery, usually a wide resection including a border of normal tissue is required to ensure complete removal of the tumour. Even in small tumours, resection can result in defects which require reconstruction. This is caused by the complex anatomical construction of the jaws, tongue, palate, pharynx, larynx and the separated respiratory and digestive tracts, which make the aerodigestive tract a functionally complicated part of the body. Side effects of radiotherapy can be severe and may include xerostomia, mucositis, or can cause complications like osteoradionecrosis (Dreizen *et al.*, 1976). Next to that it should be noted that ionising radiation is tumourigenic as well and comprises the risk of malignant transformation of tissues.

Large lesions (T3-T4) require a planned combination of surgery and radiotherapy of the primary tumour and cervical metastases. So far, chemotherapy has not been successful in the curative treatment of head and neck tumours. It is used in clinical trials in combination with surgery and/or radiotherapy or for palliative treatment (Zagars *et al.*, 1993). Recently it was proposed to investigate the possibility of chemoprevention of oral cancer by the dietary intake of retinoids (Boyle *et al.*, 1995).

The 5 year survival rates of patients with head and neck tumours vary from 80% for early stage tumours to less than 25% for advanced stage tumours (Zagars *et al.*, 1993). The volume of the primary tumour and the number and extent of regional nodal metastases are the most important prognostic factors.

To obtain a greater success in the management of tumours of the upper aerodigestive tract new techniques for diagnosis and treatment are desired. From the literature it became apparent that detection with photosensitizer based fluorescence localisation and treatment with photodynamic therapy (PDT) might be alternatives for the currently used methods. Fluorescence localisation of dysplasia or tumours by using fluorescent probes may yield additional information in the diagnostic work-up of a patient. Especially the possibility of the detection of dysplastic mucosa and small superficial tumours seem interesting. Damage to normal tissues induced by photodynamic therapy heals with regeneration rather than scarring (Kleeman *et al.*, 1996). Photodynamic therapy has shown some promising results in the treatment of human mucosal dysplasia and small localised squamous cell carcinomas of the upper aerodigestive tract (Gluckman, 1991; Biel, 1995; Feyh *et al.*, 1990). The results on treatment or palliation of large tumours using PDT vary from satisfactory (Tong *et al.*, 1996) to disappointing (Gluckman, 1991). In the next chapter the most essential aspects of PDT are discussed in more detail.

1.2 AIM OF THIS THESIS

As described above, for improving the management of tumours of the upper aerodigestive tract new techniques for diagnosis and treatment are desired. Therefore, fluorescence localisation and photodynamic therapy of dysplasia and squamous cell carcinoma of the oral mucosa, using aluminium phthalocyanine disulphonate (AlPcS₂), were investigated.

The aims of the present study were:

- To investigate whether AlPcS₂ induced fluorescence, can be exploited as a mean for the localisation of epithelial dysplasia and squamous cell carcinoma of the oral cavity.
- To investigate the localisation of AlPcS₂ in normal and dysplastic oral mucosa and squamous cell carcinoma.
- To determine the time interval between injection of AlPcS₂ and the moment of its highest accumulation in dysplastic lesions and squamous cell carcinoma of the rat oral mucosa.
- To evaluate the short and long term effects of AlPcS₂-based PDT on the normal tissues of the oral cavity and to find a sufficient treatment dose which will induce reparable damage without impairment of essential functions.
- To study the potential value of AlPcS₂ based PDT as a therapy of oral mucosal dysplasia and squamous cell carcinoma.

1.3 PHOTODYNAMIC THERAPY AND FLUORESCENCE LOCALISATION

GENERAL PRINCIPLES OF PHOTODYNAMIC THERAPY

The basis for photodynamic therapy (PDT) are drugs (photosensitizers) which accumulate in tumours and can be activated by light. At the active sites of the photosensitizer-molecules, light (energy) is absorbed which results in an elevated energy state of electrons (figure 1.3.1). These excited electrons can undergo several processes of which some are important in PDT.

After absorption of a photon the electrons can decay back to the ground state, emitting light which is referred to as fluorescence (figure 1.3.2). This can be detected by sensitive equipment and is exploited as a means for tumour-detection. To generate a photodynamic effect, the photosensitizer should be transferred to the triplet state by a process referred to as "intersystem crossing". During this process the excited electrons undergo electron spin conversion to a lower intermediate state, the triplet state. For photosensitizers to be effective, a long-lived triplet state is necessary. Therefore, not all light-absorbing chemicals are photodynamically active. From this triplet state 2 types of photochemical reactions can occur. In Type I reactions the excited photosensitizer reacts with substrates in the proximity. The nature of this reaction is proton or electron transfer, basically a radical/redox reaction, resulting in photosensitizer-substrate products (Ferraudi *et al.*, 1988; Feix *et al.*, 1991; Buettner *et al.*, 1985). In Type II reactions, energy is transferred to oxygen and yields excited oxygen molecules (Rosenthal *et al.*, 1986). In this type of reaction only energy is transferred

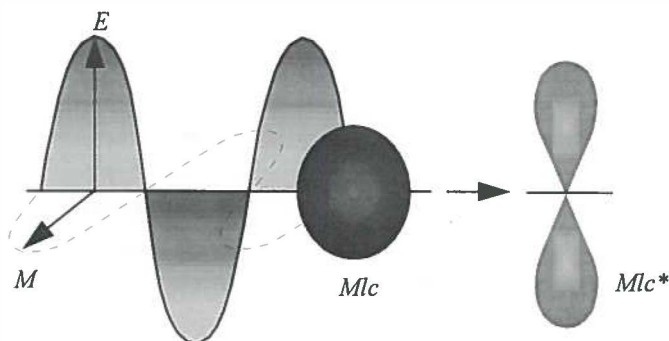


Figure 1.3.1 Schematic drawing of absorption of electromagnetic radiation (=light), with an electrical (E) and magnetic (M) component, by a molecule in the ground state (Mlc), resulting in an electronically excited state of the molecule (Mlc*). In the excited state the electrons of the molecule are in a different orbit than in the ground state.

and the photosensitizer and oxygen molecules are not permanently altered. Oxygen in the singlet state is a highly reactive molecule which can react with DNA, proteins and unsaturated bonds in lipids. These reactions can result in lethal damage to cellular functions. The Type II reactions are considered to be important for PDT (Weishaupt *et al.*, 1976), although no unequivocal proof has been provided that singlet oxygen is ultimately responsible for tissue necrosis (Harriman, 1995).

The toxicity of photosensitizers for living cells strongly depends on the oxygenation of the tissues (Gomer *et al.*, 1984). Higher concentrations of oxygen will yield more singlet oxygen and more necrosis. The presence of various biomolecules which can act as a substrate also influences the process and therefore Type I and II reactions will both occur during PDT. The photosensitizer-molecule will be altered during irradiation because of Type I reactions or due to destruction by singlet oxygen. This process of photosensitizer degradation can be observed during irradiation with light as a diminishing of the fluorescence intensity of the photosensitizer (photodegradation).

THE USE OF LIGHT IN PDT

For effective treatment of tumours, light should penetrate sufficiently into the tissue. Upon entering the tissue, light (in this case it is convenient to envisage light as a photon beam) is

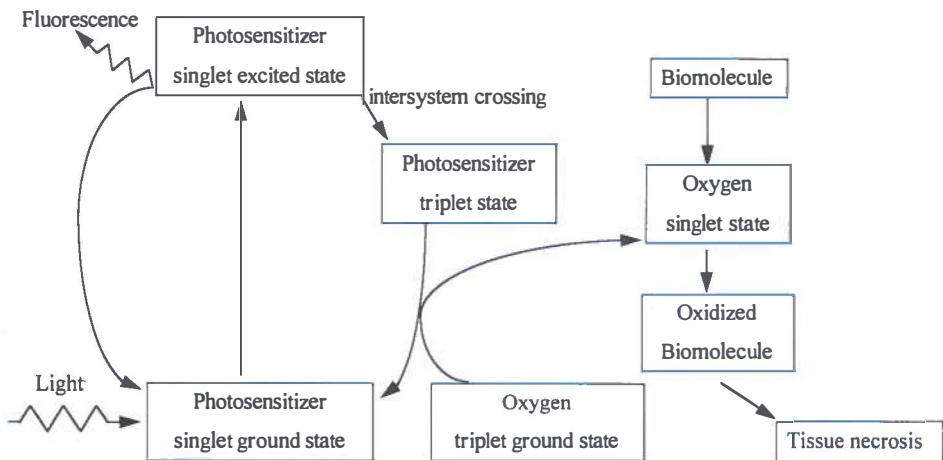


Figure 1.3.2 Schematic drawing of photosensitizer excitation and emission of fluorescence and a Type II photoreaction important for PDT.

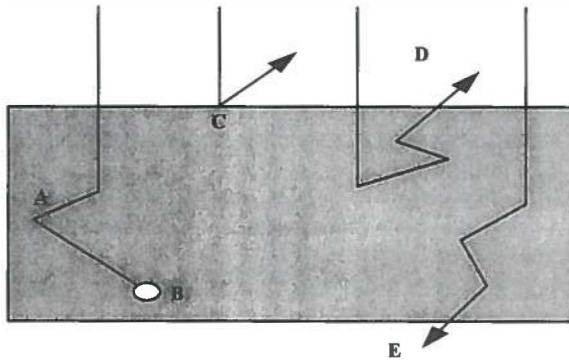


Figure 1.3.3 Scattering (A), absorption (B), reflection (C), back scattering (D) and forward scattering (E) of photons in tissue.

subjected to two major processes namely absorption and scattering (figure 1.3.3). When absorbed, the energy from photons is transformed to either heat or chemical energy by naturally existing chromophores in the tissue. When scattered, the direction of the path of the photons is altered and this process depends on variations of refractive indices at e.g. cell boundaries and other structures in the tissue. Both absorption and scattering determine the optical path length, that is the average distance a photon will travel before being absorbed or scattered in tissue. In human and animal tissues light is mainly scattered forward (figure 1.3.3, E). Furthermore, it is known that most naturally existing chromophores absorb at short wavelengths (<600 nm). At a higher wavelength of approximately 700 nm the penetration is deeper owing to the lack of chromophores in the tissue which are able to absorb light of this wavelength. In the range of 500-700 nm the scattering-coefficient of tissues does not dramatically alter, and therefore the lack of chromophores will yield a deeper penetration of light. For this reason, PDT with photosensitizers with absorption bands in longer wavelength regions will result in deeper tissue necrosis than photosensitizers with absorption bands in shorter wavelength regions.

Due to scattering and absorption the applied light dose in tissue will be different from the incident light dose. The effective light dose depends on the concentration and distribution of the photosensitizer in the tissue. These parameters influence the threshold destructive dose, that is the light dose needed for inducing tissue necrosis. Light-sources used for PDT should be capable of generating sufficient optical power to amount to the threshold destructive dose within an acceptable treatment time. Conventional light sources like xenon or halogen lamps are able to yield sufficient optical power. In fact, successful PDT treatments have been carried out using light from a slide projector. However, these

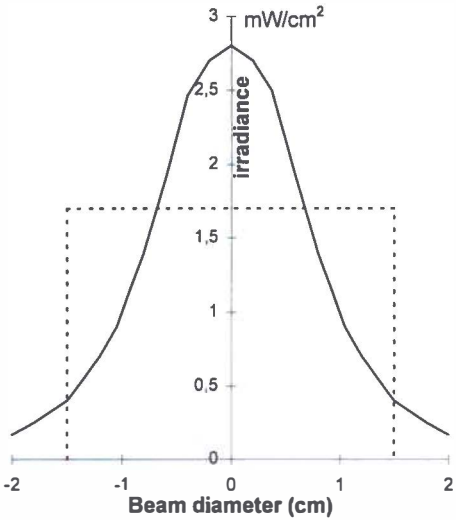


Figure 1.3.4 Example of an ideal beam with a flat profile (dotted line) and a light beam with a bell shaped profile (continuous line), both having approximately the same power density

lamps generate polychromatic light which makes dose calculation difficult. This problem can be overcome by using a laser as a light source. Lasers generate light of a single wavelength at high optical power. In combination with a dye laser, this wavelength can be altered depending on the dye used. The power density of a light beam is expressed as Watts per unit of surface area (W/cm^2) and the light dose as Joules per unit of surface area (J/cm^2). The incident light dose can be calculated from the dose rate of the incident light beam (irradiance) multiplied by the

irradiation time ($1 W=1 J/s$). The effects of scattering and absorption should be included when calculating the applied light dose.

A practical problem in PDT is the geometry of the light beam. When for instance a light beam has a power density of $10 mW/cm^2$ the distribution of the incident light beam is not homogeneous but bell shaped (figure 1.3.4). This results in a lower irradiance at the periphery of the irradiated area than in its centre, whereas an ideal beam would show a homogeneous distribution of the irradiance.

PHOTOSENSITIZERS

In the past century several light sensitive chemicals were discovered which were able to generate a PDT-like tissue necrosis. Photosensitizer-based PDT for the treatment of tumours evolved when a derivative of hematoporphyrin (HpD) was discovered. This derivative showed high tumour uptake in mice and was later considered interesting for clinical use (Lipson *et al.*, 1961; Dougherty *et al.*, 1975). After the first clinical investigations of HpD the interest of using photosensitizers for photodynamic therapy expanded rapidly. For a long time HpD was the only photosensitizer available.

The optical absorption spectrum and the absorption efficiency largely determines the efficacy of a photosensitizer in photodynamic therapy. In addition, a photosensitizer should obviously possess good tumour localising properties. Furthermore a long-lived triplet state, a good singlet oxygen yield, a chemically pure and stable molecule and a high fluorescence yield are considered other important features. HpD has shown good localising properties and photodynamic action in several experimentally induced tumours and human tumours (Grossweiner, 1987; Wenig *et al.*, 1990; Feyh *et al.*, 1990). However, there are several disadvantages using HpD as photosensitizer. Patients injected with HpD have a high skin photosensitivity for normal daylight for a period of approximately 6-8 weeks. HpD is a mixture of porphyrins of which its monomers probably are responsible for tumour fluorescence while its oligomers are the photodynamically active components, which makes prediction of therapeutic effects difficult (Kessel, 1982; Dougherty, 1987). Furthermore, the absorption bands of HpD often used for PDT are situated around 500 and 625 nm at which the absorption efficiency is relatively low. For superficial treatment this can be sufficient, however, for larger tumours a photosensitizer with a higher absorption efficiency as well as absorption bands at longer wavelengths seems to be preferable. After the introduction of HpD the search for better photosensitizers was intensified (powerful and rapid clearance from the body). This resulted in the introduction of metallo-phthalocyanines as possible photosensitizers for PDT (Van Lier *et al.*, 1989; Rosenthal, 1991). Besides metallo-phthalocyanines several other photosensitizers are under investigation. These are beyond the scope of this thesis and will not be discussed here.

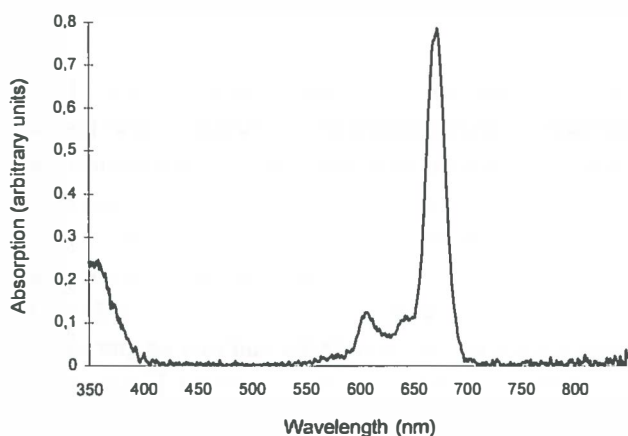


Figure 1.3.5. Typical absorption spectrum of AlPcS₂ in methanol

Metallo-phthalocyanines (MPC's) are chemically synthesised molecules and possess many of the characteristics favourable for photosensitizers. The energy involved in the excitation to the photosensitizer-singlet state is much lower for MPC's than for porphyrins. Thus, the major absorption-band is situated at a longer wavelength, between 650-700 nm with a peak at 670 nm (figure 1.3.5). For clinical use this is interesting because a deeper tissue effect can

be expected due to a deeper penetration of light. In animals phthalocyanines showed almost no skin photosensitivity, with the exception of Caesium-Pc (Brasseur *et al.*, 1987; Tralau *et al.*, 1989). The photochemical properties of MPC's can be influenced by altering the metal ion (Chan *et al.*, 1987; Wu *et al.*, 1985; Langlois *et al.*, 1986; Rosenthal *et al.*, 1987). This influences the triplet life time of the molecule and the fluorescence yield. Aluminium and zinc have been proposed as most suitable metals for phthalocyanines (Berg *et al.*, 1989a; Ambroz *et al.*, 1991). One important disadvantage of MPC's is the insolubility in water. This can be overcome by adding up to 4 side chains substituents of sulphonic acid. This will result in mono-, di-, tri- and tetra-sulphonated phthalocyanines. During the sulphonation a mixture of these compounds will be formed and separation is necessary because the degree of sulphonation is essential in the localisation in cells and tissues. Among the various MPC's, aluminium phthalocyanine disulphonate (AlPcS₂) seems the most promising for PDT and has been the subject of numerous investigations. AlPcS₂ has shown to possess good tumour localising, fluorescence and necrotising properties (Rosenthal, 1991; Spikes, 1986). For AlPcS₂ 16 different isomers are possible, with difference in lipophilic(hydrophilic) characteristics. Complete separation of these isomers is not feasible. It was found that the difference in lipophilicity will show difference in PDT-activity (Paquette *et al.*, 1988; Ali *et al.*, 1988). The AlPcS₂ with its sulphonic acid groups adjacent (cis-isomer) will show amphiphilic (i.e. possessing both lipophilic and hydrophilic properties) characteristics, and may be efficiently taken up by cells, whereas the isomer with opposite sulphonic acid groups (trans-isomer) will behave more lipophilic. For this study we obtained an isomer of AlPcS₂ which was analysed by others and seems to be amphiphilic of nature (Ambroz *et al.*, 1991).

FLUORESCENCE LOCALISATION

For sulphonated AlPc's, excitation often is performed at the absorption bands at 300, 610 or 670 nm. Emitted fluorescence can be detected by photomultipliers or Charge Couple Device (CCD) cameras. Basically these instruments transform the absorbency energy of a photon into an electric signal which can be processed by a personal computer. Fluorescence imaging is a useful technique to study the localisation of photosensitizers in single cells or in tissue.

The degree of sulphonation of the AlPc molecule largely determines the uptake and localisation in cells and tissue (Paquette *et al.*, 1988; Chan *et al.*, 1990; Peng *et al.*, 1991a). It was found that *in-vitro* the less sulphonated AlPc's are taken up faster and to a greater extent in cells than the more sulphonated AlPc's (Berg *et al.*, 1989b; Chan *et al.*, 1990). Furthermore, AlPcS₁₋₂ located diffusely in the cytoplasm while AlPcS₃₋₄ showed a granular pattern in cultured cells (Peng *et al.*, 1991a), indicating a different intra-cellular localisation among the sulphonated AlPc species. The localisation of AlPcS₂ alters during irradiation, which makes

analysis of the damaged sites in the cells complicated (Ambroz *et al.*, 1994). *In vivo* experiments showed that the localisation in the tissues of the sulphonated species varies substantially. AlPcS₂ accumulated intracellularly while AlPcS₄ seems to localise in the tumour stroma (Peng *et al.*, 1990). Furthermore, the time interval between injection and maximal tumour concentration as well as the amount of tumour uptake varies (Chatlani *et al.*, 1991; van Leengoed *et al.*, 1993a). Time intervals of maximal AlPcS₂ fluorescence in tumours of 2-48 h were reported in the literature.

PHOTODYNAMIC THERAPY

Two processes are responsible for tumour necrosis by PDT: the PDT-induced direct cell necrosis and the indirect necrosis due to shutdown of tumour vessels. There has been much debate on which of both is the most essential for tumour necrosis. *In vitro* experiments showed that in cellular necrosis several cellular functions may be damaged like plasma membrane leakage and inhibition of transmembrane transport systems (Steveninck *et al.*, 1983; Dubbelman *et al.*, 1991), mitochondrial disruption (Moan *et al.*, 1982) and inhibition of DNA excision repair (Boegheim *et al.*, 1987). It was recently shown that the ultimate cause of necrosis may vary per cell line, depending on its weakest link (Penning *et al.*, 1994). In this study cell death occurred due to inhibition of enzyme activity in some cells while others were sensitive to mitochondrial damage or failure of transport systems.

Several studies clearly indicated that indirect tumour necrosis due to vascular shutdown is an important feature of PDT. It was shown that the clonogenicity of tumour cells did not alter when they were harvested from the host animals and cultured *in vitro* immediately after PDT (Henderson *et al.*, 1985). Furthermore, a reduction and even cessation of bloodflow was observed after PDT in a transplanted tumour in a window observation chamber, which lead to tumour necrosis (Star *et al.*, 1986). Several vessel responses were noted varying from initial vasodilatation to constriction and obstruction of the lumen by blood clots (Menezes da Silva *et al.*, 1995; Fingar *et al.*, 1993). Endothelial damage and the release of clotting factors from blood cells yield thrombosis (Fingar *et al.*, 1992; Fingar *et al.*, 1990; Ben-Hur, 1988). In addition, the tumour vessels are often rapidly formed due to an increased need for nutrients by the tumour cells. Therefore this vasculature is of a lesser quality, and possibly more sensitive for PDT than normal pre-existing vessels (Chaplin, 1991). Hypoxia or ischemia and lack of nutrients will consequently lead to tissue necrosis distal from the obstruction.

The efficacy of tumour necrosis varies for each of the sulphonated AlPc's species. Mono-sulphonated phthalocyanines seem to be less attractive as tumour localisers but yield substantial PDT induced necrosis whereas tetra-sulphonated phthalocyanines are good tumour localisers but yield limited tissue damage (Berg *et al.*, 1989; van Leengoed, 1993b). *In vitro*

studies showed uptake of ALPcS₂ in cells and a higher cytotoxicity than HpD (Chan *et al.*, 1991; Peng *et al.*, 1991a). *In vivo* studies on the effect of the central metal ion and degree of sulphonation show that ALPcS₂ displays a high tumour fluorescence and tumour necrosis after illumination (van Leengoed *et al.*, 1993c). ALPcS₂ seems a promising photosensitizer for clinical use of PDT due to both its tumour-localising and photodynamic properties and it is therefore interesting for further investigations.

1.4 CHARACTERISATION OF AN AUTOLOGOUS TUMOUR MODEL FOR THE INVESTIGATION OF FLUORESCENCE LOCALISATION AND PDT OF THE ORAL MUCOSA

INDUCTION OF DYSPLASIA AND SQUAMOUS CELL CARCINOMA USING 4NQO

To investigate detection and treatment of oral squamous cell carcinoma by photodynamic therapy (PDT) an animal model is necessary which mimics the human situation. To investigate the applicability of PDT in the treatment of early cancer of the oral mucosa, a model with the dysplastic stages preceding invasive cancer is desirable. Oral epithelial dysplasia and squamous cell carcinomas induced by 4 nitroquinoline-1-oxide (4NQO) on the hard palate of the Wistar albino rat emerged as a possible model (Wallenius and Lekholm, 1973). This location seems suitable for investigating the effects of PDT on the oral mucosa as well as on several surrounding tissues like bone and teeth. The effect of 4NQO application on the mucosa of the hard palate as well as on other parts of the oral

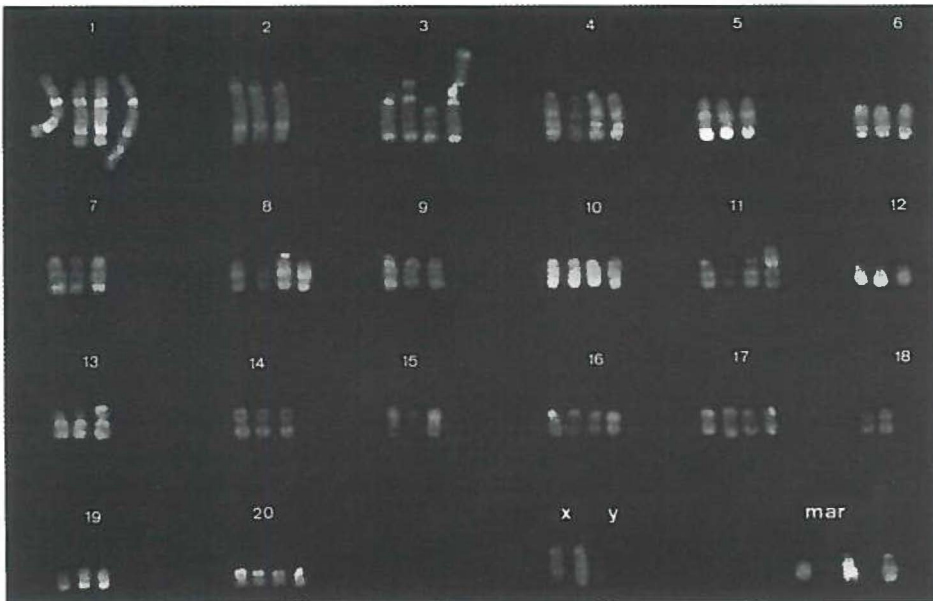


Figure 1.4.1 Karyotype of a cell line derived from keratinocytes treated with 4NQO for 16 weeks *in vivo*, stained for R-banding. The karyotype was interpreted as: add(1)(q5?3),-2,add(3)(p1),del(3)q11q23, add(3p)(qter→p11::hsr?::3q23→qter),-5,-6-7-9,add(11)(p?11)[50%],-15,-19,+2 to 8 markers.

cavity (tongue, buccal fold) was investigated. A common protocol for the induction of dysplasia and squamous cell carcinoma on the oral mucosa of the rat is the repeated application of 4NQO on this tissue (Prime *et al.*, 1986; Fisker, 1978). A safe method for handling the carcinogenic 4NQO is to dissolve it in propylene glycol at a concentration of 0.5% (w/v) and apply that solution with a small brush to the palate. After approximately 26 weeks of 4NQO treatment tumours evolve from premalignant dysplasia to infiltrative squamous cell carcinoma. Like most oral squamous cell carcinomas (depending on the anatomical location), the 4NQO-induced tumours have a delayed tendency to metastasise to lymph nodes (Stenman, 1981). It appeared that lesions on the palate were reproducible while the other locations were less suitable for creating reproducible dysplastic lesions and squamous cell carcinoma (Nauta *et al.*, 1996a; Nauta *et al.*, 1996b). For that reason tumour

induction on the hard palate of the rat was chosen as the model for investigating the applicability of detection and therapy of dysplasia and squamous cell carcinoma with PDT.

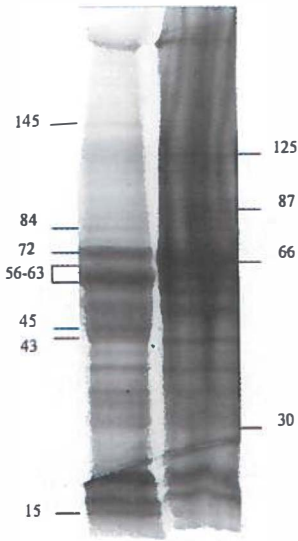


Figure 1.4.2 SDS-PAGE of 4NQO-treated (A) and normal (B) keratinocytes on a 4-20% gradient gel. Major differences in protein bands present in normal cells but not in the malignant cells and vice versa are marked, and the according mol. weights indicated (kDa). Note the pronounced band at 56-63 kDa in the malignant cells indicative for excessive keratin production

THE EFFECT OF 4NQO ON CELLS AND TISSUES

The carcinogenic 4NQO has been extensively investigated and is known to cause several types of chromosomal changes. In bacteriophages, 4NQO induces basepair change mutations (GC→AT) and deletion mutations. It has been proposed that the mutagenic action of 4NQO is based on its conversion to 4-hydroxyaminoquinoline 1-oxide which binds covalently to nucleic acids and damages chromosomes through the formation of DNA adducts (Nagao *et al.*, 1976; Daubersies *et al.*, 1992). In eukaryotic cells 4NQO induced diplochromosomes indicated a disturbed chromosome reproduction (Sutou, 1973). In general, 4NQO-induced chromosome aberrations resemble those induced by UV light (Kondo, 1981). Little is known about the genotype and phenotype of oral keratinocytes that were malignantly transformed by 4NQO. It has been shown that in 4NQO-treated oral keratinocytes, both *in vivo* and *in vitro*, an

aneuploid chromosome number is not an early marker for a malignant growth pattern (Crane *et al.*, 1989). Analysis of the effects of 4NQO on cultured keratinocytes derived from 4NQO- induced squamous cell carcinoma of the oral mucosa showed numerous genetic alterations (figure 1.4.1). Two studies are available investigating the alterations in the karyotype after 4NQO treatment and in both tetraploid populations were found with defects (deletions, translocations, gain or loss of chromosomes) to chromosomes 3 and 12 (Witjes *et al.*, 1995a; Patel *et al.*, 1995).

Treatment of the oral mucosa with 4NQO *in vivo* can result in a change in cytokeratin expression (Witjes *et al.*, 1995a; Boyd *et al.*, 1991). In culture, malignant keratinocytes derived from rat palatal mucosa treated with 4NQO *in vivo*, produced substantial amounts of keratin (figure 1.4.2). *In vivo*, the induction of cancer with 4NQO often is accompanied by excessive keratin production.

The development of early dysplastic stages to invasive carcinoma of the oral mucosa can be followed accurately by means of histological analysis. Using the Epithelial Atypia Index (EAI, see addendum A) (Smith *et al.*, 1969) for histopathological tumour grading, severe dysplastic changes in the mucosa correlate with an increasing EAI number (Nauta *et al.*, 1996a). Analysis of the palatal mucosa of 4NQO treated rats showed a strong correlation of 0.88 between the application time and the EAI of the mucosa (figure 1.4.3, Spearman

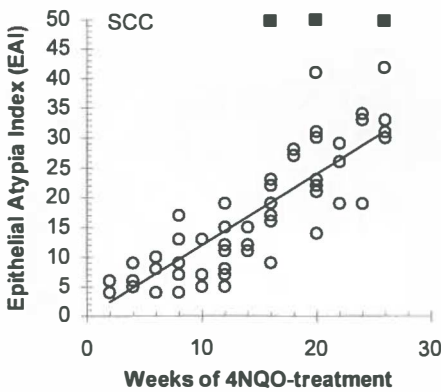


Figure 1.4.3 Results of histological analysis of rat palatal mucosa treated with 4NQO using the Epithelial Atypia Index (EAI). The correlation between the application period and the increase of dysplasia was 0.88 (total n=68, ■ =squamous cell carcinoma n=8).

correlation analysis, $p < 0.0001$). Furthermore the type of dysplasia shows distinct similarities with the human situation as well (Nauta *et al.*, 1995). Especially, the possibility of expressing the degree of dysplasia of the mucosa numerically is an important feature of this model. Squamous cell carcinoma can not be graded by the EAI (only dysplasia can) and is therefore separately noted.

A typical progression of dysplasia is shown in figures 1.4.4A-D. The histological signs of dysplasia are summarised in the EA-Index (addendum A). After an initial

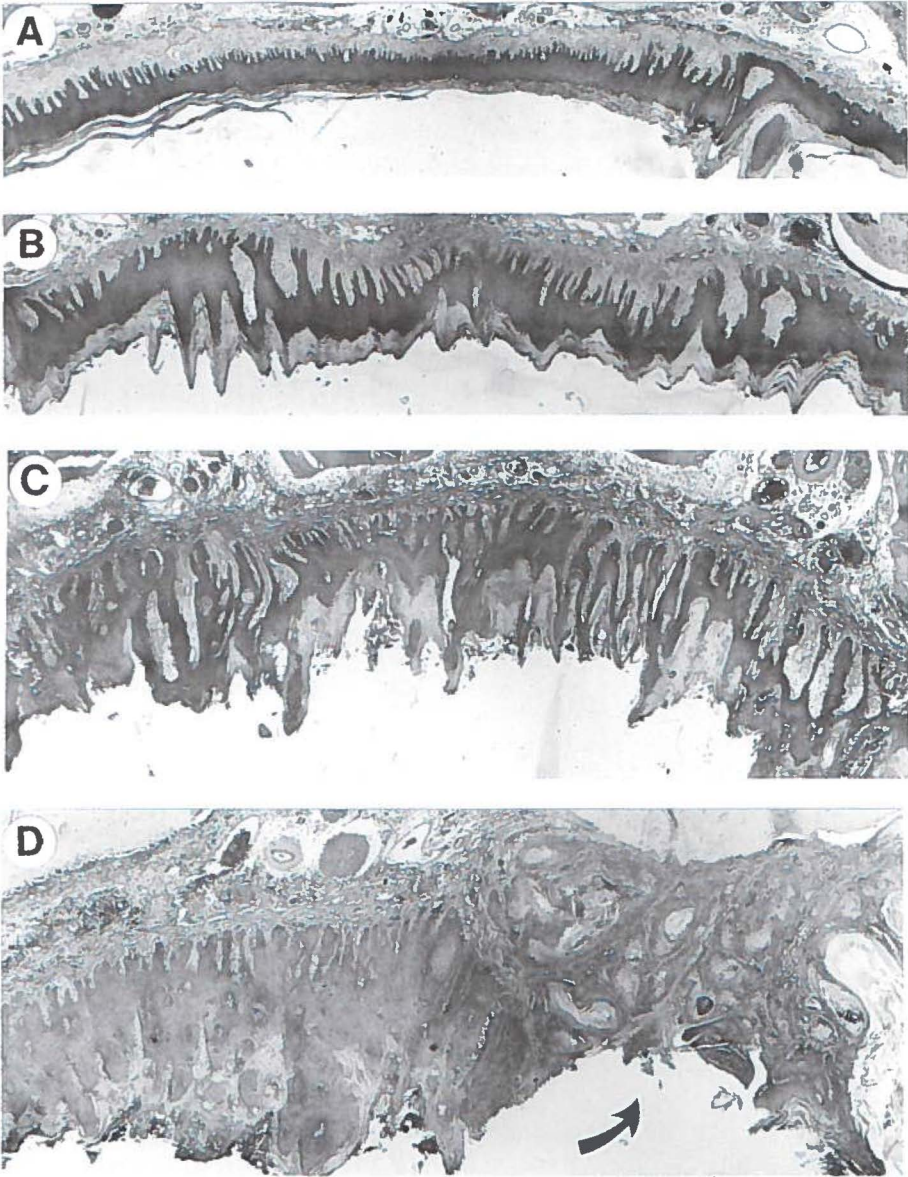


Figure 1.4.4A-D: Histological slides of rat palates treated for 8 (A), 16 (B) and 26 (C&D) weeks with 4NQO. An increasing 4NQO treatment period coincides with elongation of the rete ridges of the epithelial layer, an increase in thickness of the epithelial layer and excessive production of keratin. Cellular atypia develop during this period resulting in slight (A), moderate (B) and severe dysplasia (C) or in invasive carcinoma (D).

inflammatory reaction which can last several weeks, the epithelial layer starts to show hyperkeratosis, hyperplasia and elongation of the rete ridges. Then, acantholysis appears as well as keratinisation of cells beneath the keratinised layer. At the cellular level the nucleus increases in size and a difference in cell size and shape becomes apparent. Increase in mitotic activity and bizarre mitoses are seldomly seen. Invasive tumour growth is usually present after 26 weeks of 4NQO-treatment. Only in a few rats tumours evolved after 16-20 weeks of treatment. The growth pattern of 4NQO induced lesions is predominantly well differentiated squamous cell carcinoma although rapidly invasive tumours with perineural growth have been observed as well (Nauta *et al.*, 1996a; Crane *et al.*, 1986; Prime *et al.*, 1986).

In conclusion, the 4NQO- rat palatal model seems an appropriate tumour model for investigating PDT of premalignant lesions and early cancer of the oral cavity.

A grey square containing the Roman numeral 'II' in a large, black, serif font.

II

FLUORESCENCE LOCALISATION OF DYSPLASIA AND SQUAMOUS CELL CARCINOMA

2.1 *IN VIVO* FLUORESCENCE KINETICS AND LOCALISATION OF ALUMINIUM PHTHALOCYANINE DISULPHONATE IN AN AUTOLOGOUS TUMOUR MODEL

INTRODUCTION

Photosensitive drugs can be used for therapy and detection of cancer. The therapeutic modality is called photodynamic therapy (PDT) and the detection modality is generally referred to as photodiagnosis or photodetection (PD). After administration, the ideal drug for PDT or PD accumulates preferentially in premalignant or malignant tissue. If more photosensitizer is retained in tumour than normal tissue, drug fluorescence can be used for tumour localisation or detection.

Most *in vivo* fluorescence studies were performed with animal models in which xenografts were used to mimic the clinical situation. It is known that differences exist between the actual clinical situation and the tumour xenografts like the presence of a fibrous layer surrounding the implanted material or other host responses (Fodstat, 1988). A tumour model which has a human counterpart will have the advantage of being clinically comparable.

It has been shown that porphyrins accumulate in chemically induced premalignant and malignant tissues in animals (Mang *et al.*, 1993; Crean *et al.*, 1993). The tumour model used in the present study is based on the induction of squamous cell carcinomas with 4-nitroquinoline 1-oxide (4NQO) in the hard palate of the Wistar albino rat which closely resembles the clinical and histological appearance of human squamous cell carcinoma (Prime *et al.*, 1986; Nauta *et al.*, 1995). After sufficient 4NQO application the whole mucosal area between the molars becomes dysplastic and tumours arise locally, sometimes in multiple spots. When the 4NQO application is continued more tumours arise and the existing tumours expand.

To detect sensitizer fluorescence *in vivo* several systems have been developed which include endoscopes connected to devices like intensified charge couple device (CCD) cameras or photomultipliers (Profio *et al.*, 1983; Brodbeck *et al.*, 1987; Andersson *et al.*, 1987; Rogers *et al.*, 1990). Promising results have been established with endoscopic detection of tumours in clinical settings with HpD or Photofrin (Monnier *et al.*, 1990; Kato *et al.*, 1992), although it has been noted that most papers are case reports and that real value of sensitizer based PD needs to be established (Bown, 1993). We have developed an endoscope-based imaging system for the detection of sensitizers in the palate of the rat. The aims of this experiment were to study the fluorescence kinetics of aluminium phthalocyanine disulphonate (AlPcS₂) in the 4NQO-palate tumour model and the ability of AlPcS₂ to localise in non-invasive epithelial disorders and squamous cell carcinoma of the mucosa of the hard palate.

MATERIAL & METHODS

Photosensitizer

AlPcS₂ was obtained from Porphyrin Products Inc. (Logan, UT, USA) and was prepared via the direct sulfonation method. After receiving the AlPcS₂ the purity was analysed by High Performance Liquid Chromatography in a gradient from 20% to 90% MeOH. The fraction consisted of >90% pure AlPcS₂ of one isomer. For injection the drug was first dissolved in 0.1 M NaOH (pH 12). This solvent was diluted to an injectable volume with phosphate buffered saline (PBS). The pH was adjusted by adding an amount of 0.1 M HCl equal to the amount of NaOH.

Imaging system, AlPcS₂-excitation and -fluorescence detection

A schematic drawing and description of the palatoscope developed for the purpose of illumination and acquisition of fluorescence images is presented in figure 2.1.1. The region of interest was the mucosa of the hard palate between the molars of the rat. With this endoscope a fairly homogenous beam was obtained which illuminated an area of approximately 1 cm in diameter. From the centre of the beam the light intensity gradually

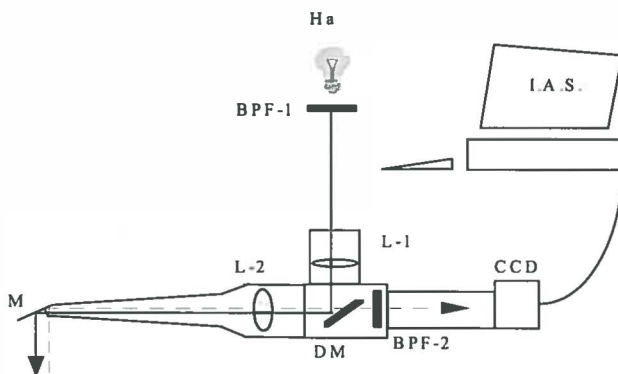


Figure 2.1.1 Schematic drawing of the imaging system. Excitation light is obtained from a halogen lamp, passed through a band pass filter (BPF-1) and further transported through a liquid light guide to a lens L1. The light is then reflected by a long pass dichroic mirror (DM) and passed through the imaging objective L2 to create a nearly parallel beam that is reflected by a mirror M to become perpendicularly incident on the palatal surface. The emitted fluorescent light (dotted line) is reflected by the mirror, passed through L2, DM and a band pass filter (BPF-2) to select the emission band of the photosensitizer, and is recorded by an intensified CCD-camera. The images are stored on the hard disk of a PC-based image analysis system (IAS).

diminished to not less than 90% at the outer part of the beam. The imaging system projected a full screen view of the hard palate including the molars, and allowed detailed analysis of the mucosa. The images were digitised by a Personal Computer based framegrabber and averaged over 16 frames (van Leengoed, 1993b). The detection range of the CCD camera was between 0-30 nW/cm², and fluorescence was detected in the linear part of the range between 10-25 nW/cm². The images were analysed by imaging software (TIM by Difa Measuring Systems B.V., Breda, The Netherlands) using a pixel measurement program which allows to measure grey-scale values of fields of interest and to subtract different recorded images.

The technique of dual wavelength excitation (Baumgartner *et al.*, 1987) was used to detect the AlPcS₂ fluorescence. The AlPcS₂ as purchased showed a typical aluminium phthalocyanine absorbance spectrum in the monomeric form with a minimal absorbance between 400 nm and 550 nm followed by a small peak at 590 nm to 615 nm and a large absorbance peak at 672 nm (figure 2.1.2). Since the monomeric form is responsible for phthalocyanine fluorescence (Wagner *et al.*, 1987) it was expected that AlPcS₂-fluorescence *in vivo* could be excited at a wavelength around 610 nm. In pilot experiments we found that autofluorescence images of the palate excited at 460 ±20 nm and at 610 ±15 nm did not differ very much in fluorescence intensity and pattern. The excitation light was blocked with a high pass dichroic mirror (DM) transmitting light above 550 nm or 650 nm respectively, while the fluorescence of both excitation wavelengths was detected at 675 ±15 nm. After subtraction of the images of the two wavelengths, less than 10% of the original value remained (fig 2.1.3).

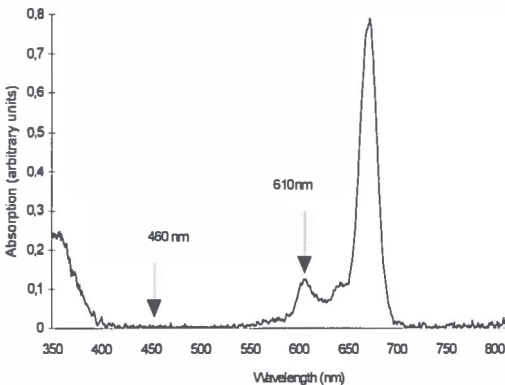


Figure 2.1.2 Absorbance spectrum of AlPcS₂ in methanol. The arrows are positioned at the wavelength areas used for excitation of autofluorescence at 460 nm, and AlPcS₂-fluorescence at 610 nm.

Also the autofluorescence images obtained at 460 ±20 nm did not alter after drug injection (fig 2.1.3), while excited at 610 ±15 nm AlPcS₂-fluorescence was easily detected at a dose of 1 μmol/kg. Satisfactory fluorescence intensities for recording images were obtained with light generated by a halogen-lamp (Ha) with an irradiance of 0.2 mW/cm², after passing through the excitation filter. The power of the lamp was checked regularly during the experiments but no adjustments were necessary.

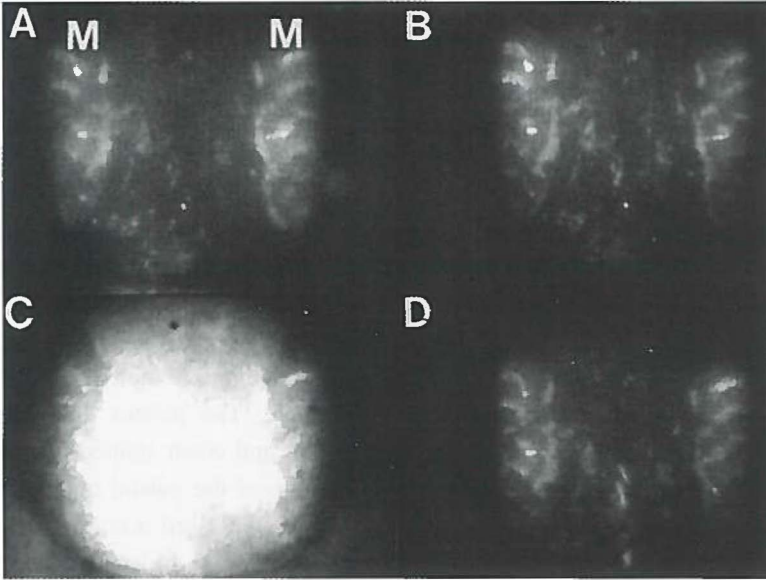


Figure 2.1.3 Four digitised fluorescence images of a palate of the same 4NQO-treated rat. On each image on the left and right the molars (M) and the region of interest between the molars can be seen. **A:** Autofluorescence-image of the palate excited with 460 nm. **B:** autofluorescence-image excited with 610 nm, both prior to the injection of AlPcS₂. When these images are subtracted almost no autofluorescence remained (not shown). **C:** The fluorescence image excited with 610 nm 6 h after injection of 1 $\mu\text{mol/kg}$ AlPcS₂. Clearly, AlPcS₂-mediated fluorescence dominates this image. **D:** The 460 nm autofluorescence-image of the same rat also 6 h *after* injection of 1 $\mu\text{mol/kg}$ AlPcS₂. No change of fluorescence was observed compared with the 460 nm-image before injection (A). When image D is subtracted from image C only the specific AlPcS₂ fluorescence will remain (not shown).

Experimental procedure and assessment criteria

Squamous cell carcinomas and epithelial dysplasia were induced by a three times weekly application of 4NQO. The rats were briefly anaesthetised by mixture of N₂O/O₂/halothane and painted with 4NQO on the mucosa of the hard palate. During the application period the rats were housed under standard housing conditions. For this experiment 22 Wistar albino rats divided into 5 groups were used. Each group was subjected to a different 4NQO-application period, namely 8, 12, 16, 20 and 26 weeks. Two untreated animals served as controls.

Ideally, the light beam should be perpendicularly incident on the whole palatal surface. However, this is only partly possible due to the anatomical curvature of the palate. Also accurate repositioning of the animal is required. This was achieved by anaesthetising the animals with a mixture of O₂/N₂O/Ethane, and placing them in a stereotactic frame which

was fixed on an XY-table. The endoscope was fixed to the table on a photographic standard which was adjustable in height.

After recording autofluorescence images all rats were injected with 1 $\mu\text{mol/kg}$ AIPcS₂ via a tail vein. Fluorescence images were recorded at 2, 4, 6, 8, 10, 24, 32, 52, 72, 100 h post injection. The rats were sacrificed with an intra-cardial overdose of pentobarbital after the last fluorescence image was recorded. The palate with the surrounding hard and soft tissues, including the skull, were removed in one piece. The palates were fixed in 4% formalin, decalcified with 25% formic acid with 0.34 M trisodium citrate dihydrate for approximately 4 weeks. The degree of decalcification was checked by X-ray analysis. Punch biopsies of 3 mm in diameter (Biopsy Punch, Stiefel, Germany) were taken at locations which displayed as strong fluorescent spots (hot spots) in the fluorescence image or which were clinically suspect for squamous cell carcinomas but did not fluoresce. The palates and biopsies were cut transversely and processed for standard hematoxylin and eosin stained histological sections. The slides of the biopsies and the adjacent epithelium of the palatal mucosa were examined with light microscopy and the epithelial dysplasia was assessed according to the Epithelium Atypia Index (EAI) grading list by Smith/Pindborg by an independent observer without knowledge of 4NQO-treatment time or of the outcome of the fluorescence measurements (Smith *et al.*, 1969). The average grey-scale value of the total area between the molars at every fluorescence recording after subtraction of autofluorescence was measured for all rats. The grey-scale values of the fluorescent hot spots were measured and compared to the total area measurements.

RESULTS

Fluorescence intensities and EAI of palates

The images of normal rat palates show an identical AIPcS₂-fluorescence pattern. A small band along the molars fluoresces strongly and the intensities decrease in the middle of the palate. This was also seen in the 4NQO-treated rats and this pattern slightly interfered with the diagnosis of hot spots because it made the interpretation of the images more complex (fig 2.1.3). We were able to reduce the autofluorescence signal to a negligible level of approximately 5 pixels for all groups (0 h) by subtracting the 610 nm and 460 nm images. The grey-scale levels of AIPcS₂ fluorescence after subtraction were for the normal rats (with the lowest AIPcS₂ fluorescence of all groups) approximately 80 pixels. Therefore analysis of AIPcS₂-localisation was not hindered by autofluorescence. Two rats which were treated for respectively 8 and 26 weeks with 4NQO were lost during the experimental procedure. The fluorescence intensity of AIPcS₂ increased with increasing 4NQO treatment. Figure 2.1.4A

shows the course of the detected AlPcS₂-fluorescence of the mucosa between the molars of a rat, treated for 26 weeks with 4NQO. As hot spots were only present between 2 and 10 h after injection it was decided to restrict statistical analysis to that period. No hot spots were observed anymore 24 h after injection. The area under the curve as presented in figure 2.1.4A, between 2 and 10 h should give a good impression of the fluorescence kinetics of tumour tissue. The area was approximated by means of a weighted sum of the fluorescence measurements at times 2, 4, 6, 8 and 10 h, respectively using 'weights' 1, 2, 2, 2 and 1. Figure 2.1.4B shows the approximated areas vs. the number of weeks of 4NQO application for every rat. An extension of the Wilcoxon rank-sum test (Stepniewska *et al.*, 1992; Cuzick, 1985) was used to confirm a positive trend between the area under the curve (between 2 and 10 h for all rats) and the number of weeks of 4NQO application ($p < 0.04$). Figure 2.1.4C shows the EA-Indices vs. the 4NQO application period. As was expected, a highly significant relationship is present between the 4NQO application period and the EAI (extension of Wilcoxon rank-sum test; $p < 0.001$). In figure 2.1.4D the approximated areas vs. the EAI is plotted. The EA-Index was originally designed for assessing the severity of the dysplasia and has a maximum score of 45. Invasive squamous cell carcinoma (SCC) was not included in the grading system. We did not exclude SCC from the data analysis since it is an important feature of the model. It was previously observed that the dysplasia induced in this model eventually will lead to invasive SCC. For these reasons we assigned the number 50 for all cases of SCC. The height of this number is arbitrary, however, varying this number between for instance 50 and 100 does not affect the outcome of the analysis since the essence of the test is an analysis of rank-order. The approximated area's under the curve vs. the EAI showed a positive trend (extension of Wilcoxon rank-sum test; $p < 0.05$)

This increase in fluorescence can not be explained by variations in the individual amount of AlPcS₂ administered due to differences in weight. The rats in each group were treated for different periods with a possibility of allowing the longest treatment group (26 weeks) to gain more weight. In figure 2.1.5 the average weight per group is plotted. Initially, the weight increased with prolonged treatment due to ageing, but the body weight of the rats in the group that were treated for 26 weeks was lower than the 20-weeks or 16-weeks group, although it had the highest fluorescence intensities. These rats probably lost weight as a result of their malignancy.

Fluorescence intensities and EAI of biopsies

Images of 4NQO treated rats showed some clear fluorescent hot spots varying in diameter from 1-4 mm (fig. 2.1.6). These spots occurred between 2 and 10 h after injection. No hot spots were seen after this time interval. The maximum level of fluorescence differs per

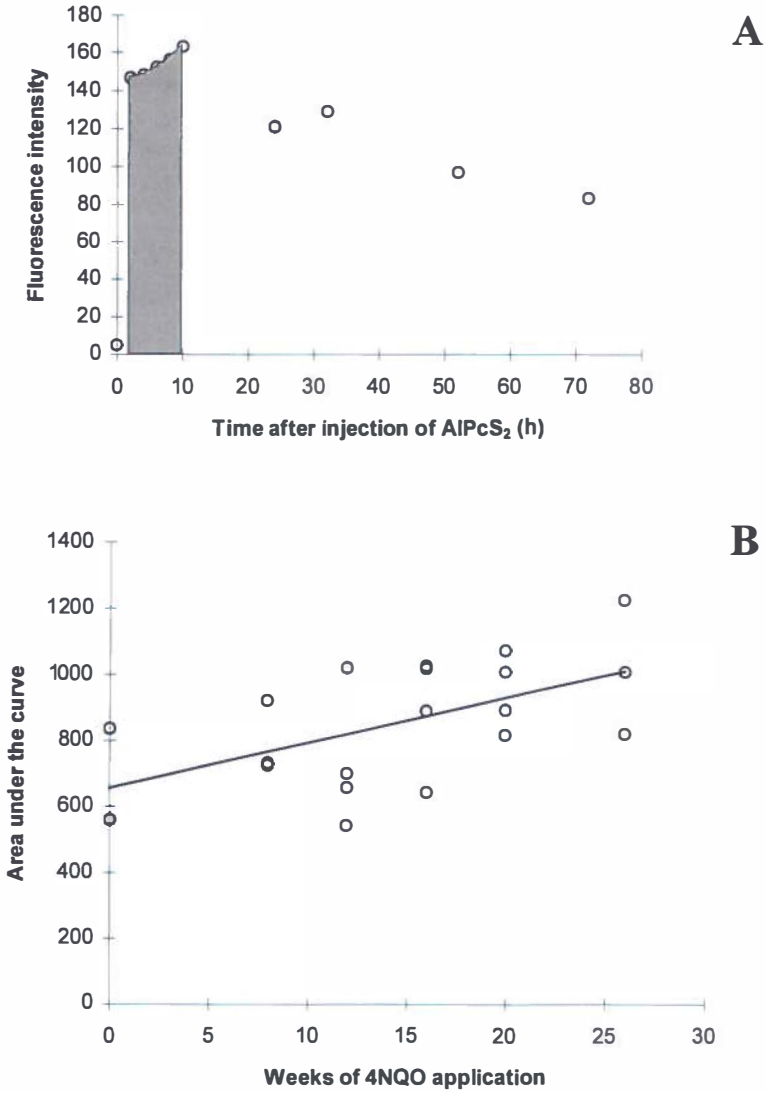


Figure 2.1.4 A: A typical example of the fluorescence intensities plotted vs. the time (h), of one rat. The area under the curve between 2 and 10 h (shaded area) was used for the statistical analysis of fluorescence kinetics since we observed hot spots only in this time segment. **B:** Calculated areas under the curve for each rat are plotted against the weeks of 4NQO-application. There was a significant trend ($p < 0.04$) indicating an increasing fluorescence signal when the application period is longer.

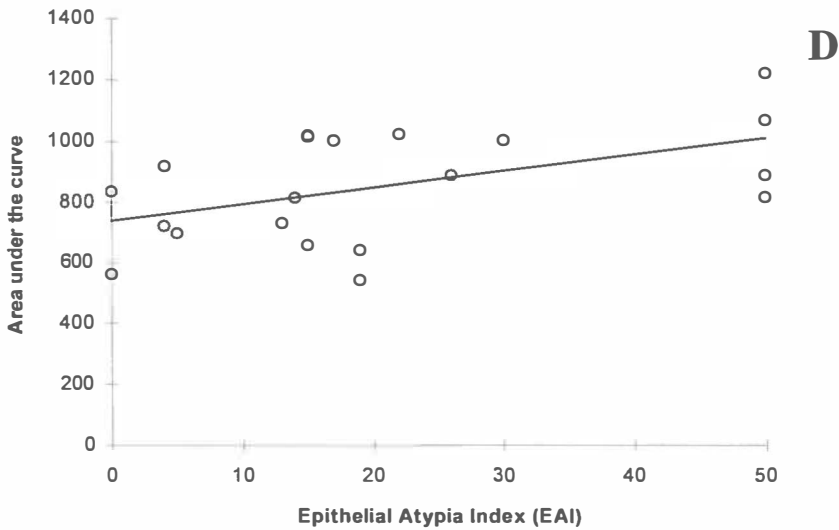
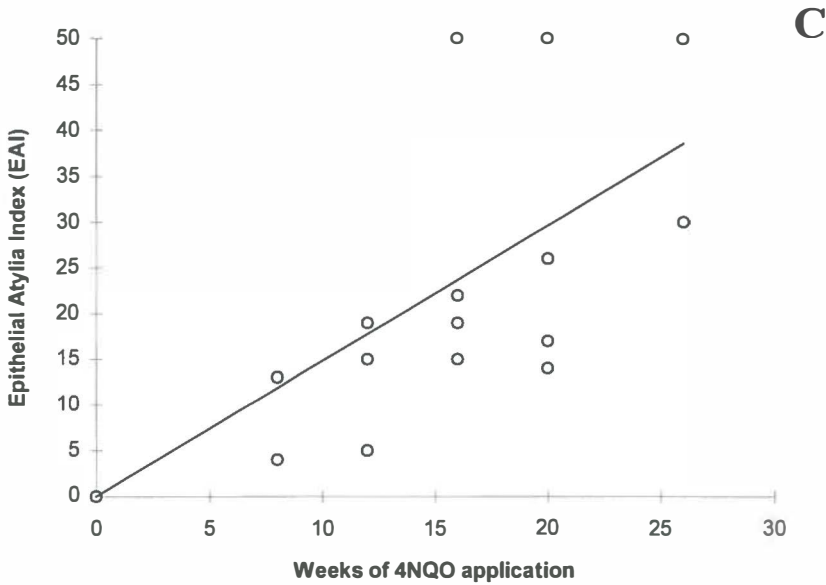


Fig 2.1.4 continued C: The EA-Indices plotted against the weeks of 4NQO application ($p < 0.001$). **D:** The areas under the curve (see B) for each rat plotted against the EAI ($p < 0.05$). We attributed the number 50 to squamous cell carcinoma (SCC). In figures B, C and D the line indicates the trend of the data.

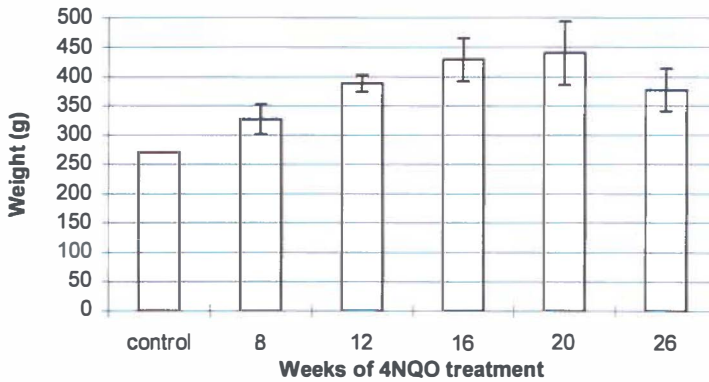


Figure 2.1.5 Average weight of the rats ordered per treatment group. The weight increases slightly due to ageing. However, the 26-weeks treatment group, which were the oldest rats and showed the highest fluorescence intensities, weighed less than the 20-weeks or 16 weeks group.

spot, as well as the time interval between administration of AlPcS₂ and the peak levels. Some hot spots had their maximum at 2 h and some at 4 or 8 h after injection. This did not only occur among different rats but also on the palate of an individual rat. A total of 21 hot spots were seen in the complete group. The grey scale values of the hot spots varied considerably. The average intensity of the hot spots was 35% (s.d. ±22%) higher than the grey scale values of total palatal intermolar area measurements (range 8 to 115%). The intensity of the spot did not reveal information about a possible malignancy. This wide range indicates that the decision about whether something can be considered a fluorescent spot can only be made on visual information, guided by the fluorescence pattern on screen.

Six of the 21 hot spots proved to be invasive squamous cell carcinoma. In another 8 biopsies inflammation was present. In most cases the inflammation was caused by included hairs or dietary fibres and macrophages, lymphocytes and foreign body giant cells were present (fig 2.1.7). Possibly the dysplastic mucosa is easily penetrated by such fibres. In 7 of the fluorescent hot spots no specific alterations were found histologically. The EAI-number did not differ from the EAI-number of the surrounding palatal mucosa in these biopsies. By this biopsy-method a sensitivity of 67% was achieved when squamous cell carcinoma and inflammation are regarded as alterations to the mucosa, but a tumour specificity of only 29%. In 3 rats squamous cell carcinomas were found during histological analysis in areas where no hot spots were seen, resulting in 15% false negatives. The spots which represented squamous cell carcinoma were not always clinically suspect for invasive cancer (fig 2.1.8).

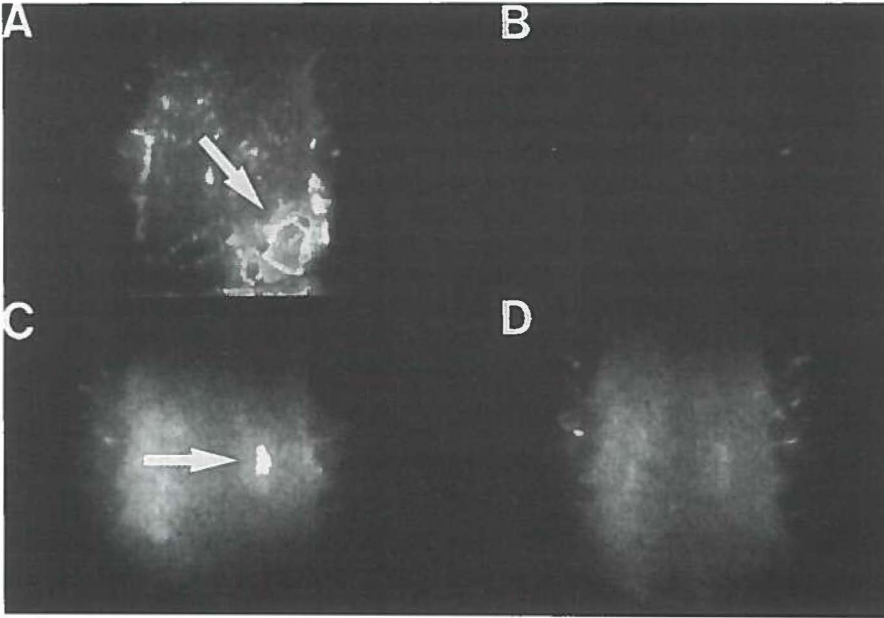


Figure 2.1.6 Fluorescence images of two rat-palates after subtraction of the autofluorescence. **A:** The fluorescence image of a rat (no. 1) treated for 16 weeks with 4NQO recorded at 6 h after injection of AIPcS₂. The indicated spot (arrow) represents a malignancy, and this spot had a true dimension of 4 mm in vivo. **B:** Image of rat no. 1, 24 h after injection. The fluorescent spot has completely disappeared and the image resembled that of a normal rat. **C:** Image of another rat (no. 2) recorded at 4h after injection. The arrow indicates a spot localisation which represented inflammation caused by the inclusion of dietary fibres (true dimension of the spot was 1.5 mm). **D:** Image of rat no. 2, 24 h after injection; no spots are visible.

DISCUSSION

In this study we found that it is possible to localise squamous cell carcinomas induced by 4NQO with AIPcS₂ mediated fluorescence. AIPcS₂ proved to be a sensitive probe for alterations in the mucosa but not very tumour specific, as only 29% of the biopsies was squamous cell carcinoma. However, when the grade of dysplasia increased, the fluorescence intensities of whole palates increased as well. The EA-Index (or the 4NQO application period) increased monotonically with the AIPcS₂-fluorescence. There is an optimum time interval for the detection of hot spots in mucosa between 2 to 10 h after injection. After this interval AIPcS₂-fluorescence could still be detected, up to one week after injection, but did not selectively localise in tumour tissue. The technique of dual wavelength excitation is suitable for fluorescence detection of AIPcS₂. Tumours on the palate induced by 4NQO have a high

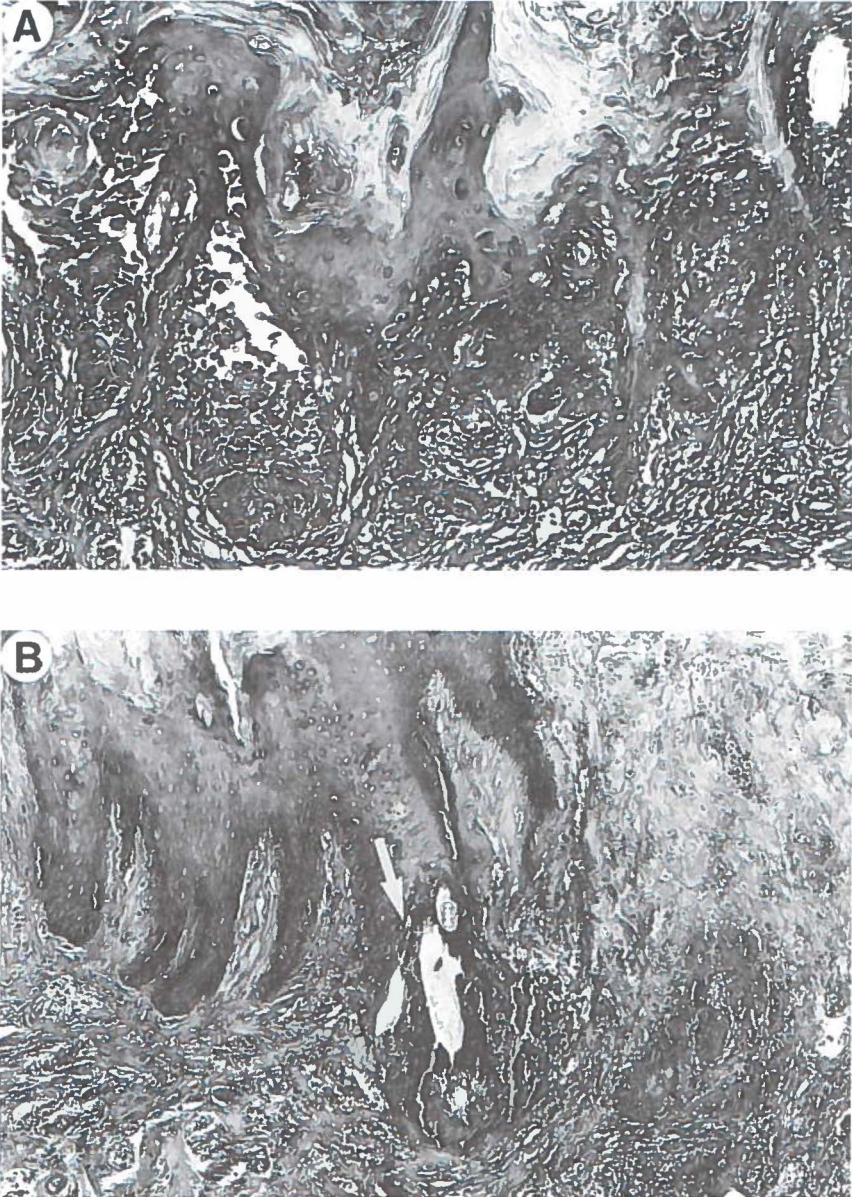


Figure 2.1.7 A: Histological slide of spot of rat no. 1, as shown in figure 2.1.6A. The histology proved severe dysplasia with suspicion of micro-invasive carcinoma. **B:** Histological slide of spot of rat no. 2, as shown in fig. 2.1.6C. The dysplasia was mild, but the included hair (arrow) caused a severe inflammation.

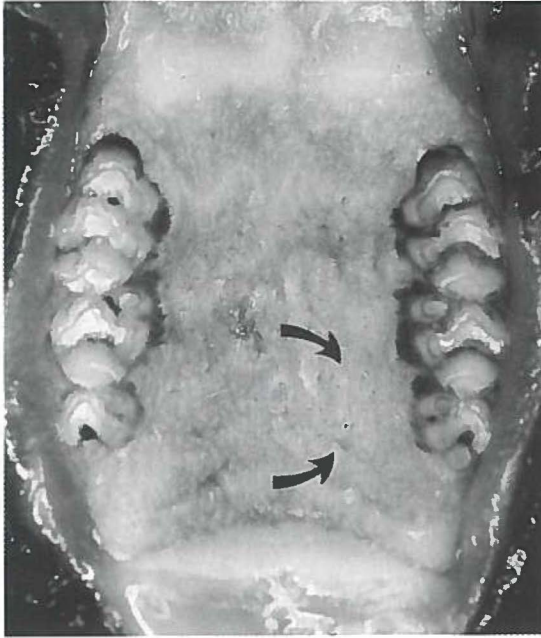


Figure 2.1.8 Photograph from the palate of rat no. 1 (13x). The arrows indicate the area of the hot spot as seen on the fluorescence image in figure 2.1.6, however no clinical signs of squamous cell carcinoma are present.

production of keratin and this creates a high background fluorescence on the image. By choosing the excitation wavelengths properly, it was relatively easy to reduce the (keratin) autofluorescence to an insignificant level. The photochemical properties of phthalocyanines are mainly determined by the macrocycle (Rosenthal *et al.*, 1987). Therefore this technique can be applied independent of the number of sulphonate groups.

The AlPcS₂ fluorescence detected in this experiment is composed of 3 levels: 1) non-specific fluorescence of AlPcS₂ present in the vessels, connective tissue and normal epithelial tissue. 2) AlPcS₂ fluorescence in dysplastic/neoplastic epithelial tissue and 3) small areas with high fluorescence intensities displayed as hot spots on fluorescence images. Regarding the second fluorescence level, a significant relation was found in this experimental set-up between the fluorescence intensities of whole palates and an increasing severity of dysplasia. However, to be able to discriminate between normal tissue and dysplastic tissue by numerical analysis of the fluorescence image in a clinical setting a well calibrated detection system is needed as well as knowledge about the uptake of AlPcS₂ in different types of normal or inflamed tissues.

The results found in the 4NQO-tumour model need to be interpreted differently from xenograft tumour models when measuring tumour to normal tissue ratios, because no clinically visible borders exist between normal tissue, dysplasia and tumour. The 4NQO-treatment will make large areas dysplastic so that an abrupt border of tumour-no tumour will not be present. It was possible to establish the outline of the strong fluorescent spots of the epithelium in the 4NQO model. Remarkable was the variation in time interval for the fluorescence intensities of the hot spots to reach their maximum values. Some spots were present at 2 h and had completely disappeared at 8 h whereas others started to appear at 4-6 h. We found no difference between the grade of dysplasia of the biopsies that showed no invasive carcinomas and that of the adjacent mucosa. We expected a clear correlation between the presence of severe dysplasia or invasive tumour and fluorescent hot spots but most of the positive spots were associated with inflammation of the tissue. No conclusions regarding the nature of the tissue alterations could be drawn from the appearance of the spots on the image. The invasive squamous cell carcinomas and inflammation had no histological similarities except a loss of integrity of the basal membrane. Also the presence of macrophages in case of inflammation has been associated with increasing fluorescence levels (Korbelik *et al.*, 1991). The significantly increased fluorescence levels of the complete palate-measurements, due to increasing dysplasia, and the hot spots may have a different origin. The pathways to the cell are possibly passive diffusion or endocytosis of free phthalocyanine or LDL-receptor mediated uptake of bound phthalocyanine (Ben-Hur *et al.*, 1987a; Ricchelli *et al.*, 1991; Jori, 1993). Which of these is the most prominent or whether other unknown pathways are responsible for sensitizer uptake remains to be established (Hamblin *et al.*, 1994). An increasing turn over rate and the accompanying high lipid metabolism of dysplastic cells possibly leads to a higher phthalocyanine uptake as seen in rats with a higher EAI number. The phenomenon of the spot-fluorescence, which occurred as a result of a high local accumulation of AlPcS₂, in our opinion can be interpreted as follows: hot spots seem to arise as a result of the improved availability of AlPcS₂ to the epithelial cells due to loss of biological barriers like the basal membrane. By (micro) infiltration of tumour cells into the stroma or mechanical destruction and inflammation, the process of the AlPcS₂ uptake can be much more efficient for epithelial cells in areas where the barrier is lost. Likewise a higher uptake of AlPcS₁₋₄ in tumours has been correlated in the presence of greater vessel permeability (Poon *et al.*, 1992; Roberts *et al.*, 1993). Also the insertion of polyvinyl sponges induces a high accumulation of porphyrins in these sponges (Straight *et al.*, 1985). It has often been mentioned that the mechanism for the localisation of sensitizers in tumours is based upon a longer retention-time of a sensitizer in tumour tissue than in normal tissue. Based on the kinetics of the complete palate analysis and the spot localisations seen in this study we conclude that more AlPcS₂ is taken up by tumour

or dysplastic epithelium than by normal epithelium but is also more rapidly cleared from the tumour than from the normal (underlying) tissue. Tumour uptake and clearance of sensitizers probably depends on the type of tumour, the mechanism of tumour induction (autologous or xenograft) and its anatomical location (Chan *et al.*, 1989). Possibly, the results from this study are only accurate for epithelial disorders, and other abnormalities (for instance sarcomas) at the palate may interact differently with AlPcS₂.

An important question is whether an optimum interval determined by fluorescence represents the best time interval for PDT treatment of tumours. The results of this study would suggest a time interval of 4 to 10 h post injection may yield optimal tumour necrosis while sparing the normal tissue as much as possible. However, we expect it to be difficult to induce necrosis solely in tumour tissue because of high normal tissue levels of AlPcS₂. In most studies of PDT effects the time interval for illumination of AlPcS₂ was chosen at 24 h after injection but not all fluorescence kinetic studies show an optimal uptake of sensitizer at that point (van Leengoed, 1993b; Pope *et al.*, 1991; Barr *et al.*, 1991; Peng *et al.*, 1991; Biolo *et al.*, 1991; Chatlani *et al.*, 1991). In fact, the maximum uptake in tumour tissue varies from 1 h to 48 h post injection, probably depending largely on the type of tumour and tumour-host tissues which are being studied.

In conclusion, AlPcS₂ can be used for photodiagnosis of premalignant and malignant disorders in epithelium and a fluorescence optimum can be expected between 2-10 h after injection instead of the earlier reported time interval of 24 h. It would be interesting to study the possible influence of the time interval between injection and illumination on the selectivity of PDT induced tumour necrosis.



2.2 DISTRIBUTION OF ALUMINIUM PHTHALOCYANINE DISULPHONATE IN AN ORAL SQUAMOUS CELL CARCINOMA MODEL. *In vivo* fluorescence imaging compared with *ex vivo* analytical methods

INTRODUCTION

Aluminium phthalocyanine disulphonate (AlPcS₂) is investigated as a probe for the detection of oral squamous cell carcinoma. To date reports on tissue concentrations of sulphonated phthalocyanines as a function of time after injection are inconsistent. In table 2.2.I the results and most important parameters of several published studies are summarised. These results reflect the shortcomings of the generally used methods. *In vivo fluorescence measurements*, using endoscopes or optical fibres, are non-invasive and allow real-time analysis of fluorescence kinetics of photosensitizers. However, the precise location of the fluorescence cannot be established since fluorescence is detected simultaneously from several layers of tissue. *Fluorescence microscopy* reveals the detailed localisation of a photosensitizer in soft tissues but is an invasive method because it requires a biopsy and, as *in vivo* fluorescence, does not provide information on the exact amount of the fluorescent compounds. *Spectrofluorimetric* analysis of tissue extracts is sensitive and quantitative but does not discriminate between compounds with similar spectroscopic properties. Even when the fluorescence excitation wavelength is sharply demarcated and a correction for background fluorescence is performed, it remains a non-specific detection technique when complex biological samples are under study. In addition, the extraction procedure, usually performed with 0.1 M NaOH for AlPcS₂, changes the biochemical matrix of the AlPcS₂. More precise and detailed analysis of the extract is possible with *high-performance liquid chromatography (HPLC)* in combination with *diode laser-induced fluorescence (DioLIF)*. This sensitive technique allows quantitative detection of AlPcS₂ and the separation of its signal from other fluorescent compounds (including other isomers), but requires the same sample handling as used for the spectrofluorimetric technique (Mank *et al.*, 1993).

The results from several studies presented in the literature are not consistent enough to determine for instance the optimal time interval between administration of AlPcS₂ and photodetection of cancer or photodynamic therapy. To investigate whether the differences were caused by using the various techniques we compared the use of *in vivo* endoscopic fluorescence imaging, fluorescence microscopy, conventional spectrofluorimetry and HPLC—Dio-LIF for the detection of AlPcS₂ in experimentally induced oral squamous cell carcinoma. Furthermore, we noted that most fluorescence kinetic studies were performed at doses between 5-20 mg/kg, which is considered a 5- to 10- fold higher dose than generally

Table 2.2.I Overview of literature concerning in vivo/ex vivo detection of AIPcS_n

Author	Sensitizer purity & dose	<i>In vivo</i> excitation/detection	<i>Ex vivo</i> excitation/detection	Tumour model	Time interval of maximal tumour: normal tissue ratio
Tralau <i>et al.</i> , 1987	mixture of AIPcS ₁₋₄ 5mg/kg, i.v.	Not applicable	610 nm exc. 675 nm det. fluorimeter	DMH-induced colon tumour in rats. DOP-induced pancreas tumour in hamsters. Transplanted glioma mice	colon: 48 h, ratio 2,8:1; pancreas: 24-48 h ratio 3:1 glioma: 24 h ratio 28:1
Chan <i>et al.</i> , 1990	AIPcS ₁₋₄ , mix and individual isomers 0.1 ml of 2.27 mM, i.v.	Not applicable	605 nm exc. 673, 675 or 677 nm peak det. fluorimeter	Transplanted colon tumour cells (colo-26) in flank of mice	24-48 h for all, except AIPcS ₁ (no selectivity)
Chatlani <i>et al.</i> , 1990	90% AIPcS ₂ >90% AIPcS ₄ 5mg/kg, i.v.	Not applicable	633 nm exc. 665-700 nm det. for flu-microscopy; 603 nm exc. 673 nm det. fluorimeter	Normal colon rat	mucosa: 1 h (AIPcS ₂) 5 h (AIPcS ₄). High correlation for the methods
Peng <i>et al.</i> , 1990	90% AIPcS ₂ 90% AIPcS ₄ 10mg/kg, i.v.	Not applicable	633 nm exc. >640 nm det. Laser scanning flu.microscopy	Transplanted human melanoma in flank of nude mice	48 h (AIPcS ₂) AIPcS ₄ not present in cells
Peng <i>et al.</i> , 1991b	95% AIPcS ₄ 20mg/kg, i.p	Not applicable	350 nm exc. 550-700 nm det. fluorimeter	Transplanted human melanoma in nude mice in flank	18-24 h tumour: muscle 8-10:10.25-24 h skin: tumour 0.8-1:1
Loh <i>et al.</i> , 1992	90% AIPcS ₂ 5 mg/kg, i.v.	Not applicable	633 nm exc. 665-700 nm det. fluoresc. microscopy	Normal stomach rat	2 h (mucosa)
Poon <i>et al.</i> , 1992	95% AIPcS ₄ 5mg/kg, i.v.	337 nm exc. 300-800 nm det. LIF, fibre	610 nm exc. 675 nm peak-det. fluorimeter	C6BAG- glioma celsuspension in rat-brain	24 h ratio 40:1

COMPARISON OF FLUORESCENCE IMAGING AND EX VIVO ANALYTICAL METHODS

Author	Sensitizer purity & dose	<i>In vivo</i> excitation/ detection	<i>Ex vivo</i> excitation/ detection	Tumour model	Time interval of max. tumour : normal tissue ratio
Chen <i>et al.</i> , 1993	mixture of AIPcS ₁₋₄ 20mg/kg, i.p	633 nm exc. 685 nm peak-det. LIF, fibre	610 nm exc. 685 nm peak det. fluorimeter	Transplanted sarcoma in hind leg of mice	in-vivo: 24 h, 2.4:1; ex vivo: 36 h ratio 4.4:1
Frisoli <i>et al.</i> , 1993	Mixture of AIPcS ₁₋₄ , i.v. 10mg/kg	610 nm exc. 300-800 nm det. LIF, fibre	610 nm exc. 677 nm peak-det. LIF, fibre	DMBA-induced SCC tumour cells inserted in hamster buccal pouch	2 h highest accumulation. 48 h highest selectivity
van Leen-goed <i>et al.</i> , 1993	AIPcS ₁ AIPcS ₂ AIPcS ₄ purity not mentioned all i.v.	610 nm exc. 665 nm det. image analysis	Not applicable	Rat mammary carcinoma in skin fold on back	AIPcS ₁ : no selectivity. AIPcS ₂ : tumour: normal tissue 4:1 (6 h) AIPcS ₄ : tumour: normal tissue 3.8:1, 15-120 min
Peng, <i>et al.</i> , 1995	90% AIPcS ₂ 90% AIPcS ₄ both 10 mg/kg i.p.	Not applicable	350 nm exc. 550-750 nm det fluorimeter. 365 nm exc. >600 nm det. fluorescence microscopy	Transplanted CaD2 mouse mammary carcinoma in C ₃ D ₂ /F ₁ mice (hind foot)	Tumour peak: AIPcS ₂ : 2-24 h AIPcS ₄ : 2 h Maximal ratios AIPcS ₂ : 48 h tumour:muscle 13:1 AIPcS ₄ : 24-120 h tumour: muscle 12:1
Witjes <i>et al.</i> , 1996a	>90% AIPcS ₂ 1 µmol/kg i.v.	Image analysis 610 nm for AIPcS ₂ excitation. Subtraction of 460 nm auto-fluorescence. Det. 675 ± 15 nm	Not applicable	Autologous squamous cell carcinoma induced by 4NQO in rat palatal mucosa	4-10 h localisation in tumour

Abbreviations : i.v. = intravenously; i.p. = intraperitoneally; exc. = excitation wavelength; det. = wavelength band for detection of emission; LIF = laser induced fluorescence; SSC = squamous cell carcinoma; DMH = 1,2-dimethylhydrazine dihydrochloride; DOP = 2,2'-dioxodi-*n*-propyl nitrosamine; 4NQO = 4 nitroquinoline 1-oxide

necessary for treatment (Boyle *et al.*, 1992). These high doses may not yield the same localisation/distribution as lower therapeutic doses. For these reasons we compared the various *in vivo* and *ex vivo* analytical techniques for the detection of AlPcS₂, administered at a dose also suitable for PDT.

MATERIALS & METHODS

Chemicals

AlPcS₂ was purchased from Porphyrin Products Inc. (Logan, UT, USA) and its purity was determined by HPLC. It consisted of mainly one isomer (>90%). The single AlPcS₂-isomer used in the present study was obtained via the direct sulphonation method (Porphyrin Products, personal communication) and an identical compound was analysed by others (Ambroz *et al.*, 1991). This isomer is more hydrophobic than other sulphonated isomers obtained via the condensation method. It has been proposed that the AlPcS₂-isomer with the sulphonate substituents in adjacent position is the most hydrophobic (Ali *et al.*, 1988) and owing to its amphiphilic nature, promotes cell uptake and results in good intra-cellular targeting for photodynamic therapy (Paquette *et al.*, 1992). Before injection the AlPcS₂ was dissolved in 0.1 M NaOH and the pH was adjusted to approximately 7, by addition of an equal amount of 0.1 M HCl and buffering with phosphate buffered saline. For HPLC, water was demineralized using a Milli-Q (Millipore, Bedford, MA, USA) water purification system before use. HPLC-grade methanol was obtained from Baker (Deventer, The Netherlands).

Animals

Tumours were induced with 4-nitroquinoline-1-oxide (4NQO) in the mucosa of the hard palate of the rat. The 4NQO-palate model allows the study of AlPcS₂ uptake in tumour as well as in the surrounding normal tissues of the oral cavity. The palates of 8 week-old male Wistar albino rats were painted 3 times per week for 26 weeks with 4NQO (0.5 % w/v) dissolved in propylene glycol. During this 4NQO-treatment the rats were briefly anaesthetised with a mix of O₂/N₂O (1:3) and 2.5 % Halothane. Following each 4NQO-treatment the rat was deprived of water for approximately 2 h after which it had food and water available *ad libitum*. During the 4NQO-treatment period the rats were kept under standard housing conditions. Twenty-four 4NQO-treated male Wistar albino rats and 28 untreated rats were divided in groups of 4 rats. One group of 4 treated and one of 4 untreated rats was sacrificed before injection (controls) and 2, 4, 8, 24, 48 h after injection with AlPcS₂ respectively. The seventh group of 4 untreated rats was sacrificed 168 h after injection. All rats except the control group received 1.5 µmol/kg AlPcS₂, which is

considered to be a realistic therapeutical dose (Boyle *et al.*, 1992), administered by a single tail vein injection.

In vivo fluorescence

The *in vivo* fluorescence imaging system consisted of a the same system as was described figure 2.1.1 (chapter 2.1). Fluorescence images, excited by 460 nm (autofluorescence) and 610 nm (AIPcS₂ - fluorescence), of the palates were recorded before (0 h) and 2, 4, 8, 24 and 48 h after injection of AIPcS₂, as well as 168 h for the extra group of 4 untreated rats. The subtracted images (=‘610-460’ images) were analysed for grey-scale levels of fluorescence, for the total palatal area between the molars of normal and 4NQO-treated rats. Strongly fluorescent spots (hot spots) in 4NQO-treated rats, indicating high local AIPcS₂ concentrations, were measured separately. At each of the above mentioned time points 4 normal and 4 4NQO-treated rats were sacrificed immediately after the last image was recorded. Punch biopsies were taken from 4NQO-treated mucosa in areas of hot spots. These biopsies were either submitted to HPLC analysis or to fluorescence microscopy. The hard palate was denuded and the mucosa as well as other samples collected from the tongue, palatal bone, molars, lacrimal gland, skin, liver, spleen, kidney and serum were snap frozen in liquid nitrogen and stored at -80°C. For each organ, care was taken to collect the samples from the same anatomical region.

Fluorescence microscopy

The excitation wavelengths and the image-recording system used for fluorescence microscopy were the same as described for the *in vivo* fluorescence study (460 nm autofluorescence, 610 AIPcS₂ fluorescence, chapter 2.1). The light source was connected to a microscope (Orthoplan, Leitz, Germany) and the samples were examined at a 40x magnification. The AIPcS₂ emission band was selected by a 665 nm high pass filter. The charge couple device (CCD) camera with image-intensifier was mounted on the camera port of the microscope.

Alternating frozen sections of 10 µm and 30 µm were cut from the palatal mucosa of the 4NQO-treated and untreated rats and from the biopsies. The 10 µm sections were H&E stained and used for histological analysis and the 30 µm sections were used for fluorescence microscopy. The fluorescence intensities of the epithelial layer and the connective tissue of the subtracted palatal mucosa images were measured at five spots and averaged.

Conventional fluorimetry and HPLC-Dio-LIF

For analysis of the tissues the thawed samples were digested overnight with 0.1 M NaOH

(ratio 0.1 g wet tissue/10 ml NaOH) at room temperature. The samples were disrupted using an ultrasonic cell-disrupter (Branson, Danbury CT, USA), centrifuged at 25000 rpm (5000 g) for 15 minutes and the supernatant was filtered through a 0.2 mm FP030/30 filter (Schleicher & Schuell, Dassel, Germany).

The clear solutions were then examined with conventional fluorimetry using a LS-50 spectrofluorimeter (Perkin-Elmer, Norwalk CO, USA) equipped with a R928 photomultiplier (PMT) (Hamamatsu Photonics, Hamamatsu City, Japan). Fluorescence was excited at 610 nm (10 nm slitwidth) and emission was collected between 625 and 725 nm (5 nm slitwidth) at a scanspeed of 100 nm/min. It should be noted that at least 1 ml of the sample was necessary for this technique, corresponding to 10 mg of the original tissue. Figure 2.2.1 shows the method used to determine the amount of AlPcS₂ present in the extract from the collected spectra.

The filtered solutions used for conventional fluorimetry were further analysed by high performance liquid chromatography (HPLC) with diode-laser induced fluorescence (Dio-LIF). The technique of HPLC-Dio-LIF has been described elsewhere (Mank *et al.*, 1993). In brief, excitation light was provided by a 10 mW 670 nm diode laser (Toshiba TOLD 9215(S), Tokyo, Japan). Fluorescence was collected perpendicular to the excitation beam using a quartz fibre (600 mm core diameter, Quartz & Silice, Uithoorn, The Netherlands) inserted in a home-made quartz flow cell. The AlPcS₂ fluorescence was selected by a LS-

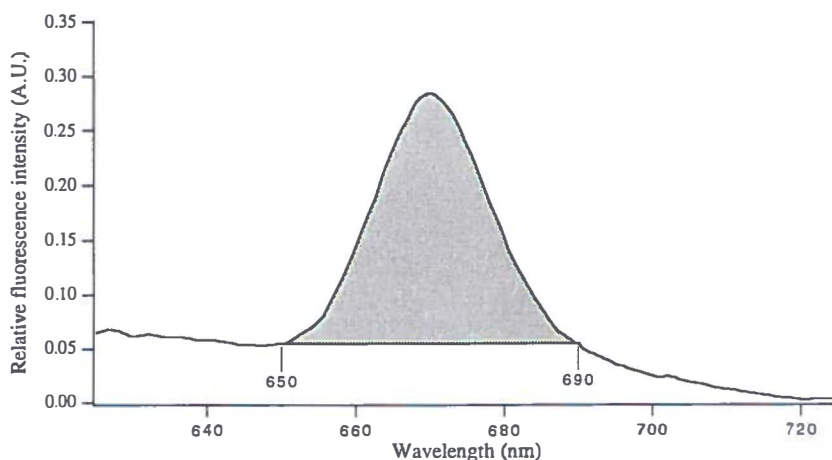


Figure 2.2.1 Presentation of the integration method for detection of AlPcS₂ by conventional fluorimetry. A baseline is drawn between 650 nm and 690 nm to remove as much of the background signal as possible, after which the area above this line is calculated. We expect this method to be more reliable than peak measurements at a single wavelength.

750 0.5" shortpass filter (Corion, Holliston, MA, USA) and two RG695 3 mm Schott filters. The collected fluorescence was focused by a 2.5 cm *f*/1 lens onto a -20°C cooled Model C-31034 GaAs PMT (RCA, Lancaster, UK). A SR400 photoncounter (Stanford Research Systems, Sunnyvale, CA, USA) with a time constant of 1 s and a threshold of -10 mV was used for signal processing. Data were recorded on a Personal Computer with a home-made program.

RESULTS

In vivo fluorescence

The autofluorescence of 4NQO-treated rats was approximately 1.5x higher than that of normal rats. For all rats the autofluorescence was effectively reduced by the subtraction technique (see Materials & Methods) to less than 10 % of the original value. Furthermore, before subtraction the AlPcS₂-induced fluorescence was at least 3-4 times higher than the autofluorescence. Examples of images obtained during the *in-vivo* fluorescence experiments are shown in figure 2.2.2. Between 2-8 h after injection strong fluorescent spots (hot spots) were seen which had disappeared 24 h after injection. This phenomenon was also observed in previous experiments (Witjes *et al.*, 1996a, chapter 2.1). Histological evaluation then revealed that the hot spots were associated with squamous cell carcinoma, severe inflammation or were of unknown aetiology (number ratio = 1:1:1). In the present paper, the hot spots were further analysed for AlPcS₂-content by fluorescence microscopy or HPLC-Dio-LIF.

Figure 2.2.3 displays the data obtained from the *in vivo* fluorescence images. The 4NQO-treated palatal mucosa contained more AlPcS₂ than palatal musosa of untreated rats ($p < 0.001$). This statistical analysis was performed using the non-paired Student T-test, comparing single identical interval-combinations of 2-2,4-4,8-8, 24-24 and 48-48 h between normal and 4NQO- treated rats. This test is allowed for comparison of single intervals only and does not need further correction. Figure 2.2.5 furthermore shows a substantial decrease of fluorescence between 8 and 24 h for normal as well as 4NQO-treated rats. Statistical analysis using the Student T-test between the fluorescence levels of 8 and 24 h showed that this decrease was significant between the time intervals in both groups ($p < 0.01$). This indicates a maximum fluorescence from the palatal mucosa around 8 h after injection of AlPcS₂.

A total of 40 hot spots was observed in the palates of 18 4NQO-treated rats. The grey-scale levels of these hot spots were on average 140% (range 110%-200%) of the mean grey-scale level of the total measured palatal area of the 4NQO-treated rats. The grey-scale levels of the hot spots were significantly higher than the grey-scale levels of the surrounding area

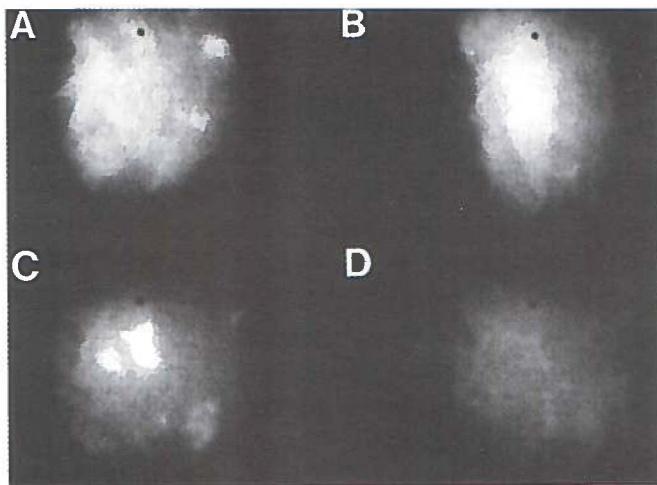


Figure 2.2.2 Four digitised *in vivo* fluorescence images of three 4NQO-treated rats. **A:** Image of rat (no. 1) shows a large area of highly fluorescent palatal mucosa 2 h after injection of 1.5 $\mu\text{mol/kg}$ AIPcS₂. **B:** Image of rat (no. 2) shows large triangle shaped fluorescent area 4 h after injection. **C:** Image of rat (no. 3) shows a hot spot of AIPcS₂-fluorescence at 8 h. **D:** Image of same rat as in C (no. 3). The hot spot completely disappeared 24 h after injection of AIPcS₂.

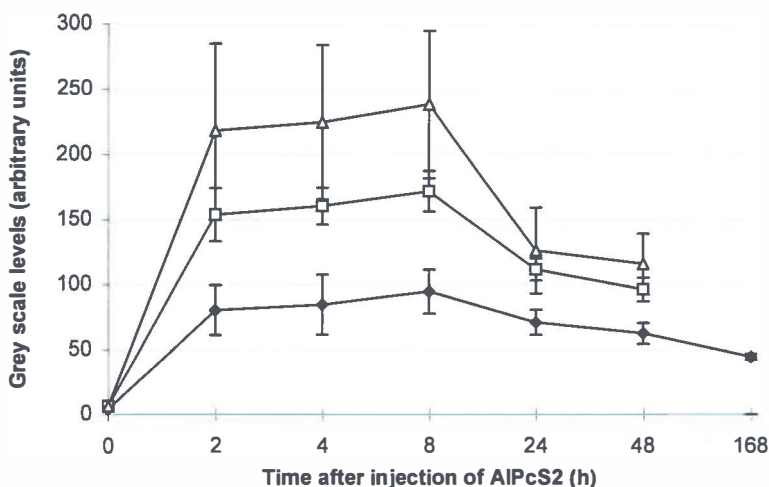


Figure 2.2.3 Results of *in vivo* fluorescence measurements. Grey-scale levels of the total palate measurements of normal (n=24, \blacklozenge), 4NQO-treated (n=20, \square) rats as well as the measurements of the hot spots (n=40, \triangle) in 4NQO-treated palatal mucosa. At every time point 4 rats were sacrificed until 4 were left at the last measurements. Error bars represent standard deviation.

of the same palate between 2-8 h after injection (p -value $p \ll 0.001$; paired Student T-test). At 24 h the fluorescence in areas where the spots were seen on the images was still significantly higher than the mean fluorescence of the total measured area ($p=0.007$). However, at this time interval it was not possible for the observers to locate the spot on the image. At 48 h there was no significant difference between the fluorescence of the spots and the mean of the total palatal area.

Fluorescence microscopy

Biopsies were taken from the mucosa in the areas at which hot spots were seen on the fluorescence image of the 4NQO-treated palates. A total of 35 biopsies were taken from the total of 40 spots. Five spots were too small to take a biopsy. From the 35 biopsies, 15 were used for fluorescence microscopy and 20 for conventional fluorimetry /HPLC-Dio-LIF measurements. The 4NQO-treated tissues remaining after the biopsies were taken, were also analysed and are referred to as "hot spotless 4NQO-treated tissues".

Figure 2.2.4A shows that the fluorescence intensities and kinetics in epithelium were identical for normal and hot spotless 4NQO-treated tissues. The fluorescence intensities of the epithelium in biopsies seemed higher than of normal epithelium, but this could not be confirmed by statistical analysis. Figure 2.2.4B shows the fluorescence levels in the connective tissues. In normal and hot spotless 4NQO-treated tissues, maximal fluorescence was detected at 2 and 4 h respectively. The connective tissue fluorescence of the biopsies showed a different kinetic pattern and was significantly different of the values of the normal connective tissue ($p < 0.04$).

Figure 2.2.5 shows examples of fluorescence microscopy images. The distinction between the connective tissue and the epithelial layer can easily be made. In normal tissues the fluorescence in the epithelial layer was always less than in the connective tissues. In biopsies, the fluorescence levels of the epithelial layer sometimes equalled the levels of the connective tissue between 2-8 h after injection. However, this was not seen 24 or 48 h after injection. In some of these biopsies the connective tissue fluorescence was remarkably high, even at 24 and 48 h after injection. Here, AlPcS₂ was retained in the connective tissue of the biopsies much longer than in the connective tissue layers of normal or hot spotless 4NQO-treated tissues. The difference between normal connective tissue fluorescence and biopsy-connective tissue levels was statistically significant at 4-48 h after injection ($p < 0.04$, Student T-Test, testing only between single identical intervals). Histological analysis showed that 4 out of 15 of the biopsies submitted for microscopy contained invasive squamous cell carcinoma (figure 2.2.6). This number is in agreement with the results found in a previous study (Witjes *et al.*, 1996a, chapter 2.1).

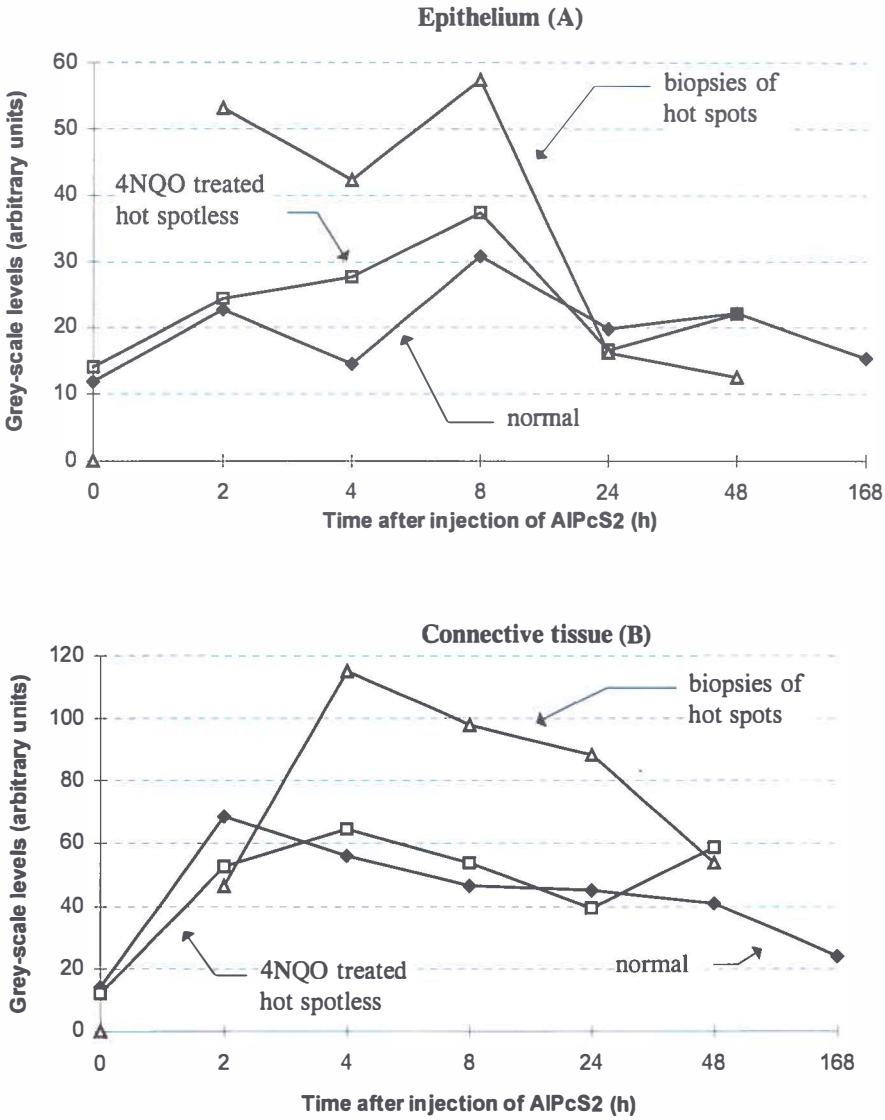


Figure 2.2.4 Grey-scale levels of microscopic fluorescence measurements of the normal and 4NQO treated epithelial layer (A) and that of the connective tissue layer (B). Symbols represent normal untreated palatal mucosa (◆), spotless 4NQO-treated mucosa (□) and mucosa of biopsies taken in areas of hot spots (Δ). N=4 for each data point of normal and 4NQO-treated mucosa. Differences were not significant, standard deviation are not depicted due to the large error bars.

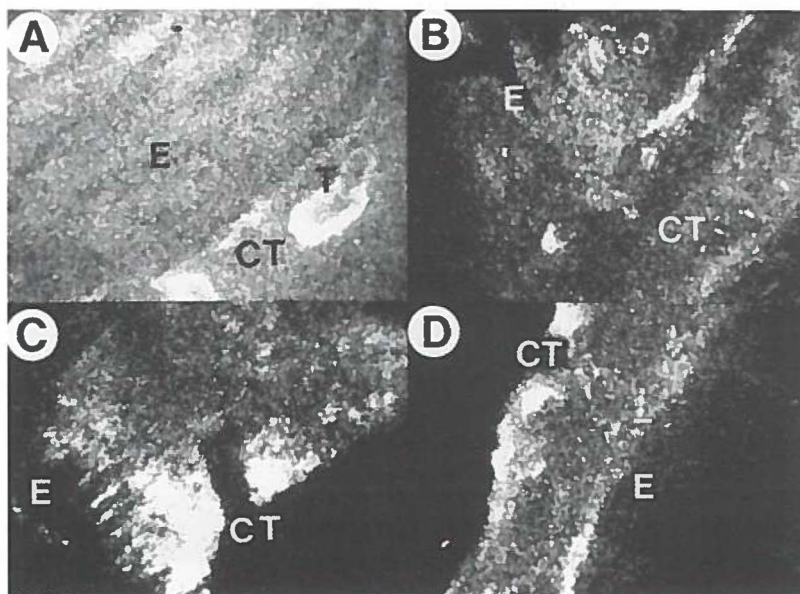


Figure 2.2.5 Digitised microscopic fluorescence images of 4 frozen sections of 4NQO-treated palatal mucosa of the same 3 rats presented in figure 2.2.2. Images excited with 610 nm and 460 nm were subtracted so that AlPcS₂ fluorescence is shown. **A:** Fluorescence image of a histological slide of rat no. 1 shows similar intensities of grey-scale levels from the epithelial layer (E) and the connective tissue (CT). Isles of invasive tumour (T) show even higher fluorescence. **B:** Fluorescence image of a histological slide of rat no.2 shows a highly fluorescent epithelial layer (E) of which the intensity equals that of the connective tissue (CT). **C&D:** At 48 h after injection the images of histological slides of rat no. 3 show that the epithelial layer (E) emits no fluorescence anymore while the connective tissue (CT) shows highly fluorescent areas.

Conventional fluorimetry and HPLC-Dio-LIF - Comparison of the methods

The extraction repeatability was determined for plasma samples with 5×10^{-8} M AlPcS₂ added (spiked samples). The relative standard deviation (R.S.D.) was 1.6 % (n=5). A detection limit (S/N = 3) of 2.5×10^{-9} M AlPcS₂ was observed for skin and spleen samples. Calibration graphs for spiked extracts from these samples showed good linearity between 2.5×10^{-9} M and 1×10^{-5} M, which can be described by formula 1:

$$Y = 3.56 \times 10^7 (\pm 0.05) X + 0.05 (\pm 0.06) \quad (R^2 = 0.998) \quad (1)$$

X and Y are the concentration in mol/l and fluorescence intensity in arbitrary units (A.U.),

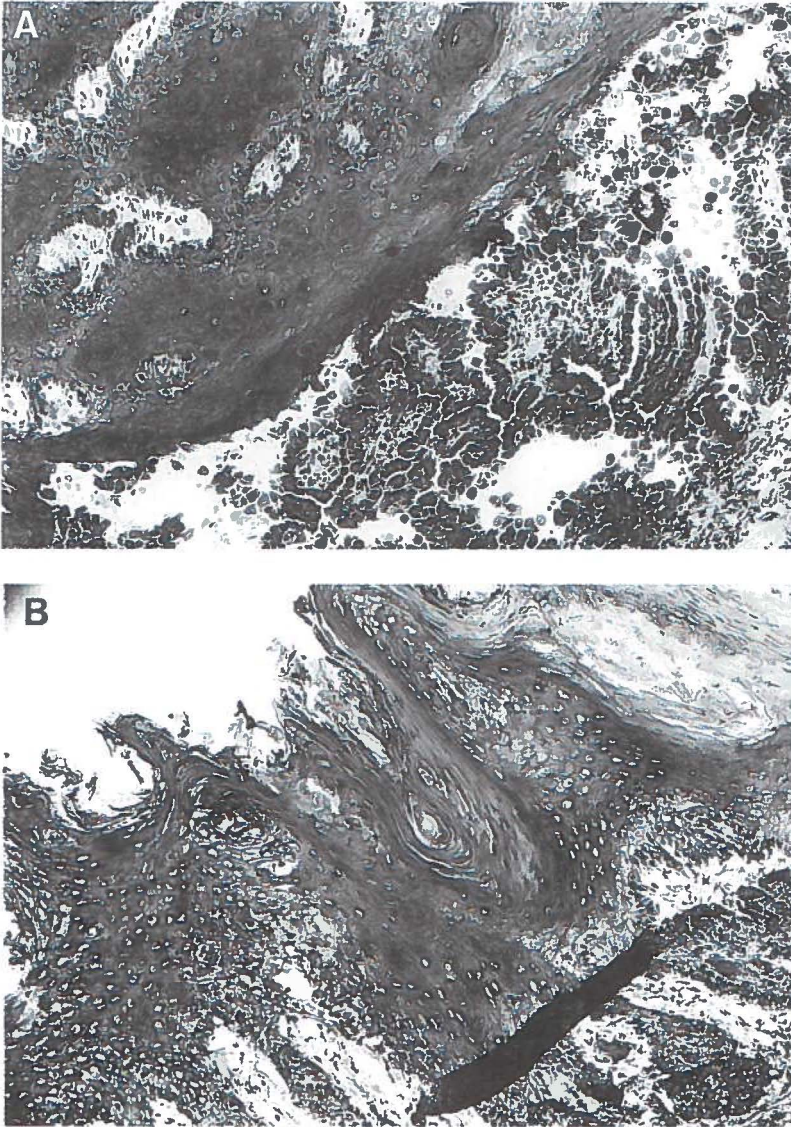


Figure 2.2.6 Photomicrographs of the stained sections corresponding to the images shown in figure 2.2.5A-D. **A:** The histological slide of rat no. 1 (40x) shows invasive squamous cell carcinoma. **B:** However the histological slide of rat no. 2 (40x) shows no histological signs of cancer although the *in vivo* endoscopic image showed a clear hot spot (fig. 2.2.2B) and its microscopy image shows a strong fluorescent epithelial layer (fig. 2.2.5B).



Figure 2.2.6 continued C: The histological slide of the biopsy taken from rat no. 3 (25x) also shows no signs of tumour or inflammation, although the endoscopic image shows a strong fluorescent hot spot (fig 2.2.2C)

respectively. For calibration eleven data points were measured in triplicate. The calibration graphs for other spiked tissues showed the same slope, but a different intercept due to the differences in background fluorescence.

The palatal mucosa and the lacrimal gland samples are shown as typical examples. Figure 2.2.7A shows the emission spectra of the mucosa samples. It is clear from these spectra that the detection limit is determined by the sensitivity of the LS-50 and only partially by fluctuations in the fluorescence background. However, from figure 2.2.9B, which shows the data for the lacrimal gland samples, the presence of AlPcS₂ can be suspected but quantitation is not possible due to the presence of interfering, naturally occurring compounds. In the lacrimal gland some of these are known to be porphyrins (Spike *et al.*, 1990). As a result detection levels in these samples were limited by differences in background for the various rats.

To examine the possibilities of the combination of HPLC-Dio-LIF, spiked samples from healthy rats were examined first. Measurements of spiked blank skin and spleen extracts, containing 5×10^{-9} M AlPcS₂ were used to establish the repeatability of measurements. The R.S.D. was 1.9 % for both types of extract (n=5), while the error of measurement was less

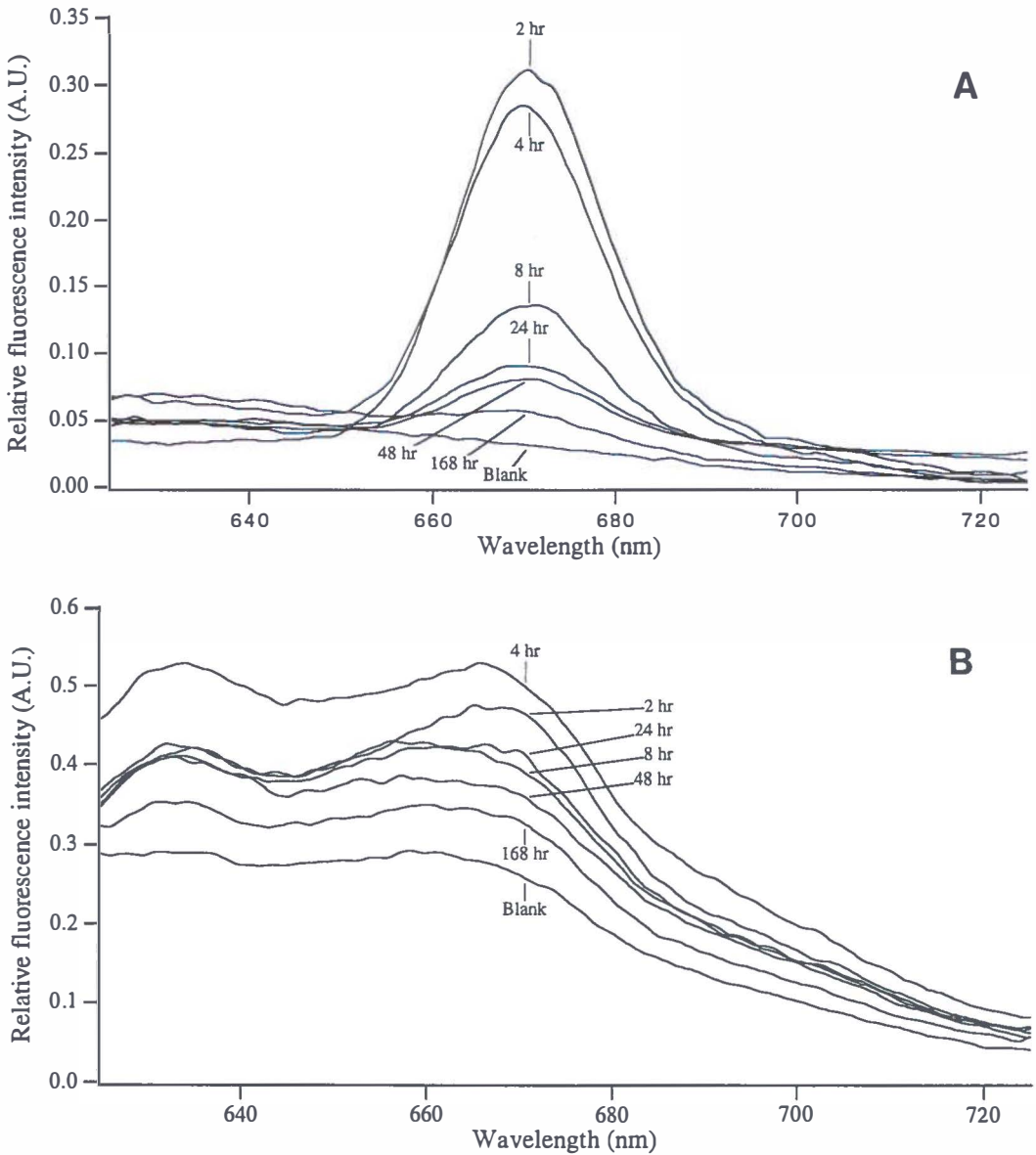


Figure 2.2.7 Fluorescence emission curves of AlPcS₂ obtained by conventional fluorimetry (excitation at 610 nm). **A:** Normal, untreated palatal mucosa samples. **B:** Lacrimal gland samples of normal rats. In mucosa AlPcS₂-mediated fluorescence is clearly detectable and quantifiable. However, the lacrimal gland samples show large background fluctuations which makes quantification impossible.

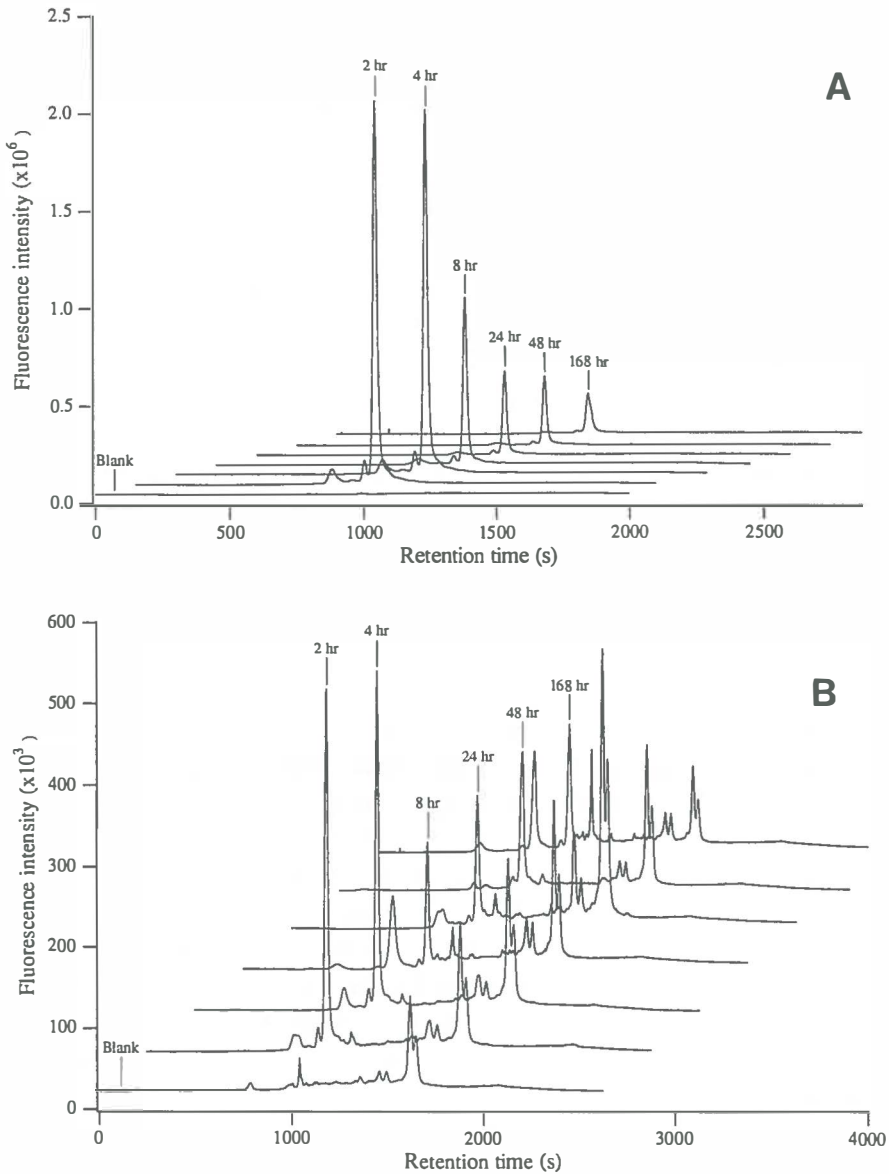


Figure 2.2.8 Chromatogram obtained by HPLC-Dio-LIF (excited with 670 nm). **A:** Normal, untreated palatal mucosa sample. **B:** Lacrimal gland of untreated rat. Relative to the lacrimal gland samples, the palatal mucosa samples show few interfering matrix components. The detection of the distinctive AIPcS₂-peak allows reliable quantification of the lacrimal gland samples.

than 5%. The detection limit was 3.0×10^{-12} M AlPcS₂ (S/N=3), determined by shot noise on the Raman-scatter related background signal. Calibration graphs for spiked extracts from skin and spleen samples showed good linearity between 3.0×10^{-12} and 1×10^{-7} M, as described in formula 2 :

$$Y = 2.5(\pm 0.1) \times 10^{14} X + 3.8(\pm 0.2) \times 10^3 \quad (R^2 = 0.999) \quad (2)$$

X and Y are the concentration in mol/l and response intensity in counted photons, respectively. For this calibration curve ten points were measured in triplicate. As a result of the selectivity added by the HPLC the background fluorescence is constant. Therefore the intercept is stable and the calibration graph is representative for all tissue extracts.

Because the AlPcS₂ contained more than 90 % of one single isomer, the advantage that this technique can distinguish between photosensitizer isomers was not used (Mank *et al.*, 1993). However, the possibility it offers to separate the AlPcS₂ signal from that of naturally occurring compounds with similar spectroscopic properties is advantageous in complex biological matrices. In figure 2.2.8A the chromatograms are shown for the same palatal mucosa samples as used in figure 2.2.7A. Clearly the detection limit with HPLC-Dio-LIF was significantly lower than that of conventional fluorimetry, even after the additional 4-fold dilution. It should be noted that only 25 ml was needed for the chromatograms and in fact, tissue samples of 1 mg containing only 1 fmol AlPcS₂ can be analysed. The chromatograms of the lacrimal gland samples, displayed in figure 2.2.8B, give more information than the corresponding emission spectra in figure 2.2.7B. Obviously, the enhanced specificity of HPLC-Dio-LIF was an advantage for these samples. This is especially clear if the AlPcS₂ concentrations determined for the rats are compared individually. Figure 2.2.10 shows the average values and standard deviations for sample extracts obtained at different times after injection with AlPcS₂ as determined with HPLC-Dio-LIF. From these data it can be concluded that the variations in results between the two *in-vitro* methods were only present in the concentration of the naturally occurring compounds and not in that of the AlPcS₂. In addition to the extracts of the lacrimal glands, those obtained from the serum, bone, kidney and the mucosa were also examined with HPLC-Dio-LIF. The results are shown in figure 2.2.10. In all cases, smaller R.S.D. values were obtained compared to the LS-50 data indicating the higher reliability of the HPLC-Dio-LIF method for biological samples.

Conventional fluorimetry and HPLC-Dio-LIF - Results of tissue measurements

The normal untreated palates had peak levels of AlPcS₂ 2 h after injection and the concentration of AlPcS₂ declined to half of the maximum value 8 h post injection as was determined with both conventional fluorimetry and HPLC-Dio-LIF (figures 2.2.9A & 2.2.10A). The kinetics of AlPcS₂ in normal palatal tissue was the same for both methods. In contrast, samples from the *same* 4NQO-treated palatal mucosa extracts showed different AlPcS₂ kinetics when analysed by conventional fluorimetry or HPLC-Dio-LIF. Conventional fluorimetry (figure 2.2.9A) indicates a significant difference between normal and 4NQO-treated palates already occurring at 2 h post injection (p<0.01, Student t-Test, comparing single identical intervals only). According to HPLC-Dio-LIF data the 4NQO-treated mucosa initially did not have a higher AlPcS₂ concentration. But in the course of time (8-48 h), 4NQO-treated mucosa retained more AlPcS₂ compared to normal palatal tissue (p<0.001 Student t-Test, comparing single identical intervals only). Therefore, completely different ratios between normal and 4NQO-treated palates were obtained with both *in vitro* methods (table 2.2.II). The concentration of AlPcS₂ present in the biopsies could only be measured by HPLC-Dio-LIF because of the small quantities of tissue available (1.5-5 mg). Remarkably the concentration of AlPcS₂ in these biopsies remained constant from 2-48 h and the point of the highest difference with normal tissues was at 48 h (figure 2.2.10A).

Table 2.2.II Ratios of fluorescence signals from normal and 4NQO-treated palatal tissue ordered per detection technique.

Time after AlPcS ₂ injection (h)	In-vivo Fluorescence	Fluorescence epithelium	Microscopy connective tissue	Conventional Fluorimetry	HPLC- Dio-LIF
	N : T : S	N : T : B	N : T : B	N : T	N : T : B
0	1.0: 1.5 : 1.5	1.0: 1.2: n.a.	1.2: 1.2: n.a.	1.0: 0.8	1.0: 0.8: n.a.
2	25 : 48 : 68	1.9: 2.1: 4.5	5.8: 4.5: 3.9	59 : 110	69 : 78 : 80
4	26 : 50 : 70	1.2: 2.3: 3.6	4.7: 5.5: 9.7	47 : 97	53 : 78 : 85
8	29 : 53 : 74	2.6: 3.2: 4.9	3.9: 4.6: 8.3	47 : 104	31 : 54 : 106
24	22 : 35 : 39	1.7: 1.4: 1.4	3.8: 3.3: 7.5	27 : 88	26 : 41 : 88
48	19 : 30 : 36	1.9: 1.9: 1.1	3.5: 5.0: 4.6	23 : 59	20 : 34 : 99

For all techniques the ratios were calculated relative to the value of its normal tissue (N) at 0 h, which was therefore set to 1.0. The connective tissue ratios were calculated relative to the normal tissue value of epithelium at 0 h. The results with the highest normal to tumour ratio are printed boldly. Abbreviations: N = Normal untreated palate; T = hot spotless 4NQO-treated palate; S = hot spot detected by *in-vivo* fluorescence; B = biopsy of hot spot; n.a. = not applicable

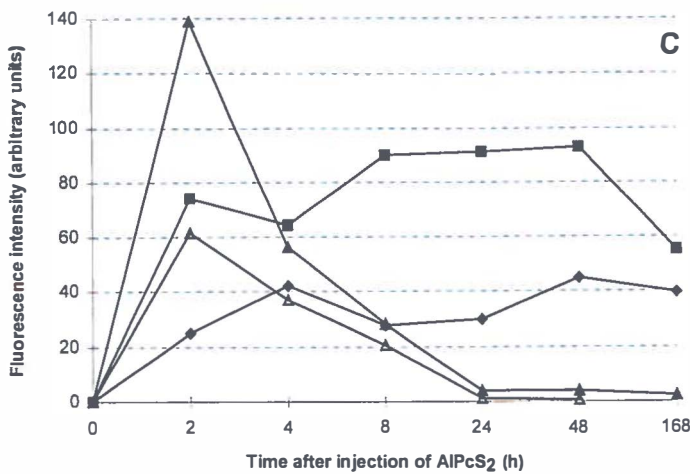
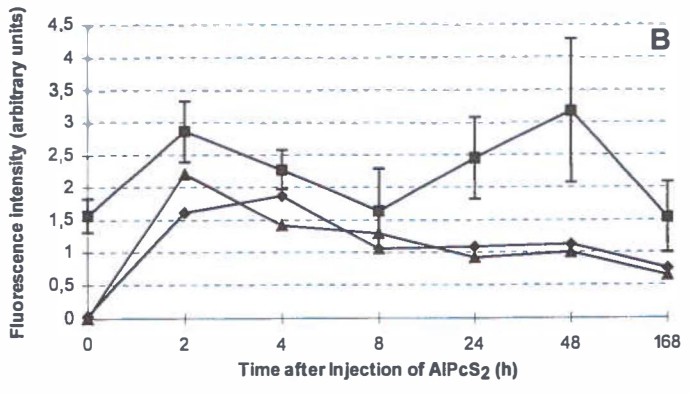
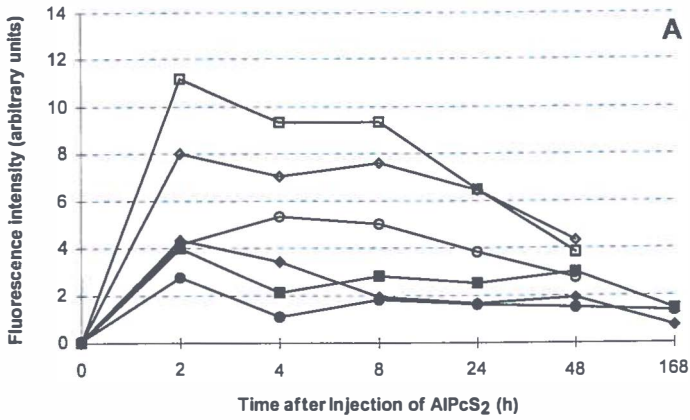


Figure 2.2.9 (previous page) Results conventional fluorimetry. Filled symbols represent measurements on samples from normal rats and open symbols represent data of 4NQO-treated rats (n=4 for each data point). The arbitrary units of figure A, B and C are directly comparable. **A:** AlPcS₂ measurements of normal (◆) and of 4NQO-treated (◊) palatal mucosa, of kidneys of normal (■) and of 4NQO-treated (□) rats and of skin of normal (●) and of 4NQO-treated (○) rats. Not only were higher signals seen for all tissues of 4NQO-treated rats compared to normal rats but also different AlPcS₂ kinetics between normal and 4NQO-treated rats. **B:** AlPcS₂ measurements of samples of molars (◆), tongue (▲) and lacrimal gland (■) of normal rats. Especially the lacrimal gland samples show large variations and error bars are depicted only for these samples (compare with figure 2.2.9B). **C:** AlPcS₂ measurements of samples of spleen (◆), liver (■) and serum (▲) of normal rats and serum of 4NQO-treated rats (Δ). For sake of clarity error bars, representing the standard deviation, were not always depicted. The differences between normal and 4NQO-treated tissues were significant for all tissues in figures A and C.

Samples from skin and kidney measured by conventional fluorimetry showed significantly higher AlPcS₂ concentrations for 4NQO treated rats ($p < 0.001$ for both, Student T-Test comparing single identical intervals only), although the blanks (0h) were similar (figure 2.2.9A). Conventional fluorimetry indicated large variations in the concentration of AlPcS₂ in serum from normal rats (figure 2.2.9C), while no differences in serum concentrations between 4NQO-treated and untreated rats were detected by HPLC-Dio-LIF (figure 2.2.10C).

DISCUSSION

In this study, 4 methods were used for the detection of phthalocyanines in the 4NQO-treated tissues. The techniques indicated different time intervals from injection for a maximal tumour concentration of AlPcS₂. The *in vivo* fluorescence measurements showed a significantly higher AlPcS₂ concentration in 4NQO-treated tissues than in normal tissue between 2-8 h after injection. Fluorescence microscopy also indicated that AlPcS₂ is mainly present in epithelium between 2-8 h after injection. Conventional fluorimetry showed a significantly higher AlPcS₂ concentration in 4NQO-treated tissue between 2-48 h and HPLC-Dio-LIF between 4-24 h. Remarkably, the AlPcS₂ concentration in the hot spots (biopsies) assessed by HPLC-Dio-LIF was constant for all time intervals and differed highly from normal tissues at 48 h after injection. The implications of using these techniques for photodetection will be discussed below.

In vivo fluorescence and fluorescence microscopy

The induction of squamous cell carcinoma with 4NQO is accompanied by a high keratin production (Nauta *et al.*, 1995) which is known to be a highly fluorescent material. Fluorescence from the keratin lining was visible on the fluorescence microscopy images and

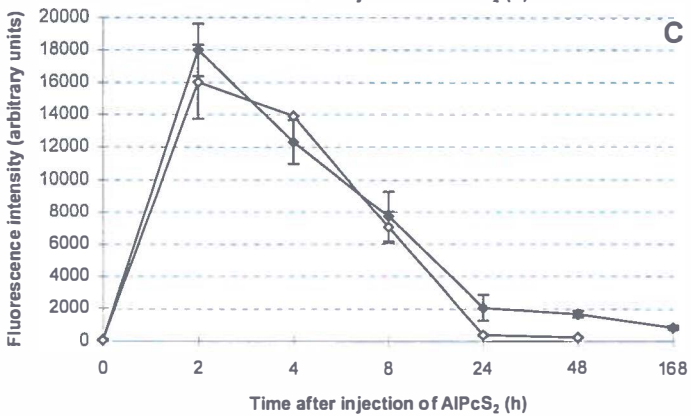
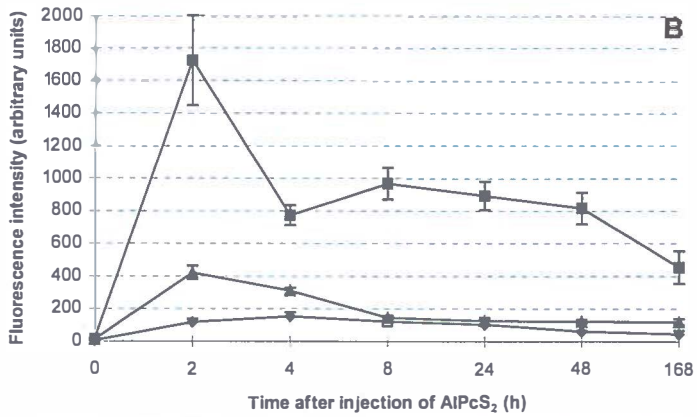
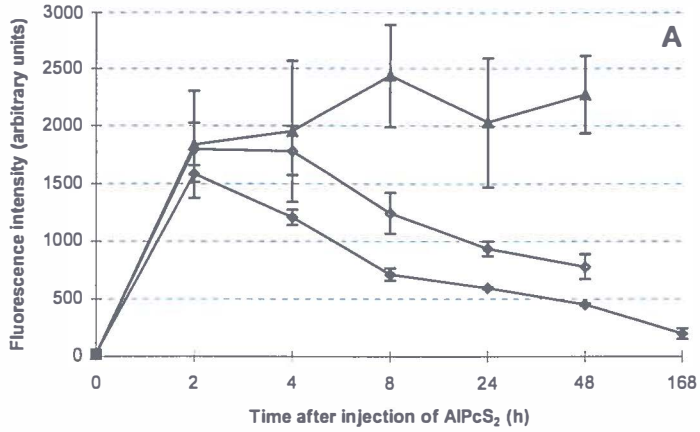


Figure 2.2.10 (previous page) HPLC-Dio-LIF measurements of AlPcS₂ in several tissue samples (n=4 for each data point). The arbitrary units of figures A, B and C are directly comparable. **A:** AlPcS₂ levels in normal palatal mucosa (◆), spotless 4NQO-treated palatal mucosa (○) and biopsies of areas of hot spots (▲). **B:** Data from AlPcS₂ measurements of samples of palatal bone (◆), lacrimal gland (▲) and kidney (n) of normal rats. The variations of AlPcS₂ concentration in the lacrimal gland samples are small (compare figure 2.2.9B). No samples of palatal bone of the 8 h group were available. **C:** AlPcS₂ concentrations in serum of normal (◆) and 4NQO-treated (n) rats. In contrast to the conventional fluorimetry (figure 2.2.9C) no differences were observed between the 2 groups. Error bars represent standard deviations.

was probably the main cause for the increase of autofluorescence in 4NQO-treated rats, seen during the *in vivo* measurements. The *in vivo* fluorescence signal is expected to be the sum of AlPcS₂ fluorescence of the epithelial and connective tissue layer. However, the observed *in vivo* fluorescence kinetics corresponded with the epithelial lining kinetics alone rather than in combination with the connective tissue. This can be concluded from the fluorescence microscopy data. The fluorescence kinetics assessed by microscopy showed AlPcS₂ uptake in the epithelial layer within the first 8 h which corresponded with the *in vivo* kinetics (figures 2.2.3, 2.2.4A+B). The fluorescence from the connective tissue showed different kinetics which was not observed by *in vivo* fluorescence. Furthermore, the high fluorescence signal from the connective tissue layer in biopsies present at 24 and 48 h, was not at all observed by *in vivo* fluorescence. Assessing what mechanisms are causing this effect is extremely difficult. However, we suspect it might be a combination of reduced penetration of excitation light, more scatter and absorption of emitted fluorescence light in the connective tissue, in spite of the relatively thin mucosal layer of approximately 1-1.5 mm and the use of a homogeneous light beam.

4NQO-treated palatal mucosa showed higher AlPcS₂-fluorescence in cancerous tissue than in normal mucosa. Likewise, in a previous study we found an increase of the *in vivo* fluorescence signal concomitant with an increasing degree of dysplasia or the presence of a malignancy of the mucosa (Witjes *et al.*, 1996a, chapter 2.1). Hot spots in 4NQO-treated rats indicated an even higher local uptake of AlPcS₂. The observed higher AlPcS₂-fluorescence in 4NQO-treated mucosa by *in vivo* fluorescence could not be confirmed by fluorescence microscopy. Apparently the fluorescence microscopy detection threshold was not low enough for these thin tissues sections. However, in individual cases the fluorescence intensity of the epithelial layer of these hot spot areas equalled the intensity of the connective tissue layer. This was not observed in normal mucosa. Both techniques showed that for fluorescence detection of autologous squamous cell carcinoma a time-interval between injection and detection of 2-8 h is optimal.

Conventional fluorimetry and HPLC-Dio-LIF

Conventional fluorimetry measurements of phthalocyanine in tissue extracts were also performed using excitation at 610 nm. The influence of the background signal was reduced by integrating the area of the fluorescence peak between 650 nm and 690 nm, which is considered to be specific for phthalocyanine fluorescence. The presence of endogenous fluorescent compounds strongly influenced the results of the conventional fluorimetry measurements. In the lacrimal glands samples, in which the background fluorescence was most prominent, it is known that endogenous protoporphyrin IX is present (Spike *et al.*, 1990). Furthermore, induction of squamous cell carcinoma by 4NQO is accompanied by high keratin production which is also a strongly fluorescent compound. Measuring fluorescence intensities of the NaOH extracts after separation by HPLC avoids the problem of background fluorescence. Conventional fluorimetry has a clear time advantage over HPLC-Dio-LIF, since the collection of a spectrum takes only 1 minute and the data manipulation does not take much longer. The HPLC-Dio-LIF detection method requires about 40 min per sample. HPLC-Dio-LIF is much more specific as a result of the chromatographic separation and more sensitive as a result of the diode laser-based detection technique. Therefore it should be used for detection in complex matrices, especially when low analyte concentrations are present.

Conventional fluorimetry and HPLC-Dio-LIF showed the same AlPcS₂ kinetics for palatal mucosa of normal rats. However, this differed from the *in vivo* fluorescence kinetics in normal and 4NQO-treated rats. *In vitro*, the highest fluorescence signal was seen at 2 h after injection, after which it rapidly declined to half the value at 8 h. The kinetics assessed *in vitro* seem to follow the pattern of the connective tissue rather than the epithelial concentrations. Apparently, the quantities of AlPcS₂ in the epithelial layer are not contributing significantly in conventional fluorimetry or HPLC-Dio-LIF. It cannot be excluded that the relatively high serum levels of AlPcS₂ influenced the *in vitro* measurements shortly after injection. In contrast, the conventional fluorimetry and HPLC-Dio-LIF data not only showed a higher concentration of AlPcS₂ in the mucosa of the 4NQO-treated rats, but also a difference in AlPcS₂ kinetics between the two *in vitro* methods (see table 2.2.II).

The induction of dysplasia by 4NQO apparently influenced the AlPcS₂ measurements. Conventional fluorimetry yielded a higher fluorescence signal in serum, skin and kidneys of 4NQO treated animals compared to samples from normal rats. Analysis by HPLC-Dio-LIF showed that the difference between the serum samples of normal and 4NQO treated rats was not caused by AlPcS₂. 4NQO is known to have some systemic effects on vital organs like liver, stomach, lungs and pancreas when applied or injected subcutaneously (Kondo, 1981),

resulting in various types of tumours. In this study no tumours were found in other organs distant from the palate by macroscopic evaluation. The induction of tumours on the palate is accompanied by high production of nasal and lacrimal fluids, which contain porphyrins, probably as a result of inflammation. This production of porphyrins possibly interfered with the conventional fluorimetry measurements of serum. We have no HPLC-Dio-LIF data on the skin and kidney samples.

Fluorescent hot spots

The phenomenon of the hot spots is not fully understood. It is clear that they appear between 2-8 h after injection and that they represent locally high drug concentrations in epithelial tissue. There was a poor correlation with SCC (27%). In another study we found the hot spots to be associated with SCC, inflammation or of unknown aetiology (Witjes *et al.*, 1996a, chapter 2.1). Fluorescence microscopy showed that biopsies of hot spots contain large quantities of AlPcS₂ in the epithelial layer and connective tissue layer. As in the normal epithelium, the AlPcS₂ was only present in the biopsy-epithelial layer between 2-8 h after injection. In contrast, the connective tissue contained high quantities of AlPcS₂ even at 48 h after injection. HPLC-Dio-LIF measurements on biopsies showed a constantly high present concentration of AlPcS₂ (figure 2.2.10A). These measurements were probably dominated by the concentration in the connective tissue layer, with little contribution of the epithelial AlPcS₂. Remarkably, the hot spots had disappeared at 24-48 h after injection on the *in-vivo* fluorescence images. This supports the finding that fluorescence emitted from the epithelial layer is apparently more easily detected *in vivo* than fluorescence from the connective tissue.

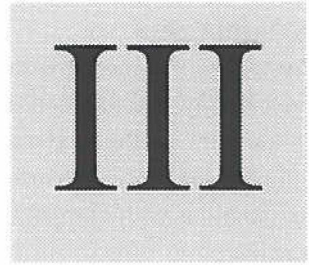
Comparison with the literature

Most studies presented in table 2.2.I investigated xenograft or transplanted tumour models. Tralau *et al* suggested that a **tumour: normal tissue** ratio of 2-3: 1 is obtainable for tumours outside the brain (Tralau *et al.*, 1987). *In vivo* fluorescence measurements of our study indeed showed a ratio for **4NQO-treated: hot spot: normal tissue** of 1.8: 2.5: 1, eight hours after injection (table 2.2.II). Other authors investigating normal epithelial lining of stomach and colon found maximum fluorescence intensities within 1-2 h (Chatlani *et al.*, 1991; Loh *et al.*, 1992). In these papers no difference in kinetics was reported between the epithelial layer and the connective tissue layer. Interesting in this respect are the results presented by Frisoli et al (Frisoli *et al.*, 1993). In this paper, a clear fluorescence signal from the epithelial layer is described 1.5 h after injection of AlPcS₁₋₄, which had disappeared at 48 h. This is in agreement with our findings that fluorescence signals from epithelial tissue can be seen during the first 8 h after injection but cannot be detected at 24-48 h. The injected epithelial tumour cells, however, showed a different time interval between injection and

optimal fluorescence than the normal epithelial layer. Tumour growth occurred in the connective tissue layer, and strong tumour fluorescence was present not only 1.5 h but also 48 h after injection. The *in situ* induced tumours in our experiments had a time interval to maximal tumour fluorescence between 2-8 h post injection. 4NQO-induced tumours showed no difference in kinetics compared to normal epithelium. The difference was only restricted to the amount of AlPcS₂ uptake. 4NQO-induced tumours did not take up any AlPcS₂ from the surrounding tissues at 24 or 48 h, even though a high amount of AlPcS₂ was present close to the tumour in the connective tissue. In contrast, the implanted tumour cells (Frisoli *et al.*, 1993) are able to take up AlPcS₂ and/or retain it 24-48 h after injection.

Conclusions

In vivo endoscopic imaging proved to be the most reliable method to establish the optimal time interval between injection and detection or PDT of AlPcS₂ in autologous squamous cell carcinoma. However, conclusions based on one detection method can be misleading. *In vivo* endoscopic detection of AlPcS₂ did not agree with the *in vitro* measurements probably due to optical effects of light propagation in multi-layered tissue and the presence of connective tissue in the tumour samples used for *ex vivo* analysis. The fluorescence microscopy measurements were crucial for determining the origin of the fluorescence. For detection as well as treatment of 4NQO-induced oral squamous cell carcinoma a time interval of approximately 8 h between administration of AlPcS₂ and illumination seems optimal. Furthermore, there seems to be a difference in kinetics, which can vary per tumour model as well as type of phthalocyanine. More attention should be devoted to possible differences between autologous and non-autologous tumour models. In the future it will be of great importance to assess the optimal time interval between administration and illumination for detection and treatment of various tumours in man.



**EFFECTS OF PHOTODYNAMIC THERAPY ON
NORMAL PALATAL MUCOSA, DYSPLASIA
AND SQUAMOUS CELL CARCINOMA**

3.1 PHOTODYNAMIC THERAPY OF NORMAL RAT ORAL MUCOSA USING ALUMINIUM PHTHALOCYANINE DISULPHONATE.

Analysis of the nature and recovery of injury

INTRODUCTION

Conventional cancer treatments like surgery or radiotherapy can have profound effects on the anatomy and function of the complex structures of the oral cavity. For instance, excision of tumours in the oral cavity easily leads to extensive defects, which sometimes need complex surgical reconstruction. Less collateral damage to the surrounding normal tissues in combination with comparable cure rates is a prerequisite for new therapies when these are considered to effectively replace the conventional ones. Photodynamic therapy (PDT) has been proposed as such a new cancer treatment. At the onset in the seventies, it was thought that certain photosensitizers would be selectively retained in tumour tissue. It was expected that a selective tumour necrosis could be obtained if tumours were irradiated after a certain time interval, with no or little collateral damage. However, after more than a decade of experience with PDT it is now thought that true selectivity is difficult to obtain with the present systemically administered sensitizers. A certain amount of damage will be induced to normal tissues. The degree in which this occurs will strongly depend on the type of sensitizer used and the light distribution in the tissues. Therefore a more appropriate term for describing the efficacy of PDT is called therapeutic ratio. This should be interpreted as the drug/light dose needed for tumour necrosis while inducing reparable damage in normal tissues without impairment of essential functions. The sensitizer under investigation in this paper is aluminium phthalocyanine disulphonate (AlPcS₂) and regarding its selectivity, fluorescence yield and PDT potential, one of the most promising sensitizers of the sulphonated metallophthalocyanines (Witjes *et al.*, 1996a). The application of phthalocyanine-based PDT is on the brink of use in humans as cancer treatment. Studies are ongoing to assess the usefulness of this group of sensitizers. Although several papers have reported favourable characteristics of phthalocyanines, little is known on the effects of these sensitizers on the functional structures of the oral cavity. In normal rabbit jaw AlPcS₂ was found to be safe for bone and molars but induced necrotising sialometaplasia in salivary glands (Meyer *et al.*, 1991). No other studies in this area are available for phthalocyanines. In other parts of the body phthalocyanines induced little collateral damage in the proximity of normal pancreas, stomach and colon at doses of approximately 1 mg/kg - 100 J/cm² (Nuutinen *et al.*, 1991; Chatlani *et al.*, 1991; Loh *et al.*, 1992). In these studies the drug and light doses varied from 0.5 to 10 mg/kg AlPcS₂ and 10 to 150 J/cm² respectively.

The aim of this study was to analyse histologically the damage inflicted upon normal oral

mucosa and the surrounding tissues of the hard palate in rats during AlPcS₂-based PDT. We have studied the effects by varying the doses of AlPcS₂ and light, in order to find an optimal drug/light-dose combination for the future treatment of epithelial dysplasia and squamous cell carcinoma. Due to scattering of light, the fluence in tissue is usually larger than the incident fluence. In addition, the actual thickness of the mucosa layer varies due to the presence of a bulk of keratin in rugae or a locally thick connective tissue layer with large vessels. Scattering and variations in mucosal thickness may cause large variations in the fluence of light. Therefore light dosimetry measurements were included in these experiments for calculating the variations in applied light dose in the tissues.

It has been suggested that the amount of photodegradation of the sensitizer during PDT may predict the damage that has been inflicted upon tissues (Ronn *et al.*, 1995). Therefore, the fluorescence intensities were measured before and after irradiation. Furthermore, results of measurements of tissue concentrations of AlPcS₂ from previous experiments have been included as well. The combination of histological analysis, fluorescence measurements, light dosimetry and AlPcS₂ concentrations in the tissues of the oral cavity, performed in this multi-disciplinary study, should provide a comprehensive view on normal tissue damage by AlPcS₂-based PDT.

MATERIAL & METHODS

Sensitizer

Aluminium phthalocyanine disulphonate (AlPcS₂) was obtained from Porphyrin Products Inc. (Logan, UT, USA). It consisted of >90% pure AlPcS₂ of one isomer. For injection the drug was first dissolved in 0.1 M NaOH (pH 12). The pH was adjusted to approximately 7 by adding an amount of 0.1 M HCl equal to the amount of NaOH and this was added to phosphate buffered saline.

Imaging and light delivery system

The light delivery system and the imaging system for recording the *in vivo* fluorescence images consisted of the same palatoscope as described in figure 2.1.1 (chapter 2.2). For PDT-irradiation a dye laser pumped with a Argon ion laser (Spectra Physics models 2040E and 375B, CA, USA) was used. A birefringent filter and a monochromator were used to tune the dye laser to emit red light of 672 ± 1 nm wavelength using 4-dicyanomethylene-2-methyl-6-*p*-di-methylaminostyryl-4H-pyran (DCM) as the dye. The laser light was fed via a 200 µm diameter optical fibre into the palatoscope. Monomeric AlPcS₂ showed an absorption peak at 672 nm in MeOH. This wavelength was chosen because only monomeric

phthalocyanine is active during PDT (Wagner *et al.*, 1987). Recently, evidence was presented that a red shift in the absorption spectrum may occur *in vivo* (Griffiths *et al.*, 1994). Whether the use of a higher wavelength will result in an more efficient tumour necrosis remains to be established. Prior to each series of experiments the beam profile along the two orthogonal axes was measured using an isotropic light dosimetry probe. The fibre coupling and lens position was adjusted until the readings at the beam periphery differed no more than $\pm 10\%$ from the centre of the beam. Next, the absolute irradiance, that is the incident fluence rate, was measured with a calibrated radiometer (United Detector Technology, model S371, FL, USA). A nearly circular beam of approximately 1 cm in diameter was produced by the palatoscope with an incident fluence rate of 60 mW/cm². This irradiance was used in all PDT experiments. For delivering a light dose of for instance 20 J/cm² a PDT-irradiation time of 5.5 minutes was necessary.

Experimental procedure

Several studies indicate that sufficient *in vivo* cell killing effects were obtained when irradiation was applied at 24 h after sensitisation with AIPcS₂. However, our previous experiments with the rat palatal model showed that AIPcS₂-fluorescence in normal and dysplastic epithelium as well as squamous cell carcinoma is maximal around 4-10 h and not the often suggested 24 h (Witjes *et al.*, 1996a; Witjes *et al.*, 1996b, chapters 2.1, 2.2). Therefore, we used a time-interval between injection and irradiation for this normal tissue damage experiment of 6 h. Thirty-six normal untreated rats were divided in 9 groups of 4 rats each and given various doses of AIPcS₂ and light (figure 3.1.3). As controls, 4 rats were irradiated without administration of AIPcS₂.

Immediately after the recording of the fluorescence images of 460 and 610 nm (see details in Materials & Methods chapter 2.1) the liquid light guide of the fluorescence excitation light was replaced by the optical fibre of the laser and PDT-irradiation started. Immediately after irradiation the liquid light guide of the fluorescence excitation light was switched back and fluorescence images of 460 nm and 610 nm were again recorded.

Rats were sacrificed by an intra-cardial overdose of pentobarbital 2 days and 2 months after PDT to study short and long term effects. The palate with the surrounding hard and soft tissues, including the skull, were removed in one piece. Standardised photographic slides were taken of the palates to evaluate the clinical appearance of the damage. The palates were fixed in 4% formalin, decalcified with 25% formic acid with 0.34 M trisodium citrate dihydrate for approximately 4 weeks. The palates were cut transversely and processed for standard hematoxylin and eosin stained histological sections. Selected slides of rats sacrificed 2 days after PDT were stained for elastin with van Gieson stain for analysing the

integrity of the elastic internal layer of the vessels. To map the histological effects in detail and to numerically express the tissue damage we designed 2 histological grading lists (addendum B&C). The items on the grading lists were subdivided in either the severity of the damage "not present - slight - marked" or the depth of the damage "mucosa - bone - beyond bone". Digits were assigned to the items with 0-not present; 1-slight; 2-marked. Higher numbers were assigned to discriminate between overlapping effects or to express the extreme severity of the damage. The calibration between 3 observers occurred in several sessions.

Light dosimetry measurements

In order to quantify the fluence distribution in palate and the skull, light dosimetry experiments were performed *ex vivo* on palatal tissue and *in situ* in the rat skull. Six normal male Wistar albino rats of 8 weeks old were sacrificed by deprivation of O₂ and an overdose of ethrane. Immediately, the lower jaws were partially dissected to a point at which the hard

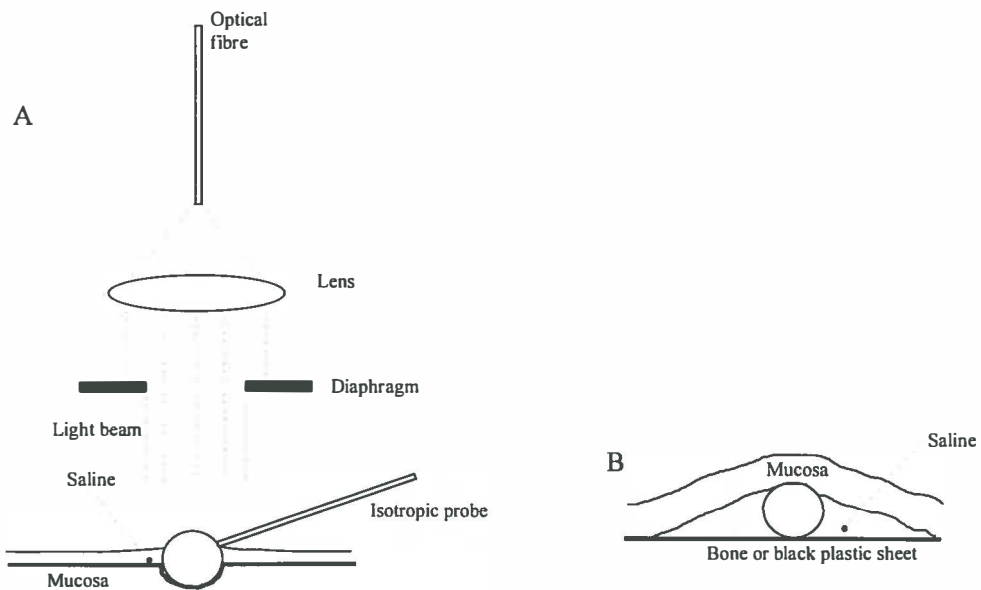


Figure 3.1.1 Schematic drawing of the dosimetry measurements. The isotropic probe (0.8 mm diameter) is gently pressed into the mucosa and also partially exposed to saline and air. Data from this type of measurement needs a correction factor of 1.15 compared to the calibration of the probe in air. In figure 3.1.2B the probe is completely surrounded by tissue and saline and therefore data obtained need a correction of 1.65.

and soft palate were directly accessible for a light beam. Care was taken to avoid bleeding of the tissues. If this occurred, the tissues were kept under pressure until it stopped. During the experiments the tissues were kept moist with saline. Prior to each measurement the nasal passage, which is a hollow structure located cranially from the palatal bone, was extensively rinsed with saline until the saline was clear. A beam of 10 mm diameter was directed to the palate simulating the light beam of the palatoscope. An isotropic probe of 0.8 mm diameter was calibrated in a parallel light beam of at 514, 625 and 672 nm. Measurements at these wavelengths were performed at several locations in the rat with the mucosa in place and after careful removal of the mucosa from the palatal bone (figure 3.1.1). The readings of the isotropic probe were corrected by a factor of 1.65 if it was in saline and by a factor of 1.15 if it was partially in saline and air (Star *et al.*, 1989; Star *et al.*, 1995). To measure light that was scattered by mucosa only, the dissected mucosa was placed on a piece of black plastic and the fluence (rate) was measured at the same locations. Comparing these results with the measurements where the mucosa was at the palatal bone yields an estimate of the light that is reflected by the palatal bone into the mucosa.

RESULTS

Photodynamic therapy - injury assessed 48 h after irradiation

Figure 3.1.2 presents the sum of the damage-index of the three anatomical locations (mucosa - bone - beyond bone). The distribution of the total damage in this graph resembles

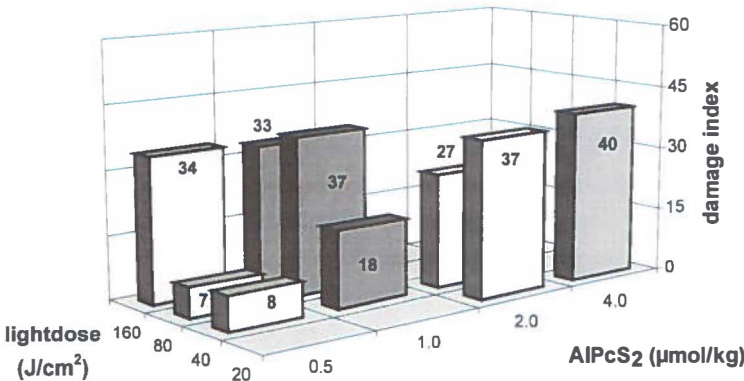


Figure 3.1.2 Results of the grading of the PDT damage 2 days after irradiation. The dose combinations investigated in this study can be read from the bar-containing fields in the graph. The numbers indicate the height of the damage. A detailed description on the method of grading is given in the text.

the damage distribution of the 3 layers, although obviously the nature of the damage is different per layer. Figure 3.1.2 shows that the damage does not increase proportionally when the light dose increases. For instance, the damage-indices from the rats treated with 0.5 $\mu\text{mol/kg}$ AlPcS₂ and 40, 80 and 160 J/cm² were 8, 7 and 34 respectively. Increasing the light dose from 40 to 80 J/cm² did not induce more damage. However, a further twofold increase of the light dose induced increased the damage by a factor 4-5. Apparently a threshold dose was passed after which the injury is much more severe. The only proportional increase of damage occurred at a light dose of 40 J/cm² and sensitizer doses of 0.5, 1 and 2 $\mu\text{mol/kg}$.

A qualitative analysis of the distribution of the histological effects in relation to the severity is presented in table 3.1.I. The first observable signs of injury are edema of the mucosa and the hematopoietic bone marrow as well as excessive necrosis of the dental pulp (figure 3.1.3B). At higher doses the edema in the mucosa becomes more severe, extending from the periosteal layer, and appears in deeper layers. When the mucosal epithelial layer is sloughed off, vessels become extremely edematous and also show clear signs of necrosis (figure 3.1.3C). Von Giesson staining demonstrated no alterations to the internal elastic lamina for all doses. Sometimes thrombi or clots of erythrocytes obstructing the vessels were seen. It seemed as if arteries were more susceptible to PDT than veins. However, this could be caused by the fact that edema of the veins could not be graded and necrosis was much more difficult to observe than in arteries. At high sensitizer doses (2 or 4 $\mu\text{mol/kg}$ AlPcS₂) and a light dose of 20 J/cm² most structures in the mucosa, bone marrow and to some extent beyond bone, showed a marked necrosis. Remarkably, no necrosis was observed of the osteocytes in the palatal bone, the nerves in the mucosa and of the lacrimal gland at any dose combination (figure 3.1.3C). The control rats, irradiated with 160 J/cm² light without the injection of AlPcS₂, did not show any histological effects.

Photodynamic therapy - permanent damage assessed 2 months after irradiation

In figure 3.1.4 the sums of the damage-indices of the three anatomical layers are presented. In contrast with the data from the 48 h histological assessment, the permanent damage to the mucosa contributes most to the total index. The permanent damage beyond bone hardly contributed to the total. The ratio was approximately mucosa:bone:beyond bone=2:1:1, except for the extreme damage at the doses 2 and 4 $\mu\text{mol/kg}$ and 40 and 20 J/cm² respectively. At these dose combinations the indices are mainly the result of the presence of a permanent fistula due to complete loss of palatal bone. The damage indices of the low drug doses 0.5 and 1.0 $\mu\text{mol/kg}$ of 2 days and 2 months after irradiation are comparable (figures 3.1.2 and 3.1.4). However, at the high dose combinations of 2 μmol

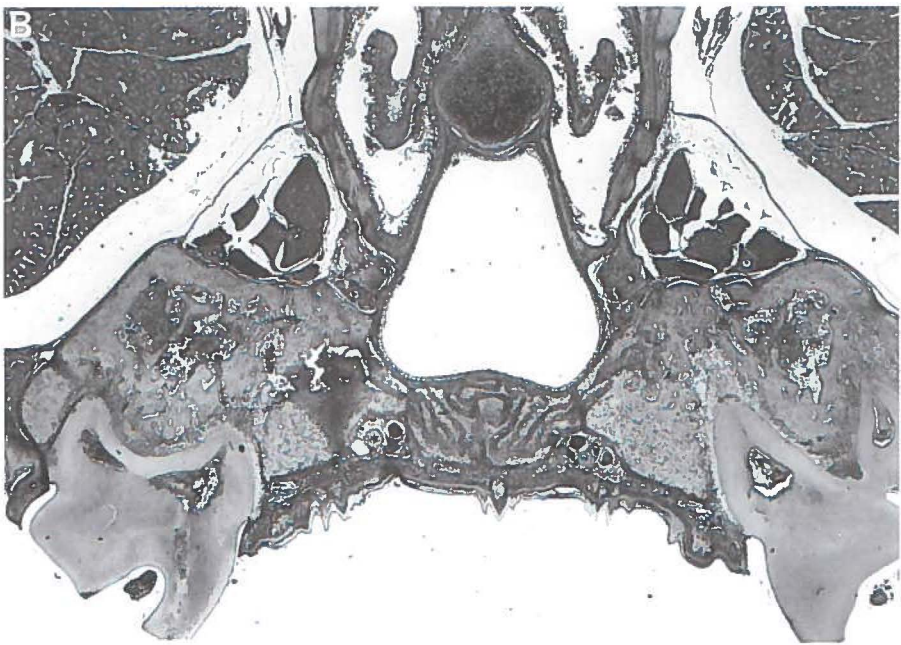
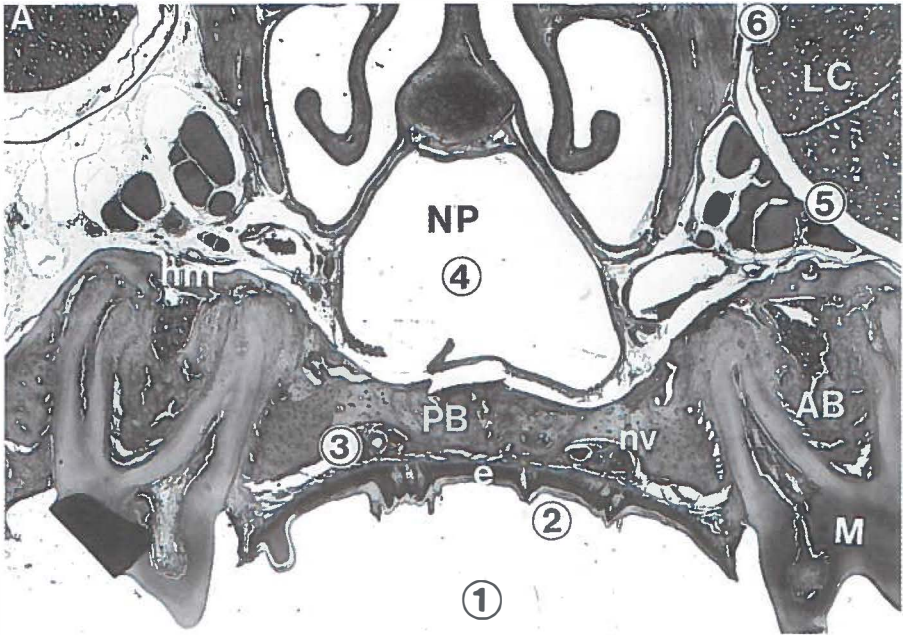




Figure 3.1.3 Photomicrographs of histological sections of rat palates (20x). **A:** Normal untreated palate with present: epithelium (e), molars (M), great palatal nerve/vessel string (nv), palatal bone (PB), alveolar bone (AB), hematopoietic marrow (hm), nasal passage (NP) and lacrimal gland (LC). The numbers indicate the positions of the isotropic probe during the dosimetry measurements and correspond with the numbers in Table 3.1.II. **B:** Palate of a rat treated with a dose of 0.5 $\mu\text{mol/kg}$ AlPcS₂ and 40 J/cm² and sacrificed 2 days after irradiation. At this low dose combination the early signs of damage are pulp necrosis, hematopoietic bone marrow bleeding and goblet cell loss of the epithelium of the nasal passage. **C:** Palate of a rat treated with a dose of 4 $\mu\text{mol/kg}$ AlPcS₂ and 20 J/cm² and sacrificed 2 days after irradiation. The epithelial layer has been sloughed off and marked edema in the connective tissue. There is extensive pulp necrosis and loss of hematopoietic cells and necrosis of the fibrous marrow. Edema extends beyond the palatal bone in the concha (arrow) and there is vascular damage with clotting of erythrocytes (arrowhead).

kg AlPcS₂ and 20 and 40 J/cm² respectively, the 2 months-indices are not consistent with the 2 days-indices. The difference in permanent damage remaining 2 months after PDT could not be anticipated from the histological analysis at 2 days.

An overview of the nature of the permanent damage and recovery is presented in Table 3.1.I. Dental hard tissue resorption at the root as well as ankylosis of the root to the alveolar bone were present in rat tissues recovering from injury of low doses (figure 3.1.6A). Foreign body reactions were usually directed against inserted hairs or dietary fibres,

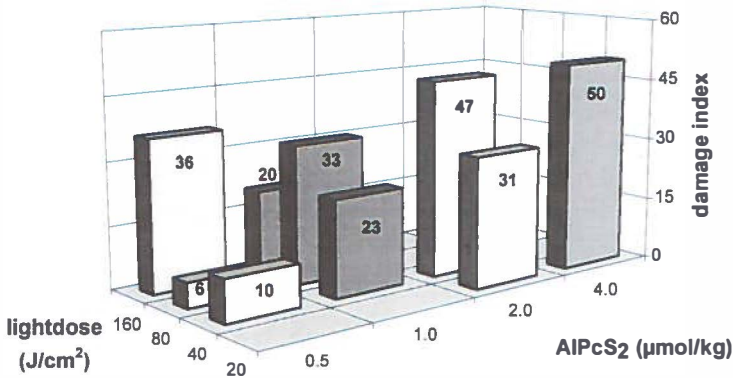


Figure 3.1.4 Results of the grading of the PDT damage 2 months after irradiation. The dose combinations investigated in this study can be read from the bar-containing fields. The height of the damage (indicated by the numbers) is in agreement with the height in damage 2 days after PDT (see figure 3.1.3), except for the high AIPcS₂ doses of 2 and 4 µmol/kg.

indicating that sloughing of the epithelial layer had preceded. The stratification of the epithelial layer was normal despite the irregular distribution of the rete ridges. Recovery also resulted in the formation of cysts-like structures and nests of epithelial cells deep in the connective tissue layer. It was not possible to differentiate whether the cysts originated from invaginations from the surface which were tangentially cut or truly formed cysts (figure 3.1.5A). Vascular effects were hypertrophy and recanalisation of the vessels. If the great palatal vessels or nerves were lost, subsequent neuronal and/or vascular proliferation was present. Sometimes vascular proliferation in the mucosal layer was present without loss of the great palatal vessels, indicating local alterations to the vascular system. In some cases either the vessel or the nerve was lost. Complete loss of bone was regarded as an extreme effect. In some cases the bone was replaced by scar tissue (figure 3.1.5B). At higher doses of 2 and 4 µmol/kg and 40 and 20 J/cm² respectively, the bone had completely disappeared leaving a fistula from the oral cavity to the nasal passage (figure 3.1.5C). One rat died of massive infection of its fistula. When a fistula was present, the epithelium of the oral mucosa was continuous with the sinal epithelium. In contrast with the palatal bone, which sometimes was partially or totally resorbed, the alveolar bone often showed a dense structure due to immoderate bone formation (figure 3.1.5A-C).

Fluorescence measurements

An example of a digitised fluorescence image of the hard palate is presented in figure 3.1.6. For all doses, AIPcS₂ fluorescence was easily detected. Fluorescence intensity was assessed as the average grey-scale level of the intermolar area. The fluorescence intensities just prior to irradiation are depicted in figure 3.1.7A. The increasing fluorescence intensity correlated

Table 3.1.I Cumulative overview of the histological features, 2 days and 2 months after PDT. Five levels of severity of damage; 1=minor, 5=maximum. Abbreviations: I.S.T.=intra suture tissue of palatal bone

	1	2 (+1)	3 (+1&2)	4 (+1,2&3)	5 (1,2,3&4)
Mucosa 2 days	-Edema-slight -Hemorrhage -Pulp necrosis marked	-Vascular edema	-Edema-marked -Hemorrhage- marked -Partial epithelial necrosis	-Total epithelial necrosis -Vascular necrosis -Congestion/ thrombosis	
Bone 2 days	-Bone marrow hemorrhage/ infiltrate	-I.S.T. edema	-I.S.T. hemor- rhage -Haematopoietic cell loss-slight	-I.S.T. necrosis palatal half -Haematopoietic cell loss-marked	-I.S.T. necrosis sinal half
Beyond bone 2 days		-Goblet cell necrosis of sinal epithelium	-Edema-slight	-Vascular edema	-Edema-marked -Hemorrhage -Vascular- necrosis -Sinal epithelial necrosis
Mucosa 2 months	-Scar tissue	-Irregular distri- bution/rete ridges -Scar tissue- marked -Foreign body reaction	-Epithelial isles &(pseudo)cysts -Vascular hypertrophy -Vascular recanalisation	-Loss of neuro vascular bundle -Vascular and neuronal proli- feration	
Bone 2 months	-Palatal bone remodelling -Dental tissue resorption slight -Ankylosis- slight	-Dental tissue re- sorption-marked -Ankylosis- marked	-Partial loss of palatal bone -Dense remodel- ling of alveolar bone	-Complete loss of palatal bone -Sequestration of necrotic bone	
Beyond bone 2 months	-Irregular dentin forma- tion			-Vascular hyper- trophy -Scar tissue -Papillary hyper- plasia sinal epi- thelium	-Permanent fis- -tula from oral cavity to nasal passage

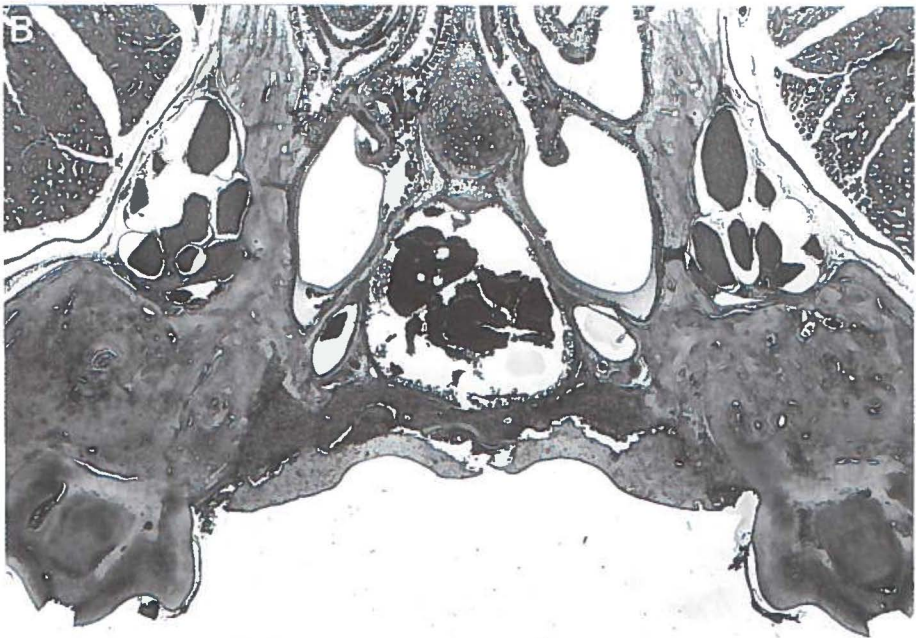
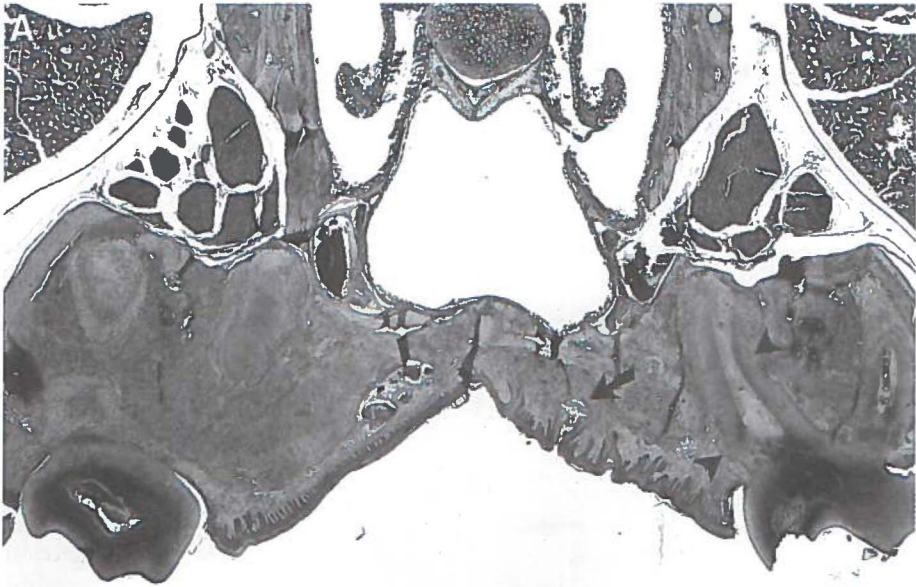




Figure 3.1.5 A: Photomicrograph of a rat palate treated with a dose of $1 \mu\text{mol/kg}$ AIPcS₂ and 40 J/cm^2 and sacrificed 2 months after irradiation (20x). In this case the cyst (arrow) appeared to be an invagination of the epithelial surface. Resorption of the roots (arrowheads) as well of the palatal bone are present. In contrast, alveolar bone shows a dense structure and show ankylotic connections with the roots. At the right side the neurovascular bundle has disappeared. **B:** Rat palate treated with a dose of $0.5 \mu\text{mol/kg}$ and 160 J/cm^2 sacrificed 2 months after irradiation (1x). The palatal bone is necrotic and being sequestered. It was replaced by scar tissue. **C:** Rat palate treated with a dose of $4 \mu\text{mol/kg}$ and 20 J/cm^2 (1x). The palatal bone has been resorbed leaving a permanent fistula between the oral cavity and the nasal passage. The oral epithelium is continuous with the epithelium of the nasal passage. The alveolar bone shows a dense structure and ankylosis with the molars.

well with the increased injected dose (correlation coefficient $\rho = 0.93$). However, the observed fluorescence did not multiply by the expected factor 2 with the injected doses of 0.5, 1, 2 and 4. The actual increase from 0.5 to 1, 1 to 2 and 2 to 4 was: 1.7, 1.5 and 1.7, respectively.

AIPcS₂ concentrations in tissues - results of previous experiments

The data are calculated from results of experiments described in another paper (Witjes *et al.*, 1996b, chapter 2.2). In brief, normal rats were injected with $1.5 \mu\text{mol/kg}$ AIPcS₂ and sacrificed at several time-points. Samples were collected of palatal mucosa, palatal bone,

lacrimal glands, extracted molars and serum. The samples were dissolved in 0.1 M NaOH using an ultrasonic cell disrupter. The AlPcS₂ concentrations were measured by sensitive high performance liquid chromatography based diode laser induced fluorescence (LC-Dio-Lif). The experimental set-up of the LC-DioLIF system has been described in detail (Mank *et al.*, 1993). The AlPcS₂ concentrations in the tissues at 6 h after injection were : mucosa : 48×10^{-10} M/l; molars : 6.6×10^{-10} M/l ; bone : 7.2×10^{-10} M/l ; lacrimal gland : 10.5×10^{-10} M/l ; serum : 501×10^{-10} M/l.

In mucosa there is approximately 6-7 times as much AlPcS₂ present as in bone or molars. However, the tissue damage was not consistent with this ratio. The dental pulp becomes rapidly necrotic, while the osteocytes seem more resistant to PDT. In spite of the higher amount of AlPcS₂ present in mucosa, damage in this tissue is observed at higher light doses than in the pulp. The lacrimal gland, which contained a slightly higher amount of AlPcS₂ than bone or molars, did not show any signs of necrosis or damage at all, even at high light doses.

Dosimetry measurements

The fluence at the several positions in the skull are given in table 3.1.II. The positions in the skull are marked in figure 3.1.3A. As can be expected, the measurements clearly show that shorter wavelengths have lesser penetration depths. Furthermore, the variations in thickness of the mucosa can have profound effects on the fluence rate. Using 514 nm light the reduction in fluence is around 18% between thin (± 0.4 mm) and thick mucosa (± 0.8 mm), and 63% when the fluence is measured underneath a ruga of keratin (± 1.5 mm). For 672 nm light, this loss of fluence was less, however irradiation will still result in a 25% difference of total light dose between thin mucosa (± 0.4 mm) and a ruga of keratin (1.5 mm). Replacing bone by a plastic black sheet results in a 40% decrease of fluence at 672 nm in the muosa.

Due to scattering effects at 672 nm, the actual fluence in mucosa is 3 times higher than the fluence of the beam and therefore the total light dose will be 3 times higher than the estimated light dose. After passing the mucosa the 672 nm light reaches the bone at a fluence varying from factor 2.85 (thin) to 2.13 (keratin-ruga) resulting in an equivalent light dose of 2.85-2.13 times the incident beam at the surface of the bone. The light dose at the nasal side of the bone is approximately 1.29 times the incident light beam. Therefore palatal bone is irradiated with a dose varying between 2.85-1.29 times the incident light beam. A variation of 156%. If a palate is irradiated with a total dose of 40 J/cm^2 , the actual light dose would be 120 J/cm^2 for mucosa and $114\text{-}52 \text{ J/cm}^2$ for bone. Approximately 61% of the incident 672 nm light beam reaches the lower lobes of the lacrimal gland.

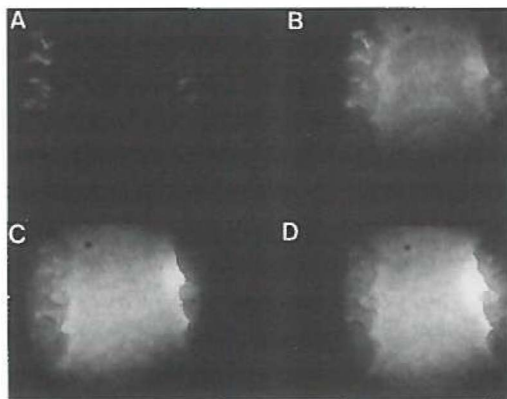


Figure 3.1.6 Digitised fluorescence images of a rat palate. **A:** Autofluorescence image prior to injection of ALPcS₂. **B:** Fluorescence image after injection of 2 $\mu\text{mol/kg}$ ALPcS₂ but prior to irradiation. **C:** Image after irradiation with 20 J/cm^2 . Clearly the fluorescence intensity has increased. **D:** The fluorescence increase continued during a 5 minute intermission without irradiation.

DISCUSSION

For cancer treatments, control over the extent of the collateral damage is a necessity. The damage to the normal rat tissues can be controlled by varying the drug and light dose. The susceptibility for PDT induced necrosis varied among the tissues from dental pulp in the molars, being highly susceptible, to osteocytes and lacrimal gland cells being not sensitive. The nature of early injury in this study was mainly edema and necrosis of the tissues. The permanent damage varied much more and ranged from dental root-ankylosis to loss of vessels/nerves, replacement of bone by scar tissue and, in case of extreme damage, the presence of a permanent fistula between the nasal passage and the oral cavity. The main purpose of these experiments was to investigate the effects of PDT on normal tissue as well as finding a dose combination for the treatment of squamous cell carcinoma. The results will be discussed below in relation to these purposes.

PDT effects

For treatment of dysplasia and squamous cell carcinoma it is desirable that the diseased epithelial layer is sloughed off or, in case of invasive cancer, the tumour cells are killed. Therefore, in this experiment, the dose combination at which sloughing of the normal epithelial layer was achieved was regarded as a dose combination interesting for PDT. All investigated ALPcS₂ doses showed epithelial necrosis. However, in some ALPcS₂ doses the collateral damage was unacceptable (loss of neurovascular bundle, loss of bone). In PDT,

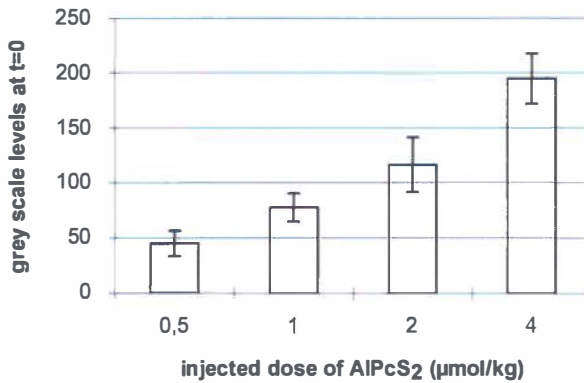


Figure 3.1.7 Relation between injected dose and fluorescence intensity 6 h after injection, just prior to irradiation. There was a strong correlation between injected dose and fluorescence levels (0.93).

vascular effects are considered crucial for tumour necrosis. In most cases of sloughing of the epithelial layer, the vessels showed necrosis. This was predominantly present in the adventitia and media of arteries. LaMuraglia (LaMuraglia *et al.*, 1993) showed that AIPcS_N was present in these layers of normal arteries 3-24 h after sensitisation. Vessel damage resulted in hypertrophy, recanalisation of the lumen or loss of the palatal vessels. When a marked vascular necrosis was observed 2 days after PDT, loss of one or both major palatal vessels was seen in rats treated with the same dose combination. Nerves of the palatal neurovascular bundles did not show any sign of necrosis or other forms of damage at any applied dose, 2 days after PDT. However, in a number of rats the greater palatal nerve had disappeared after 2 months. In contrast with our findings, irradiation of the femoral neurovascular bundle by other authors did not lead to nerve or vessel loss, even at a dose combination of 5 mg/kg AIPcS₂ and 250 J/cm² (Grant *et al.*, 1994). In these experiments the bundles were surgically separated from their environment prior to irradiation, while in our experiments the bundles were irradiated *in-situ*. This may explain the difference in outcome.

Besides loss of vessels, resorption and even sequestration of palatal bone was seen although osteocytes were not directly affected by PDT. The extent of palatal bone resorption was dependent of the dose of light and AIPcS₂ used. In contrast, alveolar bone, which supports the molars, was not resorbed but showed a more dense structure after PDT. The cause of this striking difference is not completely understood. Alveolar bone was situated at the periphery of the beam. For these reasons the tissue destruction might not have been as extensive as in the palatal bone. Also the roots of the molars partially shielded the bone from

Table 3.1.II Fluence of 3 wavelengths at various positions of probe in the rat skull during dosimetry (n=6)

Position of probe; the numbers correspond with positions in figure 3.1.3A	514 nm	630 nm	672 nm
1. Primary beam (air)	100 mW/cm ² (sem %)	100	100
2. On intact palatal mucosa covering palatal bone	207 (± 6)	291 (± 3)	305 (± 3)
3. Underneath dissected mucosa which was replaced on the palatal bone			
-Thin part (± 0.4 mm)	153 (± 13)	265 (± 8)	285 (± 4)
-Thick part (± 0.8 mm)	126 (± 17)	228 (± 9)	252 (± 7)
-Ruga of keratin (± 1.5 mm)	56 (± 22)	160 (± 10)	213 (± 8)
3. On denuded palatal bone	194 (± 6)	287 (± 4)	317 (± 4)
4. In nasal passage:			
-With covering mucosa	25 (± 9)	106 (± 9)	129 (± 8)
-Denuded palatal bone	55 (± 14)	158 (± 7)	191 (± 4)
Mediolateral of lacrimal gland			
5. -Caudal, behind molar	17 (± 24)	48 (± 14)	61 (± 19)
6. -Rostral, high at skull	1 (± 14)	6 (± 15)	6 (± 20)
Underneath dissected mucosa which was placed on a black background			
-Thin part (± 0.4 mm)	129 (± 6)	189 (± 6)	203 (± 4)
-Thick part (± 0.8 mm)	100 (± 6)	146 (± 5)	179 (± 6)
-Ruga of keratin (± 1.5 mm)	55 (± 17)	111 (± 10)	151 (± 8)
On dissected palatal mucosa placed on black underground	166 (± 7)	207 (± 3)	218 (± 2)
Calculations on fluence-description			
Percentage of increase of fluence when mucosa on bone compared to mucosa on black background	25 % (± 5.1) (SEM %)	41 % (± 1.8) (SEM %)	40 % (± 1.3) (SEM %)
Loss of fluence due to increasing thickness of mucosa, relative to thin part of mucosa when mucosa on bone in percentages			
- Thick (± 0.8 mm)	18 (± 15.9)	14 (± 5)	12 (± 3.1)
- Ruga of keratin (± 1.5 mm)	63 (± 40.2)	40 (± 6.9)	25 (± 4)
Loss of fluence due to increasing thickness of mucosa, relative to thin part of mucosa when mucosa on black background in percentages			
- Thick mucosa (± 0.8 mm)	22 (± 7.6)	23 (± 4.7)	12 (± 3.9)
- Ruga of keratin (± 1.5 mm)	57 (± 31.3)	41 (± 9.6)	26 (± 5.7)

the light.

The mere presence of AlPcS₂ in the tissues did not automatically lead to tissue necrosis after irradiation, even at a dose of light at which necrosis could be expected (160 J/cm²). This is most clearly demonstrated in the lacrimal glands, which contained slightly more AlPcS₂ than bone and molars, according to the LC-DioLif measurements, but did not show any sign of edema or necrosis. This in contrast with dental pulp tissue, which was very sensitive to PDT. Whether the dental pulp cells became necrotic due to direct cell necrosis or due to ischemia remains unclear. Goblet cells in the ciliated epithelium of the nasal passage were necrotic after PDT with low doses, while the epithelial cells of the mucosa remained undamaged. Obviously, the intra-cellular distribution of the sensitizer, the sensitivity for reactive oxygen molecules, the capability of cellular repair and pre-existing colateral vasculature are important factors in the efficacy of PDT.

Light dosimetry and fluorescence measurements

Mucosa and bone are turbid media and the fluence at 672 nm was three-fold increased due to scattering. The thickness of the epithelial layer influenced the light penetration significantly. The thickness of the epithelial layer varies from 0.4-1.5 mm thick (including the keratin layer). When 1.5 mm thick, the tissue can reduce the effective light-dose at 672 nm by 25%. At shorter wavelengths this difference becomes even greater. For superficial tumours a deep penetration is not needed to prevent collateral damage. However, treatment response will probably be poorly of PDT of bulky tumours with light of shorter wavelengths. Furthermore, the surrounding tissues influence the light dosimetry strongly. The fluence in the thin palatal mucosa was largely determined by the light that was reflected by the palatal and alveolar bone.

The fluorescence showed a remarkable increase at high doses of AlPcS₂ (2, 4 µmol/kg) after PDT. An increase of fluorescence during PDT was found by others *in-vitro*, and was explained as a release of sensitizer from intra-cellular vesicles (Rück *et al.*, 1990; Ambroz *et al.*, 1994; Peng *et al.*, 1991a; Berg *et al.*, 1991). The increase of fluorescence implies a more efficient fluorescence yield in the tissues and possibly a more efficient yield of reactive oxygen molecules. However, the influence of this increase of sensitizer-fluorescence in relation to the tissue damage is not known. The differences between fluorescence before and after PDT were not a measure for the induced damage. Furthermore, as shown by these experiments, the presence of AlPcS₂ in the tissue does not automatically lead to tissue damage

Clinical consequences for PDT

From a clinical point of view the PDT-dose for treating epithelial disorders should not induce unacceptably high permanent damage. Dental root resorption, ankylosis and to a lesser degree loss of bone may seem trivial side effects of PDT. The clinical consequences, however, are not. Palatal bone defects need reconstruction because food can enter the nasal cavity. Pulp destruction usually is very painful and ankylotic teeth are, if necessary, extremely difficult to remove. Furthermore, if PDT is used as an adjuvant therapy for squamous cell carcinoma in combination with radiotherapy, patients are possibly at risk for severe side effects like osteoradionecrosis. Side effects resulting from a combination of these two treatment modalities need to be investigated for bone-containing tissues. In our model pulp necrosis, resorption and ankylosis already occur at low doses and these effects were difficult to prevent due to the small dimensions. Results of other authors, who concluded that AIPcS₂ was safe to use in the proximity of bone and teeth (Meyer *et al.*, 1991), are in contrast with our findings. We suggest that the PDT dose for treatment of oral squamous cell carcinoma in mucosa supported by bone needs to be carefully chosen. In humans, teeth should be shielded from the beam for prevention of dental root ankylosis at any given dose. Sloughing of the epithelial layer in combination with acceptable permanent collateral damage (disregarding the root ankylosis) was present at the dose 1 µmol/kg and 40 J/cm². A lower dose of AIPcS₂ induced epithelial sloughing only after a long irradiation period also causing a high collateral damage. Increasing the dose to 2 µmol/kg leaves a small margin for controlling the damage by the light dose and is therefore not practical to use.

In conclusion, for treatment of squamous cell carcinoma in the rat palatal model a dose of approximately 1 µmol/kg and 40 J/cm² should be safe to use. Fluorescence measurements before and after PDT gave capricious results and could not predict damage. Knowledge of the light dosimetry is important for predicting the treatment outcome of tumours. Even at a wavelength of 672 nm the light penetration in the oral mucosa was considerably affected.

3.2 PHOTODYNAMIC THERAPY OF EXPERIMENTAL DYSPLASIA AND SQUAMOUS CELL CARCINOMA OF THE RAT ORAL MUCOSA USING ALUMINIUM PHTHALOCYANINE DISULPHONATE

INTRODUCTION

The currently most used modalities in the treatment of oral cancer are surgery and radiotherapy. Both modalities can have severe side effects like mutilation and radiation induced mucositis, xerostomia and osteoradionecrosis. Photodynamic therapy (PDT) has been suggested as a possible alternative for surgery or radiotherapy. PDT has potential for the treatment of localised tumours of the oral cavity without metastatic spread to lymph nodes. When metastasised to the lymph nodes in the neck region, treatment of SCC requires a completely different approach (Suen, 1989). The aim of this study was to investigate the possibility of using PDT in the treatment of chemically induced squamous cell carcinoma (SCC) and dysplasia of the palatal mucosa in Wistar rats.

The sensitizer investigated was aluminium phthalocyanine disulphonate (AlPcS₂). This drug is considered a promising second generation sensitizer with good tumour localising and cell killing properties (van Leengoed *et al.*, 1993b). In previous experiments we found a significant increase of AlPcS₂-mediated fluorescence 4-10 h after injection as the dysplasia in the rat palatal mucosa increased (chapter 2.1). Fluorescence microscopy showed that 4-8 h after injection, AlPcS₂ was localised in 4NQO-treated epithelial tissue and had disappeared 24 h after injection (chapter 2.2). Therefore a time-interval between injection and irradiation of 6 h was chosen, also because it is then possible to inject the sensitizer and irradiate the tissue on the same day. For this study a specially built endoscope was used for simultaneous light delivery and fluorescence imaging. The light beam from the endoscope will not be perfectly uniform owing to the inherent bell shaped light distribution of a flat-cut fibre and stray light in the endoscopic tube. Therefore, the profile of the light beam was measured and the effects of a non-uniform incident beam on the light distribution in multilayered tissue analysed by Monte Carlo simulations (Keijzer *et al.*, 1989). Prior to these experiments a normal tissue damage study was performed to determine an optimum drug light dose combination for therapy (Witjes *et al.*, 1996c, chapter 3.1). It appeared that a dose of 1 µmol/kg AlPcS₂ i.v. combined with 40 J/cm² of 672 nm light 6 h later was sufficient to slough off the epithelial layer but causing only acceptable permanent damage to the surrounding tissues. Dental root resorption and ankylosis were the only unacceptable permanent damage features after PDT which could not be prevented owing to the small dimensions of the rat palate.

MATERIALS & METHODS

Sensitizer

Aluminium phthalocyanine disulphonate (AlPcS₂) was obtained from Porphyrin Products Inc. (Logan, UT, USA) and consisted of >90% pure AlPcS₂ of one isomer. For injection the drug was first dissolved in 0.1 M NaOH (pH 12). The pH was adjusted to approximately 7 by adding an amount of 0.1 M HCl equal to the amount of NaOH. The solvent was diluted to an injectable volume in phosphate buffered saline.

Light delivery and imaging system

The light delivery and imaging system consisted of a specially built endoscope (palatoscope) connected to an intensified charge couple device (CCD) camera as described in chapter 2.1 (Materials & Methods). However, during the present experiments the halogen lamp was not used. For PDT-irradiation a dye laser pumped by an Argon ion laser (Spectra Physics models 375B and 2040 respectively, San Jose, CA, USA) was used. A birefringent filter and a monochromator (Oriel model 77320, Stratford, CT, USA) were used to tune the dye laser to emit red light of 672 ± 1 nm wavelength using DCM as the dye. The laser light was fed via a 200 mm diameter optical fibre into the palatoscope. Prior to each series of experiments the beam profile along the two orthogonal axes was measured using an isotropic light dosimetry probe. The fibre coupling and lens position were adjusted until the readings at the beam periphery differed no more than $\pm 10\%$ relative to the centre of the beam. Next, the absolute irradiance, that is the incident fluence rate, was measured with a calibrated radiometer (United Detector Technology, model S371, Orlando, FL, USA). A nearly circular beam of approximately 1 cm in diameter was produced by the palatoscope with an incident irradiance of 60 mW/cm^2 . A light dose of 40 J/cm^2 thus required a PDT-irradiation time of 11 minutes. The rats were anaesthetised with a mixture of ethrane/O₂/N₂O and placed in stereotactic frame which was placed on an XY-table. The palatoscope was fixed on a photographic stand, which was adjustable in height. The small mirror (M) was placed above the mucosa of the hard palate, between the molars. Fluorescence images were recorded during the irradiation with 672 nm. Fluorescence light was selected by a 3 mm thick, 695 nm high pass Schott coloured glass filter. The fluorescence intensity was reduced using a 10% grey filter. The images were digitised by a PC-based framegrabber, averaged over 16 frames and analysed by grey-scale measurement of the pixels (256x256) (van Leengoed *et al.*, 1993a). With this set-up a full screen image of a relatively small area of 1 cm^2 can be studied.

Experimental procedure

Squamous cell carcinomas (SCC) and dysplasia of rat palatal mucosa were induced by application of 4-nitroquinoline 1-oxide (4NQO, 0.5% w/v) three times a week. The Wistar rats were briefly anaesthetised by a mixture of N₂O/O₂/halothane and painted with 4NQO on the mucosa of the hard palate. During the application period the rats were housed under standard housing conditions. For this experiment 40 Wistar albino rats were divided into 5 groups. Each group was subjected to a different 4NQO-application period, namely 8, 12, 16, 20 and 26 weeks. All rats received an intravenous injection of 1 µmol/kg AlPcS₂, 6 h prior to irradiation with 40 J/cm² incident light. The rats were sacrificed with an intra-cardial overdose of pentobarbital 2 days (n=20) or 2 months (n=20) after PDT to study short and long term effects. The palate with the surrounding hard and soft tissues, including the skull, were removed in one piece. The palates were fixed in 4% formalin, decalcified with 25% formic acid with 0.34 M trisodium citrate dihydrate for approximately 4 weeks. The degree of decalcification was checked by X-ray analysis. The palates were cut transversely and processed for standard hematoxylin and eosin stained histological sections. To map the histological effects in detail and to numerically express the tissue damage we used previously designed histological grading lists, one for tissue damage 2 days and one for tissue damage 2 months after PDT (addendum B&C). The items were graded either as "none (=0), slight (=1), marked (=2)". Higher numbers were assigned to these qualifications when the damage was extreme (i.e. total bone loss, loss of neurovascular bundle).

The dysplasia of the mucosa was graded with a separate list, the Epithelial Atypia Index (EAI, addendum A), designed by others (Smith *et al.*, 1969). This list has proven to be very useful for analysing the dysplasia in rats induced by 4NQO (Nauta *et al.*, 1995). In general, the severity of the dysplasia of the mucosa is correlated to the 4NQO application period.

Monte Carlo simulations

Computer simulations for photon propagation in multilayered tissue were performed with a Monte Carlo algorithm on a Macintosh LC-II personal computer with mathematical coprocessor. In brief, the programme simulates photons entering the tissue at a single point. Photon paths and points of absorption at several depths are calculated. For a detailed description of the algorithm see Prahl and Keijzer (Prahl, 1988; Keijzer *et al.*, 1989). The irradiated area in the rats consisted of a mucosal layer supported by connective tissue and palatal bone. The thickness of the rat oral mucosa and palatal bone was measured on histological slides. The normal palatal mucosa consist of a keratin layer of approximately 75 µm and an epithelial layer of 150 µm. The mucosa is supported by a connective tissue layer of 160 µm. The palatal bone underneath the mucosa is a structure of about 400-500 µm

thick. Therefore, the palatal mucosa and bone were represented in the model by two infinitely wide slabs of finite thickness, that is, a 400 μm homogeneous mucosal layer and a 500 μm homogeneous bone layer. The optical properties of palatal mucosa and bone, necessary for performing Monte Carlo simulations, are not known. For that reason the optical properties of bronchial mucosa and cartilage were taken. These were assessed in previous *in vitro* experiments by double integrating sphere measurements on pig bronchial mucosa and cartilage at 672 nm wavelength (Murrer *et al.*, unpublished data). In a Monte Carlo simulation the light fluence rate was calculated in a plane through the centre of a beam of 0.5 cm radius and an irradiance of 100 mW/cm^2 . For each of the 5 simulations 25,000 photons were launched. The mean light fluence rate in the mucosa and bone was calculated along the beam radius from the centre to 2 mm beyond the beam periphery. To simulate the variations in fluence rate that may occur during PDT of the palate, the irradiation was simulated for a flat (ideal) beam profile and for the actually measured beam profile with a decrease of 10% towards the periphery (see *light delivery and imaging system*)

Retrospective analysis of mucosa thickness of rats treated with 4NQO

During the histological analysis it became apparent that the thickness of the mucosa increased when the 4NQO treatment period increased. This increase of thickness influenced the treatment effectiveness. To measure the increase of thickness we analysed the H&E stained histological slides of 20 rats from a previous experiment treated with 4NQO for 8, 12, 16, 20 and 26 weeks (Witjes *et al.*, 1996a, chapter 2.1). The thickness of the keratin layer and the epithelial layer was measured using a morphometric system (Quantimed, Cambridge systems, Cambridge, UK). For each rat an average of 3 slides was obtained.

RESULTS

Photodynamic therapy of dysplasia and SCC - 2 days after PDT

Histological analysis showed that the Epithelial Atypia Index (EAI) increased with increasing 4NQO treatment period (figure 3.2.1, Spearman correlation 0.85, $p < 0.0001$). This is consistent with previous experiments using the 4NQO model (Witjes *et al.*, 1996a, chapters 1.4 and 2.1; Nauta *et al.*, 1995). Squamous cell carcinoma (SCC) can not be graded by the EAI since this was designed to assess dysplasia only. Therefore when SCC was observed this was not included in the numerical analysis, but separately noted as "SCC". Figure 3.2.2 shows the damage index relative to the EAI of rats sacrificed 2 days after irradiation. Remarkably, the total damage induced by PDT decreased when the EAI increased. Spearman correlation analysis showed that there is an inverse relationship

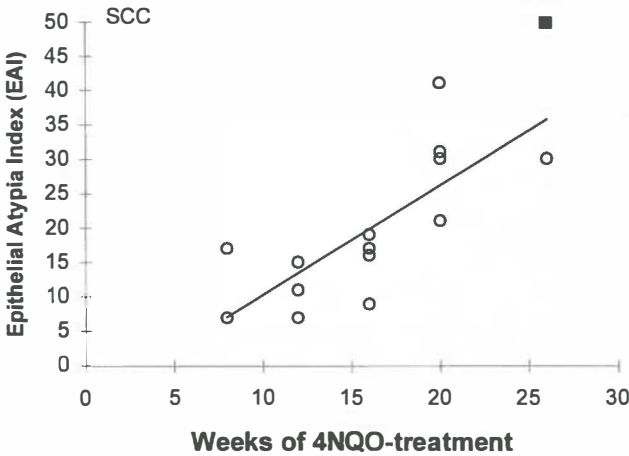


Figure 3.2.1 Plot of the degree of dysplasia of the rats sacrificed 48 h after PDT, expressed by the Epithelial Atypia Index (EAI), as a function of the 4NQO treatment. Clearly, the dysplasia increases with an increasing 4NQO application period ($r=0.85$). Squamous cell carcinoma (SCC) cannot be graded by the EAI and was therefore separately indicated (■, $n=1$).

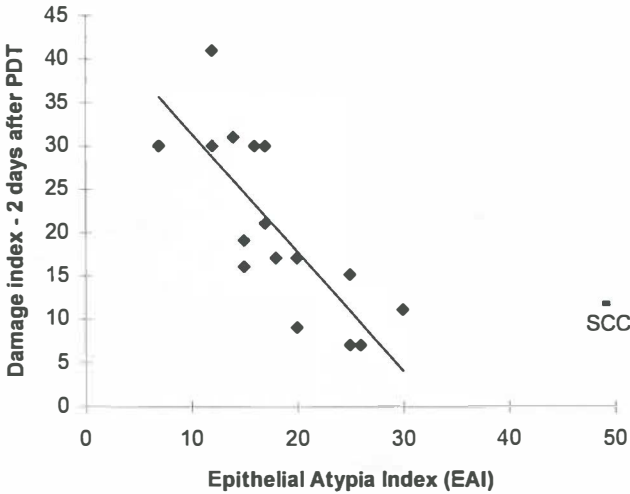


Figure 3.2.2 The PDT-induced damage assessed 2 days after irradiation vs the degree of dysplasia (EAI). Remarkably, the damage decreased as the dysplasia increased ($r=-0.86$; $n=18$). Squamous cell carcinoma (SCC) was separately indicated because it cannot be graded by the EAI (■, $n=1$)

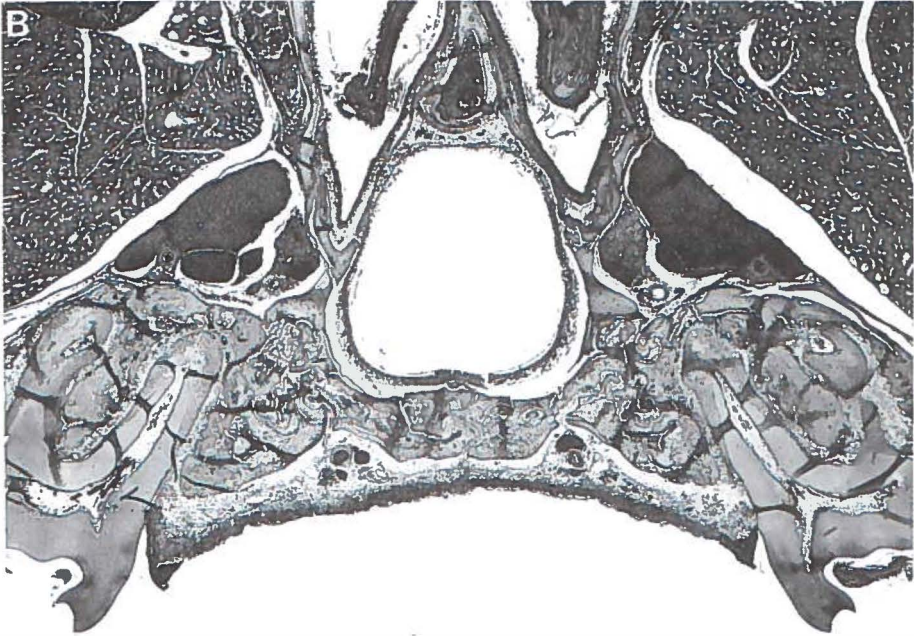
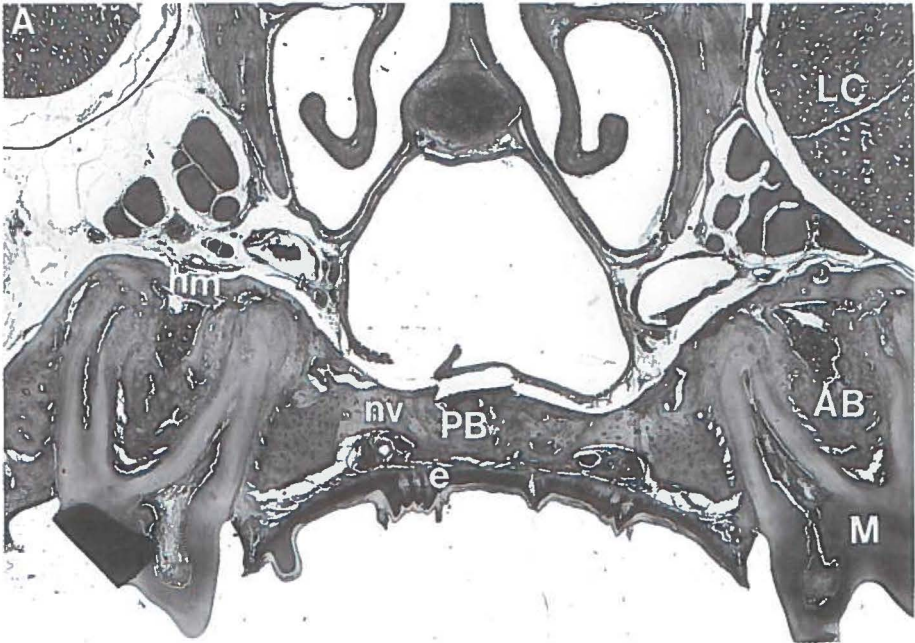


Figure 3.2.3 (previous page) Photomicrographs of histological sections of rat palates. **A:** Normal untreated palate with present: epithelium (e), molars (M), great palatal nerve/vessel string (nv), palatal bone (PB), alveolar bone (AB), hematopoietic marrow (hm), nasal passage (NP) and lacrimal gland (LC). **B:** Palate of a rat treated for 8 weeks with 4NQO and sacrificed 2 days after PDT. Clearly, the complete epithelial layer has sloughed off. There is extensive edema of the connective tissue and periost, occlusion of a great palatal artery and extensive pulp necrosis. This rat had a fluorescence intensity at the palate of approximately 114 on a gray-scale of 0-255.

between these variables (correlation coefficient $r = -0.86$, $p < 0.0001$)

The histological features of damage inflicted by PDT differed between the rats with low and high EAI. In rats with a high EAI the damage generally existed of edema, hemorrhage, partial or no necrosis of the epithelial layer, slight vascular necrosis, bone marrow hemorrhage and pulp necrosis. In palates with a low EAI the additional greater damage consisted mainly of total loss of the epithelial layer, severe vascular effects, necrosis of the palatal bone marrow and edema at deeper layers. A demonstration of the histological differences between PDT damage to rats with a low EAI and a high EAI is shown in figures 3.2.3A to D. In the rats treated for 8 weeks it was possible to remove the epithelial layer completely (figure 3.2.3B). The palatal epithelial layer in rats with an intermediate grade of dysplasia was sloughed off partially while the palatal epithelial layer in rats with a high EAI number could not be removed at all (figure 3.2.3D).

Photodynamic therapy of dysplasia and SCC - 2 months after PDT

A characteristic of the 4NQO model is that dysplasia will continue to progress towards SCC although the 4NQO-application has stopped (Nauta *et al.*, 1996). The histological analysis 2 days after PDT showed that the dysplastic epithelium was not always completely removed. Owing to this, regrowth after PDT of the epithelial layer will start from remnants of dysplastic epithelial cells, which will develop into dysplastic epithelium again. Furthermore, in a previous normal tissue damage study using AlPcS₂ it was observed that the remnants of epithelial cells are often included into the connective tissue, as in the development of traumatic epithelial cysts (Witjes *et al.*, 1996c, chapter 3.1). For that reason, the discrimination between remnants of epithelial cells included in the connective tissue after PDT and active invasion of cancerous cells was difficult. In 13 rats SCC had developed within the 2 months after PDT. These rats were 4NQO-treated for 12, 16, 20 or 26 weeks. This number was higher than was expected from a previous experiment in which the latency period between cessation of 4NQO treatment and the presence of SCC was approximately 20 weeks (Nauta *et al.*, 1996).

The permanent collateral PDT damage to the rats mainly consisted of the presence of epithelial isles/cysts, hypertrophy of the medial layer of arteries, partial loss of palatal bone,

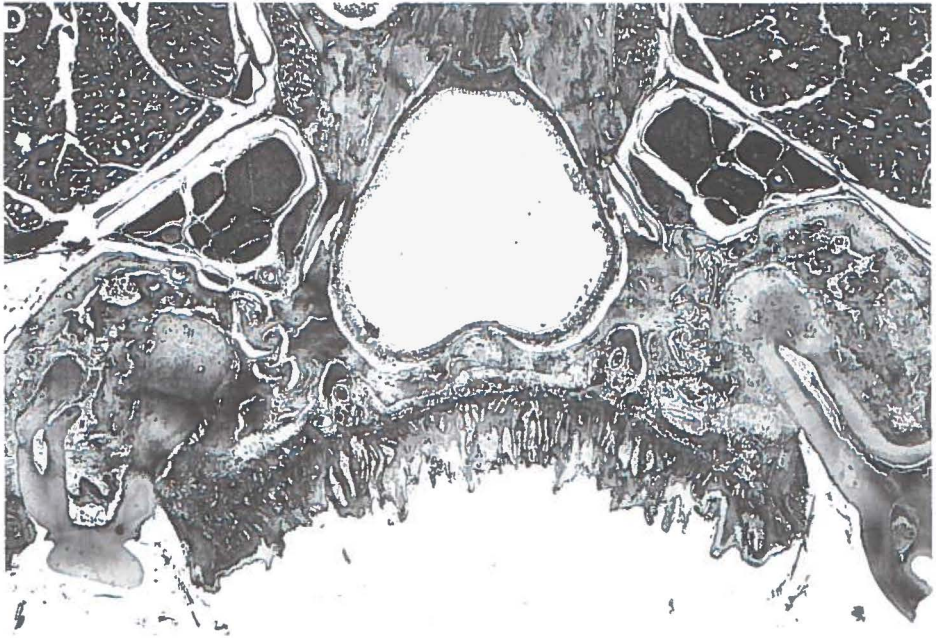
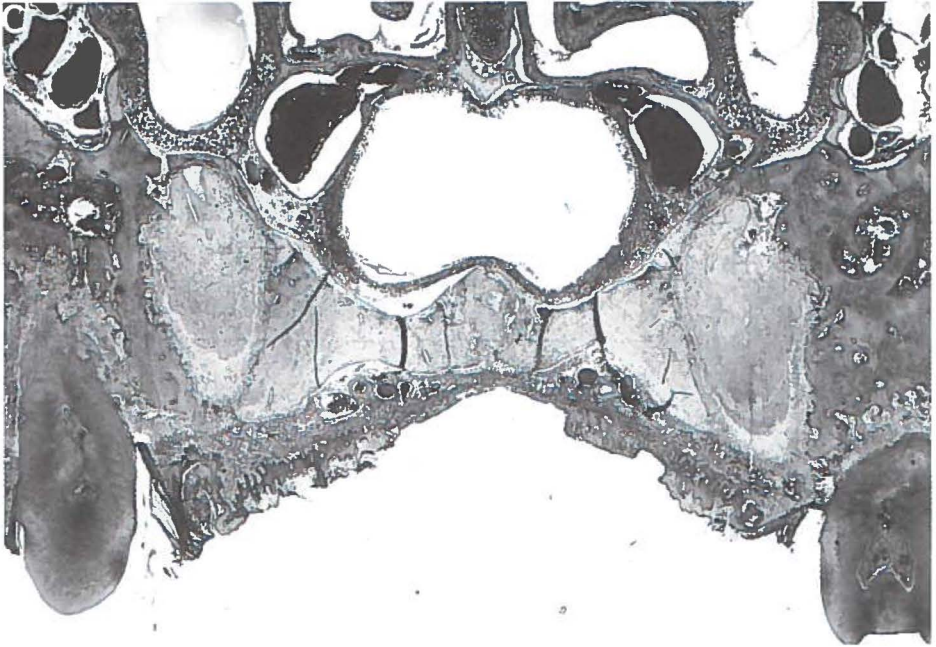


Figure 3.2.3 continued (previous page) C: Palate of a rat treated for 26 weeks with 4NQO and sacrificed 2 days after PDT. Partial sloughing of the epithelial layer and less extensive damage to the deeper layers was seen. This rat had a fluorescence intensity of approximately 130 (gray-scale 0-255) at the palate. **D:** Rat treated for 26 weeks with 4NQO and sacrificed 2 days after irradiation. The epithelial layer is intact and only edema of the connective tissue and periost and pulp necrosis can be seen. This rat had a fluorescence intensity of 190 at the palate, which was the highest measured. Remarkably, this was not reflected in the induced damage.

ankylosis and resorption of dental roots (figure 3.2.4A & B). In a few rats one great palatal nerve/vessel string was lost. In contrast to the 2 days damage index, no correlation existed between the permanent damage, graded by the damage index 2 months after PDT, and the EAI of the tissue.

Fluorescence imaging during PDT

The fluorescence intensities of the palatal mucosa between the molars of the rats at the start of PDT-irradiation are presented in figure 3.2.5. There is a significant difference in grey-scale levels between the rats treated for 8 weeks or for 26 weeks and the other groups ($p < 0.05$, Student Newman Keuls test for multiple comparison). Furthermore, Spearman correlation analysis showed a correlation of 0.7 ($p < 0.0001$) between the EAI and weeks of 4NQO treatment. Both analyses indicate a higher uptake of AlPcS₂ in rats treated longer with 4NQO. Figure 3.2.6 shows the fluorescence dynamics during PDT averaged over all rats, expressed as the percentage of fluorescence at $t=0$. Between 0 and 4 minutes of irradiation a plateau was present, with a slight increase of fluorescence at 2 min. (2%). However, there were large individual differences in the grey-scale levels after 2 minutes of PDT-irradiation which ranged from 0.71 to 1.43 times the fluorescence level at $t=0$. After 4 minutes the fluorescence intensity started to decrease to 83% of the value at $t=0$ at the end of the treatment. Figure 3.2.9 shows 4 digitised fluorescence images of a rat recorded during PDT. Clearly the fluorescence increased during treatment in this rat. The increase did not depend on the duration of the 4NQO treatment.

Monte Carlo simulations and light dosimetry

The results of the Monte Carlo estimates of the total light energy fluence are presented in figure 3.2.8. The lines represent constant fluence (isodose-lines). A light beam with a 10% decrease in fluence towards the periphery will result in a lower dose at the periphery compared to a beam with a flat profile (compare left-right isodose lines).

The results of the *ex vivo* light dosimetry measurements presented in chapter 3.1 are shown in figure 3.2.9. Owing to scatter, the actual light fluence was 3.05 times the incident irradiance at the surface of the mucosa and 2.85, 2.52 and 2.13 times the incident irradiance

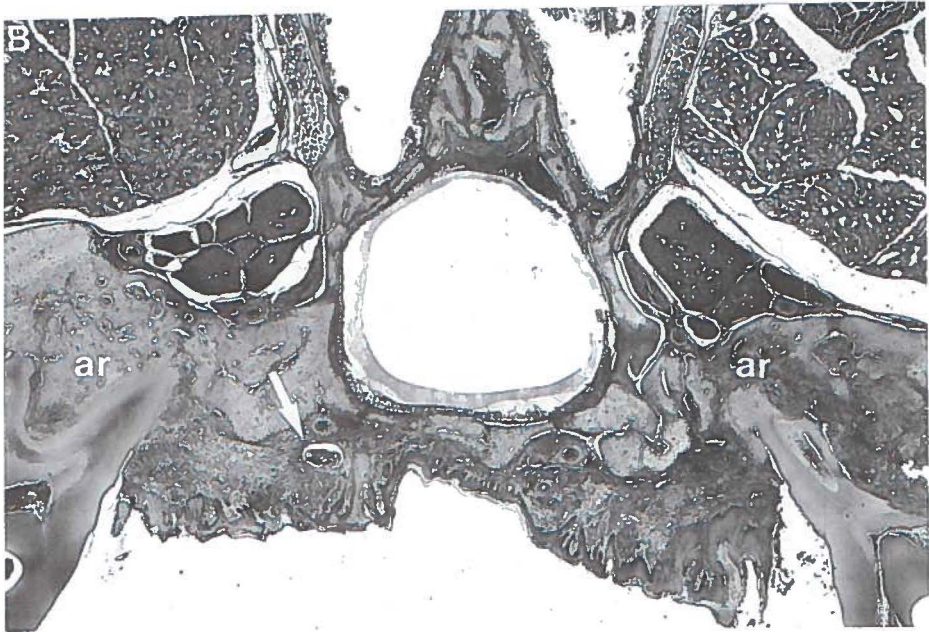
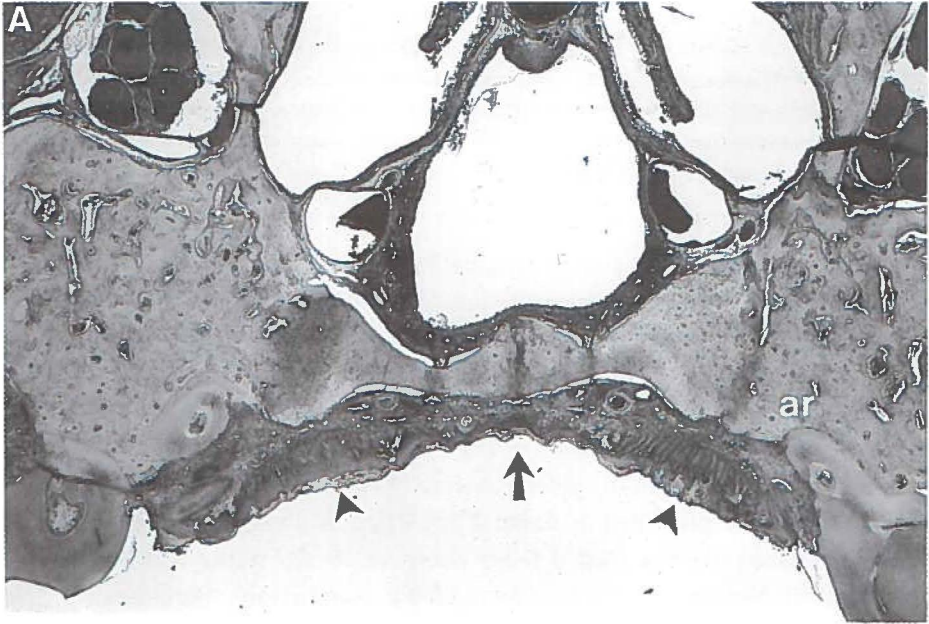


Figure 3.2.4 (previous page) Photomicrographs of histological sections of rat palates sacrificed 2 months after irradiation. **A:** Rat treated for 20 weeks with 4NQO. A therapeutic effect was only obtained at the centre of the beam (arrow). Here the epithelial layer shows less dysplasia, while at the periphery near the molars the dysplasia is severe (arrowheads). This palate had a fluorescence intensity of approximately 125 (gray-scale 0-255). The molars show bony connections to the alveolar bone (ankylosis) and areas of root resorption. **B:** Rat treated for 20 weeks with 4NQO. Again a therapeutic effect was obtained at the centre and not at the periphery. This palate had a fluorescence intensity of 150. Besides ankylosis and root resorption (ar), the connective tissue layer contains a cyst filled with keratin and lined with dysplastic epithelial cells (white arrow).

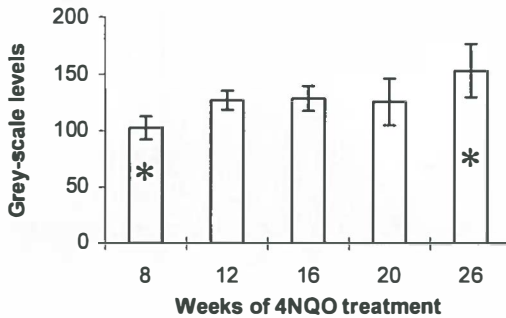


Figure 3.2.5 Results of the fluorescence measurements acquired at the beginning of irradiation. The data were analysed per treatment group (n=8 per group). The rats treated for 8 weeks and 26 weeks were significantly different from the other groups (*, $p < 0.05$, Student Newman Keuls test for multiple comparison).

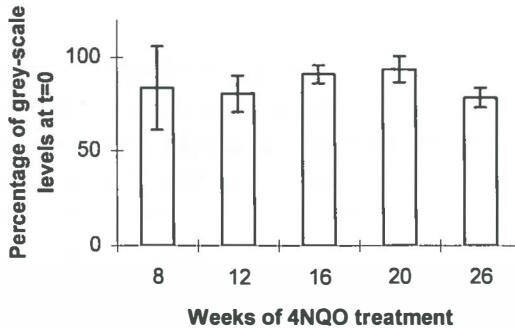


Figure 3.2.6 Results of photodegradation measurements assessed from images acquired after 11 minutes of irradiation, shown per 4NQO treatment group. The fluorescence intensity is expressed as a percentage of the fluorescence level at $t=0$ (100% is level at $t=0$). After 11 minutes an average fluorescence level of 0.83 times the level at $t=0$ for all groups remained (range 0.37-1.14).

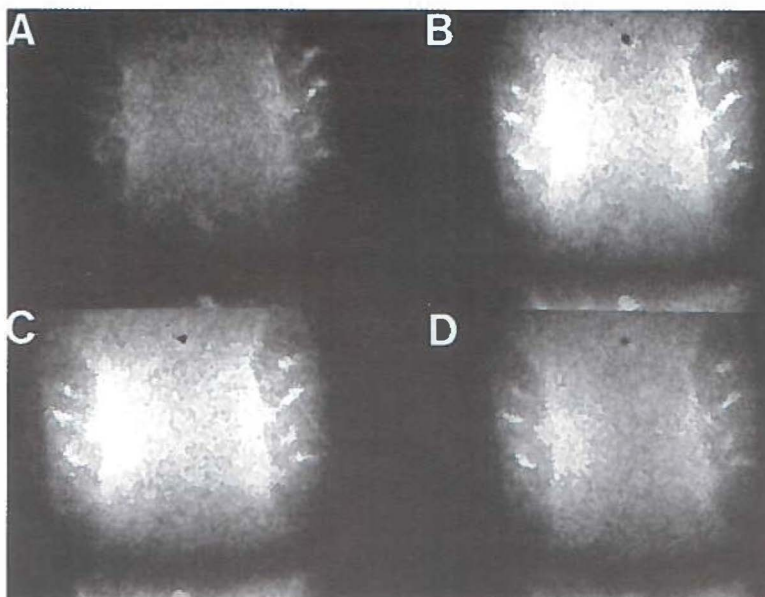


Figure 3.2.7 Four digitised fluorescence images of the same rat palate. **A:** Start of irradiation. **B:** Two minutes after irradiation. **C:** Four minutes after irradiation **D:** Eleven minutes after irradiation. The molars are indicated (M) and the area of interest is the mucosa between the molars. In figures B and C can be clearly seen that the fluorescence intensity increased during irradiation. After 11 minutes a slight decrease of fluorescence can be seen (D).

underneath 0.4, 0.8 and 1.5 mm thick mucosa respectively. The light dose can be reduced by 25% underneath areas of thick normal mucosa.

Both, the curve of the isodose-lines and reduction of light penetration, resulted in histologically observable reduction of PDT-induced damage. Calculated from the dosimetry and the Monte Carlo simulations the variation in light dose at the surface of the mucosa is between 122 ($40\text{J} \times 3.05 \times 1$) and 30.5 J/cm^2 ($40\text{J} \times 3.05 \times 0.25$). At a depth of 0.4 mm the dose was approximately 57 J/cm^2 ($40\text{J} \times 2.85 \times 0.5$) at the centre of the beam. At the periphery at 0.4 mm depth, the dose was approximately 11.4 J/cm^2 ($40\text{J} \times 2.85 \times 0.1$).

Figures 3.2.3B to D show the epithelial layer of rats treated with PDT. Generally two types of effects can be seen. First, the periphery of the irradiated epithelial layer shows residual dysplasia while at the centre the dysplasia has been ablated and replaced by normal epithelium. Second, due to increased thickness of the keratin and epithelial layer, the epithelial layer had not completely sloughed off, sometimes not even at the centre of the beam.

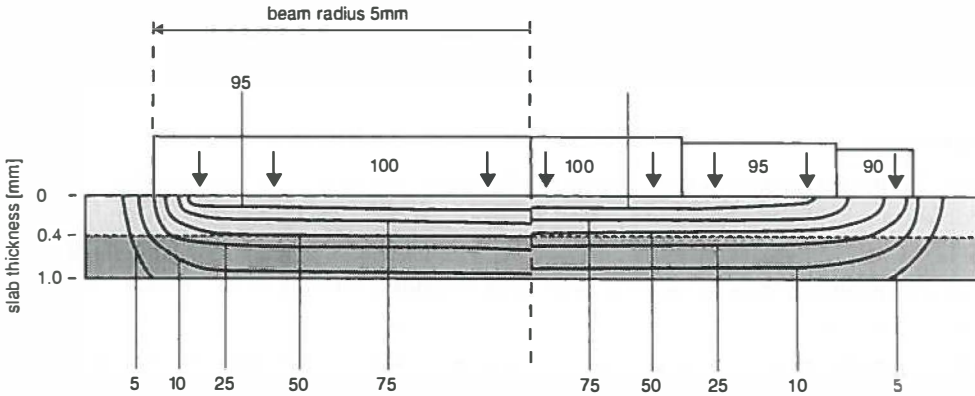


Figure 3.2.8 Monte Carlo simulations of the light distribution in mucosa and bone with a ideal light beam (left half) and the beam used in the experiments, with a 10% decrease towards the periphery (right half). The lines connect points with the same fluence (isodose-lines). The loss in fluence at the periphery in the tissue contributed to the failure of treatment. Remarkably, the beam profile was reflected in the damage pattern in the mucosa as shown in figures 3.2.3 and 3.2.4.

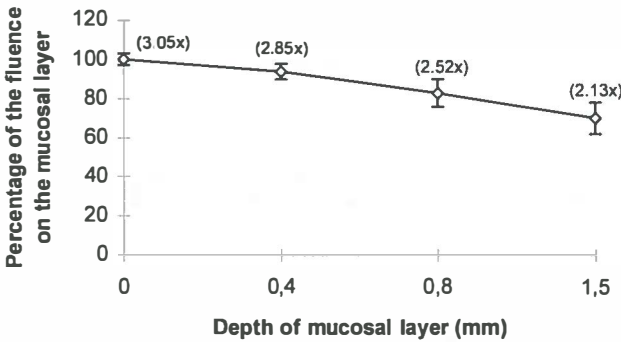


Figure 3.2.9 Results of the light dosimetry measurements under palatal mucosa. The fluence is calculated as a percentage of the fluence on the mucosa (100%). The real fluence can be calculated using the measured multiplication factors indicated between the parentheses.

Retrospective analysis of mucosa thickness of rats treated with 4NQO

Figure 3.2.10 shows the results of the morphometric analysis. Clearly, with increasing EAI the rats developed a thicker keratin and epithelial layer. Spearman correlation analysis of keratin thickness vs. EAI and epithelial thickness vs. EAI showed strong correlations of 0.93

and 0.83, respectively (both $p < 0.0001$). In absolute measures the keratin layer thickened from 73 μm (normal rat) to 356 μm (26 weeks 4NQO-treatment). The epithelial layer thickened from 151 to 581 μm , respectively.

DISCUSSION

Many studies investigating PDT, focus on the aspects of sensitizer accumulation in tumours (Peng *et al.*, 1990; Frisoli *et al.*, 1993; Tralau *et al.*, 1987). In the present and a previous study, we found significantly higher fluorescence intensities in palatal mucosa with SCC or advanced dysplasia than in mucosa with mild dysplasia (Witjes *et al.*, 1996a, chapter 2.1). However, this did not result in a larger necrotic area of the SCC containing mucosa but in a smaller necrotic area or even absence of necrosis in some rats. Light distribution in tissues, or rather the inhibition of sufficient light penetration, seemed to predominate the treatment outcome. In the 4NQO tumour model the light penetration was hampered by an increase in thickness of the keratin and epithelial layer due to the progression of dysplasia and squamous cell carcinoma.

Several studies showed that the concentration and the localisation of a sensitizer in tissue is important for the treatment outcome (Peng *et al.*, 1995; Chan *et al.*, 1988; Bown *et al.*, 1986). In general, it can be expected that increasing the sensitizer dose will result in increased tumour necrosis. In rats with normal untreated palatal mucosa, the dose combination of 1 μmol AIPcS₂ and 40 J/cm² incident light was maximal tolerated dose for normal

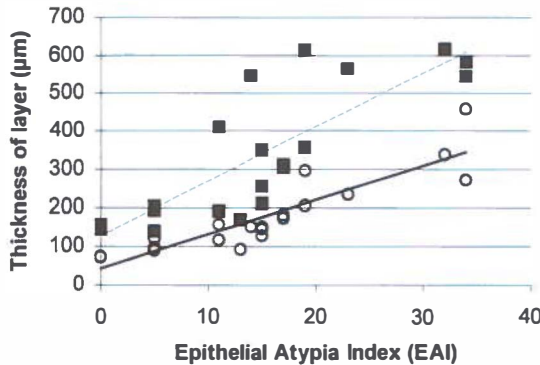


Figure 3.2.10 Retrospective analysis of the increase of thickness of the epithelial (dotted line) and keratin layer (continuous line) as dysplasia increases ($n=20$). The dysplasia is expressed as the EAI. Each point represents a measurement in triplicate. For both layers a strong correlation existed between the increase of EAI and the increase of thickness of the keratin layer ($r=0.93$) and the epithelial layer ($r=0.83$)

tissues. A further increase will result in permanent loss of bone or even fistulas in thin normal mucosa. However, this dose combination was not sufficient for sloughing off the thickened dysplastic mucosa. The light penetration was hampered in the thickened mucosa resulting in less tumour necrosis as well as less collateral damage. For obtaining the desired sloughing of the dysplastic mucosa the light dose and/or the AlPcS₂ dose can be increased. The fluorescence measurements during PDT showed that a large proportion of AlPcS₂ still is present in the tissues after irradiation (on average $83 \pm 16\%$). Therefore increasing the light dose seems preferable. Furthermore, from a previous normal tissue damage study it became clear that the collateral damage in the tissues of the palate is more difficult to control when the AlPcS₂ dose is increased than when the light dose is increased.

In vitro irradiation of tumour spheroids showed increasing resistance to PDT with increasing diameter (West, 1989). Besides the possibility of reduced light penetration in thick spheroids, the possibility of heterogeneous intracellular drug levels was postulated. Evidence for this hypothesis was found by the analysis of sensitizer-fluorescence and cell loss. Cells obtained from spheroids with a lower sensitizer-fluorescence level showed less necrosis than cells with a high fluorescence level (West *et al.*, 1989). Other authors found that PDT-induced hypoxia can reduce the efficacy *in vitro* (Foster *et al.*, 1993). During PDT, oxygen is utilised when singlet oxygen is generated. Areas of insufficient oxygenation (i.e. centre of tumour) will generate no or little singlet oxygen. All these mechanisms are able to influence the treatment outcome and need to be accounted for. However, in the present study the damage to the epithelial layer as well as to deeper layers was reduced when the EAI increased. In fact, the damage-grading list exists of a substantial number of pathological alterations to the tissue-layers beyond the epithelium. This strongly suggest that the reduced light penetration was responsible for the observed lesser damage. Evidence for light dosimetry being the limiting factor *in vivo* was found by other authors as well (Marijnissen *et al.*, 1992). They demonstrated that treatment failure of tumours was most likely caused by insufficient light dose or inadequate light dose distribution and not by sensitizer dose.

It was remarkable to find that the recovery of PDT-injury in rats often resulted in a histological profile matching the beam profile (figure 3.2.4). This resulted in areas of high dysplasia at the edges, indicating no treatment effect, and areas of less dysplastic mucosa at the centre of the palate, indicating a treatment effect. The Monte Carlo simulations showed that the use of an imperfect beam with a bell shaped profile can result in a reduction of the applied light dose at the edges (figure 3.2.8). Furthermore, dosimetry measurements showed that an increase of thickness can result in a reduction of 25% of the light dose. Altogether, the reduction of effective light penetration resulted in remnants of vital dysplastic epithelial cells after irradiation. In some rats these cells were overgrown by newly generated epithelium and were automatically included in the connective tissue layer. This is a highly

undesirable situation since it may easily lead to infiltrative carcinoma. This inclusion of dysplastic cells can be avoided by choosing a dose combination by which the epithelial cells will be sloughed off.

We did not expect to find complete cures since squamous cell carcinomas induced by 4NQO are present over a wide area of the palate which is too large to treat. Furthermore it should be noted that the geometry of these induced autologous squamous cell carcinomas is different from solid transplanted or papillary tumours. The boundaries of these solid tumours are easier to locate whereas autologous induced squamous cell carcinoma is not sharply demarcated and less easier to separate from its environment. This results in different use of the dual selectivity that PDT offers. For instance, selective necrosis was obtained when experimental colon cancer was treated with PDT using AlPcS₁₋₄ (Barr *et al.*, 1990). Although in this study the success of treatment was attributed to the higher accumulation of AlPcS₁₋₄ in the colon cancer, it is more likely that the success was a result of selective irradiation rather than higher AlPcS₁₋₄ accumulation. The colon cancer was induced by repeated injections of 1,2 dimethylhydrazine dihydrochloride (DMH) which resulted in polyps, easily separated from the normal colonic mucosa. Selective irradiation was performed with a fibre, at the top of the polyps resulting in selective necrosis. As observed in our study a higher accumulation of sensitizer not necessarily results in more necrosis.

An increase of the fluorescence intensity of the mucosa during PDT was observed. This occurred already after 2 minutes of irradiation and varied substantially among the individual rats. The data show a plateau between 0-4 minutes after irradiation, which most likely represents an equilibrium between fluorescence increase and photodegradation (figure 3.2.6). After 4 minutes the photodegradation predominated, and after 11 minutes of irradiation the levels of AlPcS₂ were 83% of the fluorescence levels at $t=0$. *In vitro* studies showed that the increase of fluorescence during irradiation is caused by intracellular degranulation and reallocation of sensitizer (Peng *et al.*, 1991a). Whether this is also the case in our experiments could not be confirmed. The exact influence of the fluorescence increase on the efficacy of the PDT treatment is not known.

In conclusion, despite the presence of a higher amount of sensitizer, the results of the treatment of squamous cell carcinomas were mainly determined by a sufficient light dose. A significantly higher AlPcS₂ localisation in tumours was not sufficient enough to generate selective tumour necrosis after PDT. Here, the treatment was limited owing to the use of a light beam with a bell shaped profile and the increase of the thickness of the keratin and epithelial layer, as dysplasia progressed towards squamous cell carcinoma. Precise knowledge of the light dose applied to the tissue as well as the depth of the desired necrosis is extremely important for successful treatment of cancer by PDT.

3.3 INCREASE OF ALUMINIUM PHTHALOCYANINE DISULPHONATE MEDIATED FLUORESCENCE DURING PDT *IN VIVO*

INTRODUCTION

Photochemical breakdown of a photosensitizer during irradiation with light in one of its absorption bands can be observed as a decrease in the intensity of emitted fluorescence light as the applied light-dose increases. This bleaching of sensitizer-fluorescence was first observed in relation to PDT *in vitro* by Moan (Moan, 1986) and later *in vivo* by Mang (Mang *et al.*, 1987), both investigating derivatives of hematoporphyrin. It was found to be an important effect since the photodegradation of sensitizers can be an advantage in controlling the PDT induced damage, or a disadvantage if a strong PDT effect is needed. A remarkable increase of fluorescence during irradiation *in vitro* was reported for both sulphonated metalphthalocyanines (MPcS_n) and sulphonated tetraphenylporphyrins (TPPS_n) by several authors (Rück *et al.*, 1990; Ambroz *et al.*, 1994; Peng *et al.*, 1991a; Berg *et al.*, 1991). It was shown to be a migration or release of these sensitizers from intracellular vesicles in the cytoplasm. This complex process depends on factors like the intracellular location of the dyes, their lipophilicity and binding-efficiency to substrates, photochemical reactions, and appears to be different from hematoporphyrin derivatives. The significance for PDT treatment of the intracellular release of phthalocyanine from vesicles is unclear. In culture, cells which showed an increase of TPPS₂-fluorescence during irradiation were more efficiently photoinactivated whereas an increase of TPPS₄-fluorescence resulted in less efficient photoinactivation of cultured cells (Moan *et al.*, 1992). To be photodynamically active, a sensitizer should be in the proximity of vital cell structures or more precisely certain target molecules, which when damaged will lead to cell necrosis. It is not known which cellular targets are ultimately responsible for cell necrosis using aluminium phthalocyanines, although damage to DNA, cell membranes and mitochondria has been observed (Rosenthal, 1991; Salet *et al.*, 1990; Ben-Hur *et al.*, 1987).

This study showed an unexpected increase of phthalocyanine-fluorescence during PDT *in vivo*. Our findings and those of others were simultaneously reported in different tissues and tumour models (Rück *et al.*, 1996; Witjes *et al.*, 1995b; Moan *et al.*, 1996). Rück *et al.* (Rück *et al.*, 1996) found an increase of fluorescence during PDT with AlPcS₄, but not for liposome bound ZnPc in a rat bladder tumour model. Moan *et al.* (Moan *et al.*, 1996) found an increase in fluorescence AlPcS₂, TPPS₄ and liposome bound ZnPc in mouse skin. Both groups explained the increase as a result of intra-cellular release of sensitizer from vesicles identical to the *in vitro* mechanism. *In vivo*, however, the mechanism of this increase is

much more difficult to assess, since an organism cannot be compared with a closed system like a petri dish. We have investigated this phenomenon in normal and tumour tissue, in relation to the time interval between administration and irradiation and following arrest of circulation.

MATERIALS & METHODS

Sensitizer

Aluminium phthalocyanine disulphonate (AlPcS₂) was obtained from Porphyrin Products Inc. (Logan, UT, USA). The fraction consisted of >90% pure AlPcS₂ of one isomer. For injection the drug was first dissolved in 0.1 M NaOH (pH 12). The pH was adjusted to approximately 7 by adding an equal volume of 0.1 M HCl after which the solution was buffered in phosphate buffered saline.

Animals and tumour model

Either normal healthy male Wistar albino rats of 8 weeks old were used or rats with chemically induced dysplasia and/or tumours. When 4-nitroquinoline-1-oxide (4NQO) is applied 3 times per week to the mucosa covering the hard palate of the rats, dysplasia of the epithelium develops. During the procedure the rats were anaesthetised with a mixture of N₂O/O₂ (3:1) and 2.5% Halothane. The 4NQO was gently applied with a small brush on the hard palate. The rats were housed under standard conditions with a 12 h dark/light period and chow and water *ad libitum*. Forty rats were divided in 5 groups of 8 rats each and subjected to 4NQO-application periods of 8, 12, 16, 20 and 26 weeks. This regime will induce very mild dysplasia, mild dysplasia, dysplasia, severe dysplasia and squamous cell carcinoma, respectively (Nauta *et al.*, 1996a).

Imaging and light delivery system

The imaging system for recording the *in vivo* fluorescence consisted of a home made endoscope (palatoscope) connected to an intensified CCD-camera as described in chapter 2.1. The images were digitised by a PC-based framegrabber, averaged over 16 frames and analysed by grey-scale measurement of the pixels (256x256) (van Leengoed *et al.*, 1993a, chapter 2.1). During all experiments the rats were anaesthetised with a mixture of O₂/N₂O (1:3) and 2.5% ethrane and placed in a stereotactic frame which was placed on an XY-table.

For PDT-irradiation a dye laser pumped by an Argon ion laser (Spectra Physics models 2040E and 375B, San Jose, CA, USA) was used. A birefringent filter and a monochromator (Oriel model 77320, Stratford, CT, USA) were used to tune the dye laser to

emit red light of 672 ± 1 nm wavelength using DCM as the dye. The laser light was fed via a 200 mm diameter optical fibre into the palatoscope. A nearly circular beam of approximately 1 cm in diameter was produced by the palatoscope with an incident power density of 60 mW/cm^2 . This irradiance was used in all PDT-irradiation experiments. For delivering a light dose of for instance 20 J/cm^2 a PDT-irradiation time of 5.5 minutes was necessary.

Experimental procedure

Three series of experiments were performed on normal rats and rats with 4NQO-induced premalignant lesions and squamous cell carcinomas. The first experiment was originally designed for investigating PDT-damage to normal palatal mucosa (chapter 3.1). The occurrence of an increase of fluorescence was not anticipated and therefore the fluorescence measurements were only performed before and after complete irradiation. Thirty-six normal untreated rats were divided into 9 groups of 4 rats each and each group was given one dose of AIPcS₂ and light. The method of fluorescence detection in this experiment has been described in chapter 2.1. Six hours after the intravenous injection of AIPcS₂, autofluorescence images were recorded using 460 ± 20 nm excitation light and a dichroic mirror of 550 nm to block the excitation light and a bandpass filter of 675 ± 15 nm to select the emission band. AIPcS₂ fluorescence was excited at 610 ± 15 nm and recorded, using a dichroic mirror of 650 nm and the 675 ± 15 nm band pass filter. The light source was a halogen lamp and the excitation intensity for both wavelengths was 0.2 mW/cm^2 . Immediately after recording of the fluorescence images the liquid light guide of the fluorescence excitation light was replaced by the optical fibre of the laser and PDT-irradiation started. Immediately after irradiation the liquid light guide of the fluorescence excitation light was switched back and fluorescence images excited by 460 ± 20 nm and 610 ± 15 nm were recorded. After a period of 5 minutes in the dark, fluorescence images were recorded again for 32 animals.

The second experiment consisted of irradiation of rats with 4NQO-induced dysplasia and SCC on the palatal mucosa, 6 h after injection of $1 \mu\text{mol/kg}$ AIPcS₂. Now, the increase of fluorescence was anticipated and therefore the fluorescence images were taken *during* PDT-irradiation with 672 nm light. The palatoscope allowed light-delivery and fluorescence detection at the same time. Fluorescence was detected using a 3 mm thick long wavelength pass RG 695 nm Schott filter. The high intensity of the AIPcS₂-fluorescence was reduced by a 10% grey filter and still enough fluorescence could be collected for imaging at this wavelength which is above the wavelength of maximum emission. PDT started 6 h after

injection and images were recorded at the beginning and after 2, 4, 6, 8 and 10 minutes of continuous PDT-irradiation.

For the third experiment 20 normal untreated rats were divided into 5 groups of 4 rats each. This experiment was performed to investigate whether an increase of fluorescence could be observed under different conditions. The rats of 3 groups received a dose of respectively 0.5, 2 and 4 $\mu\text{mol/kg}$ AlPcS₂ and were PDT-irradiated 6 h after injection. One group received a dose of 2 $\mu\text{mol/kg}$ AlPcS₂ and was PDT-irradiated 24 h after injection. Furthermore, experiments were performed on one group of rats which were injected with 4 $\mu\text{mol/kg}$ AlPcS₂ and sacrificed 6 h later, just prior to irradiation. This experiment was performed to investigate the role of the cellular fluorescence dynamics without the interference of bloodflow. After cessation of the bloodflow the cells will remain viable during the short irradiation period.

The design of the experiment was as follows: six hours after injection fluorescence images were recorded. Due to damage of some filters, the third experiment was performed as described in the first experiment instead of the preferred method of the second experiment (fluorescence imaging during PDT). The rats were sacrificed by deprivation of O₂ and an overdose of ethrane. Upon death, PDT-irradiation with 672 nm laser-light started immediately at the intermolar area. Fluorescence images were now recorded 1, 2, 3, 4, 5, 10 and 15 minutes after irradiation as described for the first experiment. At each interruption the laser optic fibre was replaced by the liquid light guide for fluorescence excitation and vice versa.

In addition, irradiation experiments with 672 nm light (60 mW/cm²) were performed with AlPcS₂ in solution to investigate its fluorescence dynamics in comparison with the *in vivo* data. The essence of these experiments is to investigate the fluorescence dynamics of aggregates during irradiation which are formed when AlPcS₂ is dissolved in serum. Cuvettes containing 4 $\mu\text{mol/l}$ AlPcS₂, dissolved in either bovine serum or methanol (MeOH), were irradiated at the same settings as the *in vivo* experiments. This concentration is approximately the amount of AlPcS₂ administered to the rats (4 $\mu\text{mol/kg}$). One set of 4 cuvettes of each solution was immediately irradiated and another set of 4 cuvettes of each solution was kept in the dark. Fluorescence images were recorded of both sets, prior to and after irradiation via the palatoscope with excitation light of 610 \pm 20 nm, 0.1 mW/cm². Autofluorescence of the solvents was negligible.

RESULTS

The digitised images displayed strong fluorescent bands along the molars of the rat (fig 3.3.1). In this figure it appears as if the increase of the fluorescence signal was more

prominent in these strong fluorescent bands than in the middle of the palate, but this could not be confirmed by grey-scale measurements comparing the two areas. Therefore the complete area between the molars was averaged. During the first animal experiment the rats injected with a high dose of 2 and 4 $\mu\text{mol/kg}$ AlPcS₂ and irradiated with a low dose of light of 20 J/cm^2 showed an increase of fluorescence of which the increase of the dose combination 4 $\mu\text{mol/kg}$ -20 J/cm^2 was significant (paired student T-test $p < 0.009$, figure 3.3.2). The fluorescence intensities after irradiation are depicted as a percentage of the grey-scale level just prior to irradiation ($t=0$). The magnitude of the fluorescence increase varied among the rats individually (range 8-40 %). During the 5 minute intermission the fluorescence intensities did not alter much in most rats. However, in 3 rats, injected and irradiated with 0.5 $\mu\text{mol/kg}$ -160 J/cm^2 , 2 $\mu\text{mol/kg}$ - 20 J/cm^2 , and 4 $\mu\text{mol/kg}$ -20 J/cm^2 , an increase of fluorescence intensity was measured from 0.36 to 0.54, 1.28 to 1.38 and 1.40 to 1.56 times the fluorescence value at $t=0$ respectively. In 8 rats the fluorescence intensities decreased slightly by approximately 10% within the 5 minute intermission.

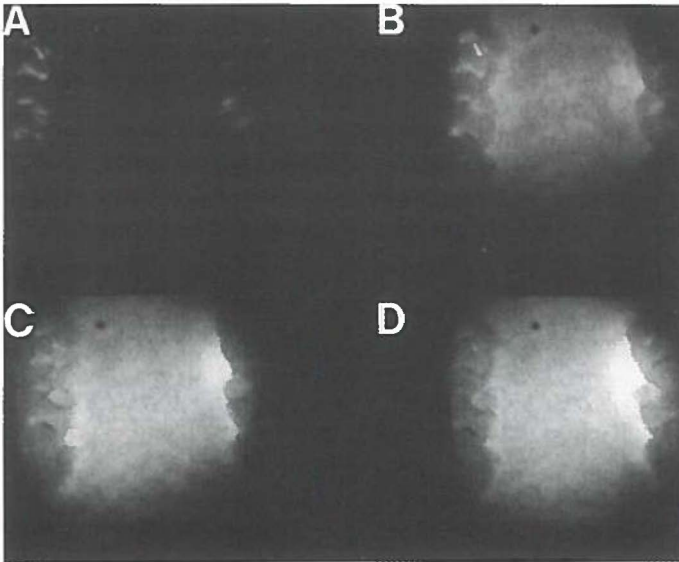


Figure 3.3.1 Four digitised fluorescence-images of the hard palate of a normal rat. **A:** Autofluorescence of the palate excited with 610 nm before injection of AlPcS₂. **B:** AlPcS₂-fluorescence after subtraction of the autofluorescence (610-460 nm) of the same palate 6 h after injection of 4.0 $\mu\text{mol/kg}$ AlPcS₂. **C:** AlPcS₂-fluorescence of the palate immediately after 5.5 minutes (20 J/cm^2) irradiation at 672 nm (60 mW/cm^2). **D:** AlPcS₂-fluorescence 5 minutes after the irradiation was stopped. Image C shows an increase of AlPcS₂-fluorescence immediately after irradiation and image D shows a further increase of AlPcS₂-fluorescence.

The results of the second experiment are shown in figure 3.3.3. From 4 rats no data could be obtained and from two rats only partially. This experiment differs from the first experiment because the fluorescence images were recorded during irradiation without interruption. On average the rats showed a slight increase of fluorescence 2 minutes after PDT-irradiation had started (2%, not significant). However, there were large individual differences in the grey-scale levels after 2 minutes of PDT-irradiation which ranged from 0.82 to 1.43 times the level at $t=0$. In most rats the fluorescence intensity started to decrease 4 minutes after irradiation. After having received a dose of 40 J/cm^2 (11 minutes of irradiation) the intensity dropped to 85% of the grey-scale value at $t=0$. Figure 3.3.4 displays digitised images of palatal fluorescence of one rat detected above 695 nm with an increase of fluorescence after irradiation. The images above 695 nm obtained during irradiation do not differ from the images obtained by subtraction of 460 nm and 610 nm images. The PDT-irradiation was not continued until complete bleaching was observed because the animals were primarily subjected to a study for PDT-effects on 4NQO-treated palates with a limited light dose (see chapter 3.2). No differences were measured among the 4NQO-treated groups indicating that the grade of dysplasia or the presence of tumours did not influence the effect.

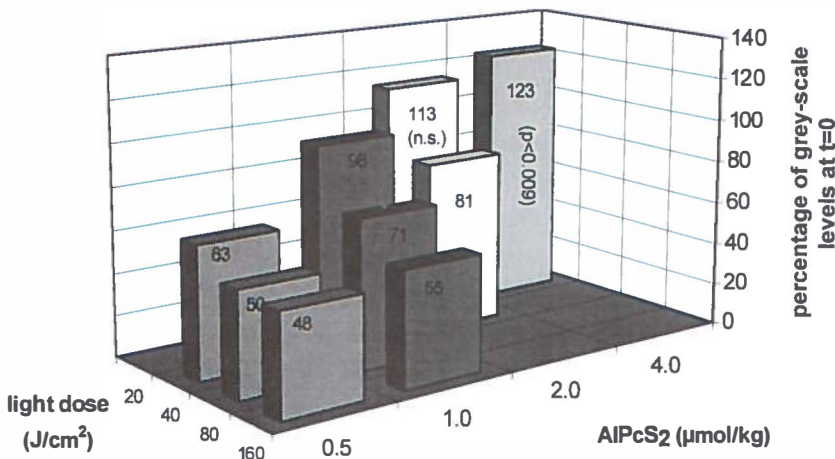


Figure 3.3.2 Results of fluorescence measurements at the palates of normal rats (experiment 1). Each bar represents an average of 4 rats and the measurements were performed immediately after irradiation was stopped. The grey-scale levels are plotted as a percentage of the measurements before irradiation ($t=0$). An increase of fluorescence was seen at the dose combinations of $2 \mu\text{mol/kg-}20 \text{ J/cm}^2$ and $4 \mu\text{mol/kg-}20 \text{ J/cm}^2$, of which the latter was significantly higher than $t=0$ (paired Students T-test, $p<0.009$). Standard deviations are not shown in the figure but ranged from 10-15%.

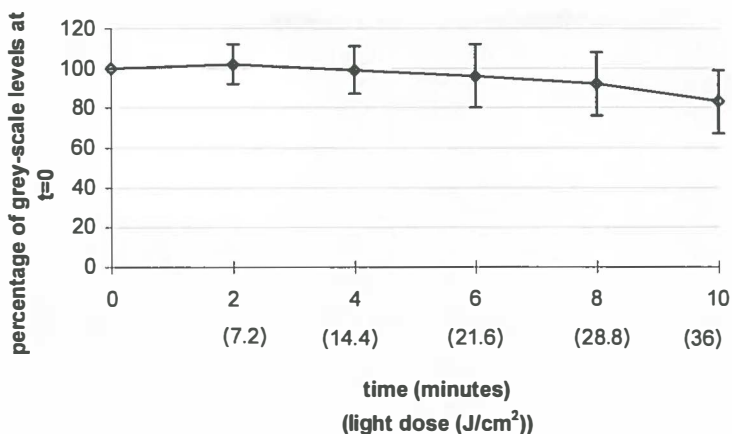


Figure 3.3.3 Results of fluorescence measurements at palates of 4NQO treated rats (experiment 2). Each point represents the average of fluorescence measurements of 36 rats. Although the differences between the fluorescence measurements are not significant, the curve within the first 4 minutes most likely represents a balance between photodegradation and an increase of fluorescence. After this time interval fluorescence decreases. Bars represent the standard deviation.

In figure 3.3.4 the results of the third animal experiment are depicted. The rats injected with 2 and 4 $\mu\text{mol/kg}$ showed an initial increase of fluorescence. This phenomenon was not influenced by a variation in time interval between injection of AlPcS₂ and start of irradiation (6 or 24 h). Three rats, injected with 4 $\mu\text{mol/kg}$, were lost during the anaesthesia and the plotted line in figure 3.3.5 representing the 4.0 $\mu\text{mol/kg}$ -group consists of data from one rat only. At t=1 the average fluorescence intensity of the 0.5 $\mu\text{mol/kg}$ group was approximately 94% of the grey-scale level at t=0. However, in one animal in this group an increase of 12% at the 2 minute interruption of PDT-irradiation was seen. No increase of fluorescence was measured in the palates of the rats which were previously sacrificed. In this group fluorescence images were recorded 6 h after injection of AlPcS₂, just before death. Upon death the irradiation started and images were recorded from 1-15 minutes after irradiation. Immediately after death a remarkably rapid decrease of 40% of the fluorescence intensity was observed in this group. This decrease coincided with the first minute of irradiation. Between 1 and 15 minutes after irradiation the fluorescence intensity decreased from 54% to 33% of the value at t=0.

The results of the fluorescence bleaching in solution experiment are depicted in figure 3.3.6. The data points represent the percentage of the grey-scale values relative to t=0. In MeOH the irradiation hardly altered the fluorescence intensity. Only after 20 minutes of

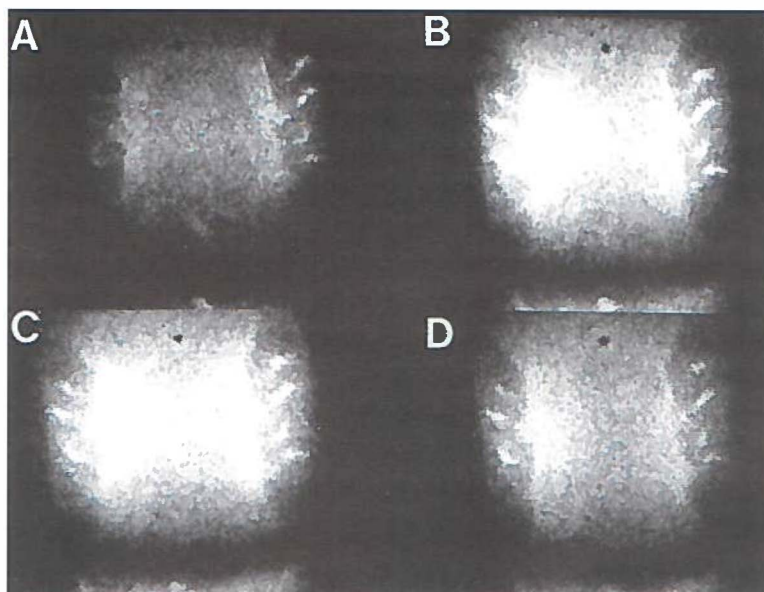


Figure 3.3.4 Sequential of digitised fluorescence images of the same palate of a rat treated for 8 weeks with 4NQO (mild dysplasia). The molars are indicated (M) and the area of interest is between the molars. Fluorescence was measured during irradiation with 672 nm (60 mW/cm^2) and detected by a long pass filter RG695. **A:** AlPcS₂ fluorescence at the beginning of the irradiation period ($t=0$). **B:** AlPcS₂ fluorescence 2 minutes after irradiation. **C:** AlPcS₂ fluorescence 4 minutes after irradiation. **D:** AlPcS₂ fluorescence 10 minutes after irradiation. Clearly an increase of fluorescence was detected which was still present after 10 minutes of PDT-irradiation.

irradiation some decrease of fluorescence was noted. This indicates that photodegradation was not induced in MeOH in the time interval which is comparable to the interval used for *in vivo* irradiation. The fluorescence intensities of the cuvettes containing AlPcS₂ dissolved in serum increased with time. Upon irradiation an immediate decrease of fluorescence was measured. However, after irradiation the fluorescence intensity increased again at a rate similar to the non-irradiated cuvettes.

DISCUSSION

The phenomenon of increasing fluorescence upon irradiation was unexpectedly observed after PDT (first *in vivo* experiment). It was reproduced during other *in vivo* experiments with an altered setting. The data from the first *in vivo* experiment show only an initial increase of fluorescence at doses of 2 and 4 $\mu\text{mol/kg}$ AlPcS₂ and 20 J/cm^2 (figure 3.3.3). Low doses of

AlPcS₂ did not show any increase of fluorescence. However, this experiment does not

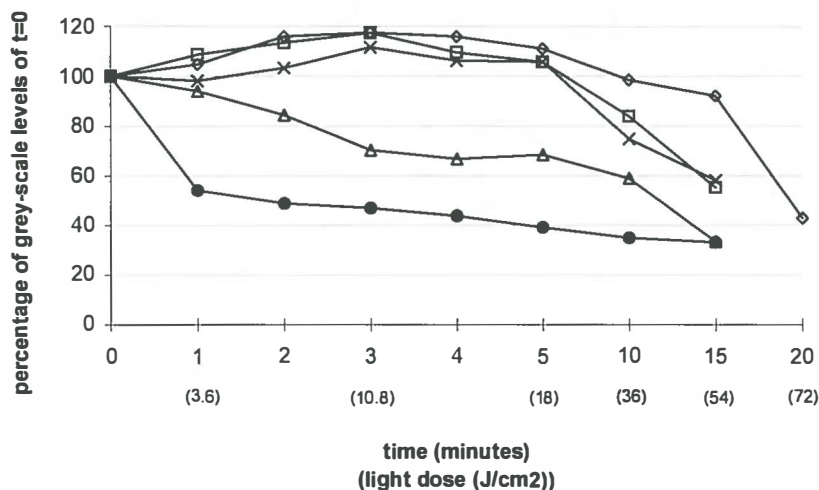


Figure 3.3.5 Fluorescence data from the palate of normal rats irradiated during the 3rd experiment. Symbols represent rats irradiated 6 h after injection of 0.5 $\mu\text{mol/kg}$ (Δ), 2 $\mu\text{mol/kg}$ (\square) and 4 $\mu\text{mol/kg}$ (\circ) AlPcS₂. The other symbols represent data from rats irradiated 24 h after injection of 2 $\mu\text{mol/kg}$ (\times) AlPcS₂ and rats sacrificed 6 h after injection and prior to irradiation (\bullet). In all rats an increase of fluorescence was seen or a slow decrease of fluorescence, except for the previously sacrificed rats. In this group the rats showed a remarkable drop of fluorescence by more than 40%. Please note the change of scale of the X-axis. Standard deviations are not shown but range from 5-14%.

provide information on the kinetics of the fluorescence intensity during the irradiation period. During irradiation an initial increase of fluorescence may have been present with low drug doses (0.5-1 $\mu\text{mol/kg}$) but the major part of the fluorescence was bleached before observation of an increase of fluorescent was possible. Evidence supporting this hypothesis was found during the second and third experiment. Firstly, during the first 4 minutes of irradiation in experiment 2, several rats did show an increase of fluorescence (by max. 40%), although they were injected with a low dose of 1 $\mu\text{mol/kg}$. Secondly, one rat injected with only 0.5 $\mu\text{mol/kg}$ and irradiated during the third experiment showed increase by 12% within the first 2 minutes of irradiation. It is possible to induce an increase of fluorescence with low doses of AlPcS₂, but this was generally not seen because of the rapid photodegradation of the sensitizer. The establishment of the plateau between 0 and 4 minutes in figure 3.3.4 most likely represents a dynamic equilibrium between the rate of photodegradation and the rate of increase of fluorescence. The existence of an equilibrium between photodegradation and fluorescence increase during the initial period of irradiation has been described *in vitro* (Rück *et al.*, 1990). However, *in vitro* it was seen within seconds

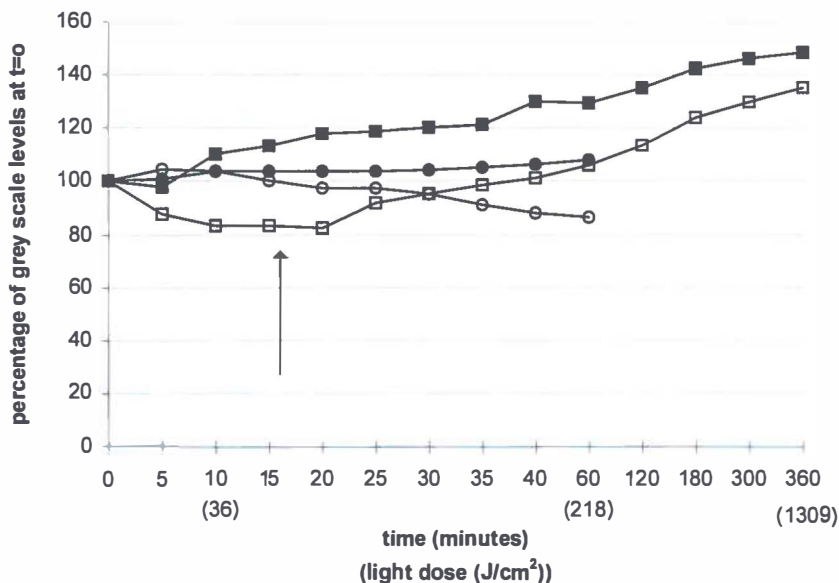


Figure 3.3.6. Data from the *in vitro* experiments with serum and methanol. Symbols represent fluorescence measurements of cuvettes with 4 $\mu\text{mol/l}$ AlPcS₂ dissolved in MeOH, not irradiated (●) and irradiated (○) or dissolved in serum, not irradiated (■) and irradiated for 20 minutes after which irradiation was stopped indicated by the arrow (□). Please note the change of scale of the X-axis. Standard deviations are not shown but range from 5-11%.

after irradiation (675 nm) and in our setting it was seen within several minutes of irradiation (672 nm). Remarkably, when the applied light doses are compared the phenomenon occurred *in vitro* at the same total light dose of approximately 20 J/cm² as in our *in vivo* experiments. Also other *in vitro* experiments using 633 nm excitation light and a dose of 30 J/cm² showed increase of fluorescence during irradiation (Ambroz *et al.*, 1994).

It was demonstrated that the increase of fluorescence in cultured cells *in vitro* is a result of release from intra-cellular vesicles or lysosomes which become permeable upon irradiation (Peng *et al.*, 1991a). In these *in vitro* experiments, spatial shifts of phthalocyanine molecules were observed, resulting in a different distribution in the cytoplasm after irradiation, indicated by a change from a granular fluorescence pattern to a more equally distributed fluorescence pattern. Single cells were irradiated and analysed for changes in grey-scale levels. *In vivo*, large quantities of cells from different layers of tissue are irradiated at the same time. Also measuring fluorescence intensities by constantly switching between the PDT-irradiation fibre and liquid light guide for fluorescence

excitation light actually results in intermittent irradiation of the tissues. The time required for recording fluorescence images was approximately 30 seconds, which can be enough for relaxation effects to occur. These effects may include the reformation of aggregates or binding to proteins (Rück *et al.*, 1990). The results of the first and third experiment could be affected by this. However, it does not explain the basic phenomenon of increase in fluorescence. During the second experiment the palatal mucosa was constantly irradiated and fluorescence measurements did not interfere with the PDT-irradiation and an increase of fluorescence was observed in some rats. Intermittent irradiation may contribute to the magnitude of the increase and interfere with the dynamics but did not cause it.

The experiments on the previously sacrificed rats were performed to exclude the possible role of circulation in increased fluorescence. We assumed that when the palate was irradiated immediately after sacrifice of the animal, cellular effects could be discriminated from possible circulatory or vessel effects like constriction or dilatation because the cells of the palatal mucosa remain viable within the irradiation period. Surprisingly, the grey-scale levels dropped by more than 40% within the first minute of irradiation. It is impossible to establish whether this was caused by simply a complete lack of circulation or induced by the absence of physiological responses. Since sacrifice had such a dramatic effect on the grey-scale levels it is clear that even if cellular effects like a redistribution or a deaggregation in the cytoplasm were present, they would be masked by the changes in circulation. We therefore suspect that the observed phenomenon of the increase of fluorescence *in vivo*, was mainly an effect of the changes of the local circulation or induced by physiological responses of the tissues, possibly in combination with effects at the cellular level but those had a relatively small contribution to the total amount of fluorescence. It has been shown that PDT with phthalocyanines can have various effects on the local circulation of irradiated tissues. The sequence of the reported vascular effects are generally described as an initial vessel dilatation followed by a vessel constriction, vessel leakage or congestion by blood clots (Moore *et al.*, 1992; van Leengoed *et al.*, 1993b; Fingar *et al.*, 1993). Sometimes vessel dilatation occurred as a consequence of a local constriction elsewhere. The palatal mucosa is a well vascularized tissue and blood contains large amounts of phthalocyanines after injection, and subsequently vessels show high fluorescence (Lamuraglia *et al.*, 1993; van Leengoed *et al.*, 1993a). A constantly present enhanced blood flow would not have resulted in a decrease of fluorescence after 4 minutes, since the circulation would supply the area with new ALPcS₂ molecules. It is therefore possible that after some time during irradiation the effects on the blood flow were reversed or the circulation was hindered by vessel occlusion (van Leengoed *et al.*, 1993b; Star *et al.*, 1986). Also from figure 3.3.3 it can be

concluded that increasing the light dose from 80 to 160 J/cm² does not further decrease the fluorescence (compare levels of 0.5 µmol/kg AlPcS₂ and 80-160 J/cm²).

Hardly any *in vitro* photodegradation was induced of AlPcS₂ dissolved in MeOH within the time segment used for bleaching *in vivo*. Apparently the AlPcS₂ molecules were minimally affected by the applied light. Bleaching of a sensitizer *in vivo* is probably caused by type I processes (Spikes, 1992). It is thought that the excited sensitizer reacts with nearby substrates like or is destroyed by its own generated singlet oxygen, and subsequently quenching of fluorescence occurs (Spikes, 1992). When AlPcS₂ was dissolved in serum a slow increase of fluorescence was seen in time in the cuvettes which were kept in the dark. Probably aggregates of phthalocyanines or weak bonds with serum proteins were formed which slowly dissolved in time. In contrast to the AlPcS₂ dissolved in the MeOH, the irradiation of AlPcS₂ dissolved in serum resulted in photodegradation, without an initial increase (fig 3.3.7). From the irradiation experiments of AlPcS₂ in solution it can be concluded that serum components are needed for inducing photodegradation. Furthermore, the rate of dissolving of the aggregates of phthalocyanines was not influenced by irradiation. It is therefore unlikely that the observed increase of fluorescence *in vivo* can be explained by light induced disaggregation of AlPcS₂ molecules.

In conclusion, the observed increase of fluorescence indicates an increase of AlPcS₂ in the monomeric form. There seems to be an equilibrium between the rate of photodegradation and the increase of fluorescence *in vivo*, which is influenced by the amount of sensitizer and total light dose. The increase was most likely associated with physiological or vascular changes rather than intra-cellular effects. However, these experiments could not completely discriminate between intra-cellular effects and other tissue effects. The phenomenon of the fluorescence increase was not restricted to tumour tissue but can also occur in normal tissue. The relevance for PDT of the increase of fluorescence, and thus more monomeric AlPcS₂ in the tissue, remains to be elucidated.

IV

GENERAL DISCUSSION AND SUMMARY

4.1 GENERAL DISCUSSION

FLUORESCENCE LOCALISATION OF ORAL SQUAMOUS CELL CARCINOMA

In the present investigations we used a specially built palatoscope which allowed full screen analysis of an area of approximately 1 cm^2 (figure 4.1.1). Small lesions of the palatal mucosa of Wistar rats of 1-2 mm can be detected and endoscopy based fluorescence imaging therefore seems a valuable tool in the detection of superficial or early cancer. It is relatively simple to apply in humans, it produces high resolution images and may be more cost effective when compared to other imaging techniques (MRI, CT, PET). Especially the possibility of detailed analysis of an area by fluorescence imaging is interesting for clinical applications. Clinically not visible extensions of a tumour may be visualised during a diagnostic work-up of a patient. Furthermore, fifteen to twenty percent of patients with oral cancer will develop a new tumour (second primary tumour) due to field cancerization of their mucosa. Early detection by regular screening of these patients for second primary

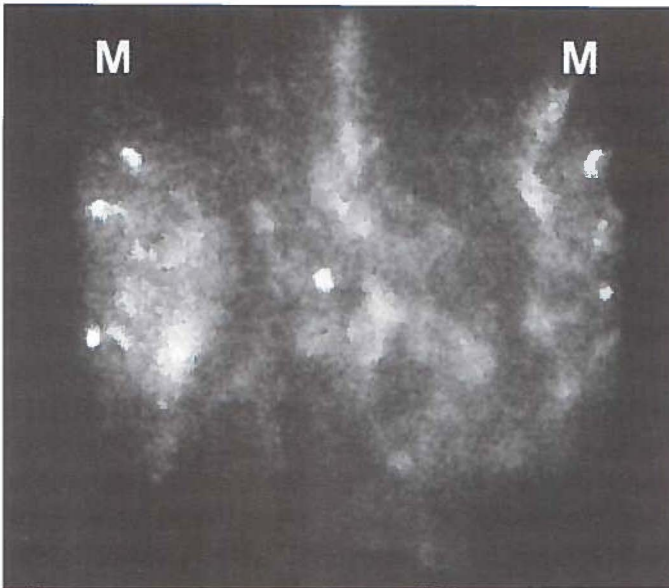


Figure 4.1.1 Endoscopic autofluorescence image of rat palate treated with 4NQO. M indicates the molars. The true dimension of this complete image is approximately 1 cm^2 . Clearly the image from the mucosa between the molars shows a lot of detail from a small area ($0.5 \times 1.0 \text{ cm}$).

tumours may yield an early treatment and therefore a higher survival rate. A disadvantage of the fluorescence imaging is that it is at best semi-quantitative. Designing a system which is well calibrated may be possible but will be difficult since the results of the fluorescence detection are influenced by the positioning of the scope above the tissue or by variations in the geometry of tissues (and thus variations in light distribution). Like other imaging techniques, fluorescence imaging is not able to indicate the nature of a detected lesion and biopsies are necessary to differentiate between malignancies and inflamed tissue.

The 4NQO-model proved to be a suitable model for endoscopic fluorescence imaging analysis. Sites of tumour development in the palatal mucosa after 4NQO treatment cannot be predicted; which makes experiments with this model challenging. Furthermore, the time interval between injection of AlPcS₂ and maximal tumour fluorescence was different in this model (2-10 h) from what usually is reported (24-48 h). The fact that this model studies induced cancer instead of transplanted tumours may be important in this respect. The applicability of fluorescence imaging depends strongly on the behaviour of the probe. In the rat palatal mucosa, AlPcS₂-fluorescence was easily detected at a low dose which makes it interesting to use. This study showed that the photosensitizer AlPcS₂ is able to accumulate in dysplastic tissue and invasive squamous cell carcinoma. However, although AlPcS₂ was very sensitive for alterations to the mucosa, the tumour specificity of the hot spots was rather low in our tumour model. This was most likely caused by the fact that AlPcS₂ also accumulates in inflamed areas. This type of inflammation, often caused by inserted dietary fibres, is a prominent feature of our tumour model.

In addition to good tumour localising properties, a photosensitizer used in fluorescence localisation should be rapidly cleared from the body to prevent skin photosensitization. This is important when fluorescence imaging is used for screening of tumours. Little is known of the skin photosensitivity of AlPcS₂. More extensive investigations are necessary on this topic before using it in humans. Other fluorescent probes, not necessarily photodynamically active, should be investigated as well as sensitizers for fluorescence imaging.

In this study we also found higher autofluorescence levels in dysplastic mucosa compared to normal palatal mucosa. Most likely this increase in autofluorescence was caused by the increase of production of certain fluorophores like keratins. The use of autofluorescence as a mean for tumour detection has been successfully applied in other areas of the body (e.g. cervix or colon, Ramanujam et al., 1994; Richards-Kortum et al., 1991). However, in the literature a limited number of studies are available. Therefore the technique of detection of dysplasia and tumours by analysing the alterations to the autofluorescence needs to be further explored.

In conclusion, the value of endoscopic based fluorescence imaging should be investigated in clinical studies. The occurrence of AlPcS₂-induced skin photosensitization should be more thoroughly investigated before using this photosensitizer in humans.

PHOTODYNAMIC THERAPY OF ORAL SQUAMOUS CELL CARCINOMA

The objectives of this study were to investigate the effect of AlPcS₂-based PDT on the normal tissues, to find an optimal time interval for treatment, to find a safe dose combination of light and AlPcS₂ and to study the efficacy of PDT on epithelial dysplasia and squamous cell carcinoma. The time interval between injection and therapeutic irradiation used in this study was based on the fluorescence studies performed on the 4NQO tumour model. We found that AlPcS₂ accumulates in dysplastic epithelium and tumour tissue within the first 10 h after injection. In the literature the reports on this optimal time interval are not consistent, although irradiation often is performed 24 or 48 h after injection of AlPcS₂. We have chosen to irradiate the palate 6 h after injection of AlPcS₂ because this allowed injection and treatment within one day.

It was striking to see the extreme collateral damage that PDT can induce in bone and teeth. When the dose is high, palatal bone may completely be resorbed and leave a permanent fistula between the oral and nasal cavity and teeth may be resorbed as well and become ankylotic. This was not only found using AlPcS₂ as a photosensitizer but also in HpD-based PDT of the rat palate (Nauta *et al.*, 1996c). The fact that such severe damage is seldomly reported in the literature (Boyle, 1992) may indicate that these occur only in this model at this location. The rat palate is a small (less than 1 cm²) and thin (1 mm) structure. During our experiments the complete palate was irradiated. In rats, a "large" tumour of the palate would only be 2-3 mm in dimension. Therefore, for a rat the irradiated area was relatively large. Bone necrosis or resorption and dental ankylosis are unwanted side effects which may pose serious clinical problems. If these effects would occur in humans, PDT would not be an advantageous modality over surgery or radiotherapy. We expect, however, that due to a favourable difference in proportions between the irradiated area and the thickness of the surrounding normal structures, the side effects will be less severe in humans. For instance the light dose in human bone will be less due to a thicker mucosal layer. Furthermore it was possible, and relatively easy, to treat the rat palatal mucosa without most severe side effects by using a low drug/light dose combination. Only ankylosis of teeth could not be prevented. Therefore, areas with teeth *in situ* should be protected and not be irradiated.

After having established an optimal time interval for irradiation and having found a suitable dose combination, we tried to treat 4NQO induced epithelial dysplasia and

squamous cell carcinoma. Although a higher fluorescence level was present in mucosa with high dysplasia or squamous cell carcinoma, the PDT-induced damage was less in these rats compared to less dysplastic mucosa. Most likely this was caused by the reduction of sufficient light penetration due to thickening of the keratin and epithelial layer and, to a lesser extent, the bell shaped energy distribution of the light beam used. The higher amounts of AlPcS₂ in highly dysplastic mucosa could apparently not compensate for the reduced light penetration. This is an important feature of PDT. AlPcS₂ was still present in the tissues after irradiation and increasing the light dose seems therefore feasible. However, the precise relation between the drug/light dose combination and the desired depth of necrosis needs to be further explored. Dose calculation should be accurate otherwise over- or under treatment will be the result.

It was not possible to completely establish the efficacy of PDT of epithelial dysplasia and squamous cell carcinoma. This was caused by the reduced light penetration of thickened mucosa but also by the tumour model. Because 4NQO is applied on the palate with a small brush and spread by the tongue movements of the rat, the localisation of the carcinogen can not be controlled exactly and therefore dysplasia and even tumours will develop outside the area of interest. Dysplasia will always be present at the treatment margin and therefore complete cures are virtually impossible to achieve. However, slight dysplastic epithelium could be sloughed off completely and it can be expected that severe dysplasia and squamous cell carcinoma can be treated likewise because most of the AlPcS₂ was still present after the irradiation period.

During irradiation a peculiar increase of fluorescence was seen in the palatal tissues. The mechanism of this phenomenon is not clear. An increase of fluorescence during irradiation was first observed by others *in vitro*. and was attributed to a release of aggregated AlPcS₂ from lysosomes or vesicles into the cytoplasm. During our *in vivo* experiments fluctuations in the vascular component seem to predominate the fluorescence levels during irradiation. What the exact effect is of this increase of fluorescence on the efficacy of PDT is not clear.

Although this study shows good results of AlPcS₂-based fluorescence detection of oral dysplasia and carcinoma, the value of PDT of oral cancer is not entirely clear. Soft tissue defects, induced by PDT, regenerated very well. Carcinomas surrounded by soft tissue seem therefore suitable for treatment by PDT. However, the following subjects should be more thoroughly investigated before deciding to use AlPcS₂-based PDT in humans:

- The effect of varying the drug/light dose combination in relation to the desired depth of necrosis in AlPcS₂ based PDT of small local (autologous) tumours in animals.

- The effect of varying the time-interval between injection of AlPcS₂ and therapeutic irradiation to investigate whether the observed maximal tumour fluorescence 6 h after injection also yields maximal tumour necrosis.
- To develop a method of applying therapeutic light in the oral cavity which ensures a well defined area of irradiation while limiting the light dose in the surrounding healthy tissue.
- The possibility of using PDT as an adjuvant therapy to, or after failure of radiotherapy. Radiotherapy, a commonly applied cancer therapy, leaves the maxillary and mandibular bone prone to osteoradionecrosis. Vascular shutdown, induced by PDT, of bone irradiated during radiotherapy may have the same adversary effect and trigger this severe form of bone necrosis.
- In addition to the patient-related studies it is desirable that more research is devoted to develop techniques for inducing small autologous tumours with clearly defined boundaries in animals. 4NQO allows induction of reproducible oral dysplasia and carcinomas, comparable with the human situation. However, the “field cancerization” of this model is an important drawback for studying cure rates of PDT.

4.2 SUMMARY

The majority of tumours in the head and neck region are squamous cell carcinomas of the upper aerodigestive tract. Curative treatment modalities for these tumours are surgery, radiotherapy or a planned combination of both. The side effects of these treatment modalities can be severe. Surgery may result in mutilation and radiotherapy may result in xerostomia (dry mouth), mucositis or worse, severe necrosis of the jaw bones (osteoradionecrosis). Furthermore, an additional diagnostic tool for detecting early cancer would be helpful in the diagnostic work-up of the patient. Our particular interest is focused on epithelial dysplasia and carcinomas of the oral mucosa. Therefore diagnosis with fluorescence localisation and treatment with photodynamic therapy of experimental oral squamous cell carcinoma was investigated.

The basis of fluorescence localisation and photodynamic therapy (PDT) of tumours is the use of light sensitive drugs (photosensitizers) which accumulate in tumours at a higher concentration than in the surrounding normal tissues. Several of such photosensitizers are available. For this study the promising photosensitizer aluminium phthalocyanine disulphonate (AlPcS₂) was investigated. This photosensitizer can be located by fluorescence imaging and be used for PDT at the same time. Fluorescence localisation comprises the technique of activating (exciting) the photosensitizer with a low dose of light after which it emits light back (fluorescence). This fluorescence can be detected with a sensitive camera (charge couple device camera or CCD camera) and images of the investigated tissues can be displayed with the use of computers. This allows the detection of tumours when the photosensitizer has accumulated in tumours. A therapeutic effect is obtained when a sufficient amount of photosensitizer is present and light is applied to the tumour (PDT). Often lasers are used because these devices are able to generate light of a certain wavelength with sufficient optical power. Irradiation will result in necrosis of the tumour. In the literature, the advantage of PDT over surgery or radiotherapy was reported to be the induction of less permanent damage to the normal surrounding tissues because damage induced by PDT predominantly heals by regeneration of normal tissue.

Our interest was focused on several aspects namely 1) the possibility of detection of dysplasia and squamous cell carcinomas with AlPcS₂, 2) the effects on normal tissue of PDT with AlPcS₂ and 3) the efficacy of AlPcS₂ based PDT on epithelial dysplasia and oral squamous cell carcinoma. A previously developed tumour model was used, the 4NQO rat palatal tumour model (Nauta *et al* 1996a), which allowed detailed investigation of these aspects of PDT. The most important characteristics of the 4NQO model are described in chapter 1.4. Squamous cell carcinomas and the preceding premalignant stadia (dysplasia) of

this type of cancer can be induced by the chemical substance 4 nitroquinoline-1-oxide (4NQO). An important aspect of this model is that quantification of the premalignant stages is possible by the use of a histological grading list. Previous experiments revealed that the grade of dysplasia is strongly correlated to the extent of the 4NQO application period which makes this a predictable and useful tumour model.

I Fluorescence localisation of AIPcS₂ in dysplasia and oral squamous cell carcinoma

The essence of the fluorescence localisation experiment was to study the possibility of tumour localisation with AIPcS₂. In chapter 2.1 a method for the detection of AIPcS₂ in the mucosa of the palates of Wistar albino rats is described. AIPcS₂ fluorescence was used to create an image of the palatal mucosa of the rat. Such a fluorescence image can be analysed for the level of AIPcS₂ fluorescence as well as the fluorescence distribution pattern. The fluorescence signal of the excited AIPcS₂ is disturbed by the fluorescence signal from the rats' own tissue (autofluorescence). We found that this autofluorescence could be reduced to an insignificant level by the technique which is referred to as the dual wavelength excitation method. Light of 460 nm (blue light) does not excite the AIPcS₂ but only the autofluorescence while light of 610 nm (orange/red light) will excite both autofluorescence and AIPcS₂ fluorescence. When the autofluorescence image excited by 460 nm is subtracted from the 610 nm image by computer, only the AIPcS₂ fluorescence will remain. This is allowed because the autofluorescence excited at 460 nm is virtually identical to the autofluorescence excited with 610 nm.

The localisation of AIPcS₂ in dysplastic oral mucosa and tumour bearing rats was studied using the fluorescence imaging technique as described above. In a group of 20 rats several stages of dysplasia and tumours were induced by 4NQO by applying this substance for 8-26 weeks. Fluorescence images were recorded via a specially designed "palatoscope" with excitation at 460 ±20 nm for autofluorescence, 610 ±15 nm for AIPcS₂-fluorescence and detection of emission at 675 ±15 nm. AIPcS₂-mediated fluorescence increased significantly when the severity of dysplasia increased ($p < 0.04$). Also the phenomenon of strong fluorescent spots (hot spots) on the fluorescence images was observed, indicating areas of locally high amounts of AIPcS₂. These hot spots were only present within the first 10 h after injection of AIPcS₂. Histological analysis proved in 67% of these hot spots a local alteration to the mucosa which was either invasive cancer (29%) or inflammation (38%). These results suggest two different mechanisms of AIPcS₂ uptake in tissue, one associated with the presence of generalised dysplasia and another associated with local changes of the epithelial/connective tissue which is not necessarily specific for tumours. In PDT, the time interval between injection of the photosensitizer and the moment of irradiation is very important because the

concentration of the photosensitizer in a tumour will be maximal for only a certain period. From these experiments it was concluded that the optimal interval between injection of AlPcS₂ and irradiation should be within the first 10 h after injection.

When comparing these results with other published data it became clear that a large variety of optimal time intervals between injection and maximal tumour concentration of the sensitizer exists. One of the reasons for this diversity could be the fact that different techniques for the detection of AlPcS₂ in tumours were used in these studies. For that reason we investigated the kinetics of AlPcS₂ in the 4NQO tumour model by the use of the four most used fluorescence detection techniques (chapter 2.2). Investigated were 1) *In vivo* fluorescence imaging (as described above), 2) fluorescence microscopy, 3) conventional fluorimetry and 4) high performance liquid chromatography (HPLC) in combination with diode laser induced fluorescence (DioLIF). It would take too much to explain these techniques in detail therefore only a short description is given here. Fluorescence microscopy analyses the AlPcS₂ content of thin histological slides of soft tissues. This technique allows a study of the localisation of the photosensitizer in the several layers of the palatal mucosa. Conventional fluorimetry analyses the fluorescence levels of AlPcS₂ in samples of tissue which were dissolved in NaOH. This is a method which allows quantification of the photosensitizer concentration. One drawback is that it does not separate between the photosensitizer and other fluorescent compounds (responsible for autofluorescence). HPLC-DioLIF is a novel technique which does separate the different fluorescent compounds and is therefore a highly precise method for the determination of the concentration of AlPcS₂ in samples dissolved in NaOH.

Dysplasia and squamous cell carcinomas were induced with 4NQO in the mucosa of the palate of 24 rats while 28 normal untreated rats served as controls. *In vivo* fluorescence images, taken after injection of 1.5 mmol/kg AlPcS₂ i.v., showed that 4NQO-treated palates had higher fluorescence signals than normal palates. Strong fluorescent spots were present in 4NQO-treated rats 2-8 h, but had disappeared 24 h after injection. After taking the *in vivo* fluorescence images the rats were sacrificed and samples of palatal mucosa, bone, tongue, molars, lacrimal glands and other organs (kidney, spleen, liver, skin) were collected. Fluorescence microscopy of the mucosa samples revealed that AlPcS₂ was present only between 2-8 h in the epithelial layer of palatal mucosa, while in biopsies of hot spots the connective tissue contained large quantities of AlPcS₂ at 24-48 h. These large quantities in the connective tissue were not observed by *in vivo* fluorescence imaging. HPLC-DioLIF showed that the relative AlPcS₂ content was highest at 24-48 h in biopsies taken in the areas of these hot spots. *In vivo* fluorescence imaging appears to show mainly fluorescence from the epithelial layer and the *in vitro* techniques mainly show the connective tissue

fluorescence. This could be an important feature of the different methods and explain partially the differences in the results presented in the literature. Therefore, care should be taken when interpreting data using one technique only. From these data it became clear that tumour localisation occurs within the first 10 h after injection. Furthermore, remarkably, the normal appearing kidney and skin of 4NQO-treated animals contained higher amounts of AlPcS₂ than non-treated animals. This effect remains unexplained.

II Tissue damage experiments on normal oral mucosa

Before PDT of squamous cell carcinoma could be investigated, a dose combination of AlPcS₂ and light had to be established with which the normal tissues could be safely treated. This was performed by investigating the effect of AlPcS₂ based PDT on normal palatal mucosa (chapter 3.1). After having established that the optimal time interval of maximal tumour concentration lies within the first 10 h after injection of AlPcS₂ we could plan the normal tissue damage experiments. The time interval between injection of AlPcS₂ and therapeutic irradiation was set at 6 h. This allows injection, fluorescence diagnosis and therapeutic irradiation within one day. For irradiation the wavelength of 672 nm was chosen because the absorbance spectrum of the purchased AlPcS₂ showed a peak at 672 nm in MeOH. Other authors found that to be photodynamically active, the phthalocyanine molecule has to be in the monomeric (not aggregated) state, which is obtained in MeOH. For that reason we assumed that light of 672 nm should be sufficient for the induction of necrosis. However, the subject of which wavelength is most efficient for excitation of phthalocyanines is under debate. Recently an increase of efficiency of PDT induced necrosis was obtained by using a higher wavelength.

Forty normal rats were injected with various doses of AlPcS₂ and 6 h later irradiated with various doses of 672 nm light. The rats were sacrificed 48 h or 2 months after irradiation to investigate the acute and long term effects. For assessing the damage two histological grading lists were developed which allowed numerical expression of the histological damage 48 h and 2 months after PDT. The nature of early damage was mainly edema and necrosis. There was a clear difference in susceptibility for PDT-damage between the tissues, which did not correlate with the AlPcS₂ concentrations in those tissues as presented in chapter 2.2. Dental pulp was very sensitive to PDT while the lacrimal glands were not, although the AlPcS₂ concentrations were similar. Permanent damage consisted mainly of vascular and neuronal proliferation, dental root resorption and ankylosis, palatal bone resorption and epithelial cysts. In some rats the palatal bone as well as the mucosa had disappeared leaving a fistula between the nasal passage and the oral cavity. This was considered an extreme effect of PDT. For the future treatment of squamous cell carcinoma

of the palate, a dose combination was desired which sloughs off the epithelial layer leaving as little permanent damage to the normal tissues as possible. This was possible at a dose combination of 40 Joules/cm² of 672 nm light and 1 µmol/kg ALPcS₂. Two unwanted side effects of PDT could not be prevented at this (or any) dose, namely the dental root resorption and ankylosis. Especially ankylotic teeth are difficult to treat. Therefore, when PDT is applied in humans, the teeth should be shielded from the therapeutic light. At almost all dose combinations relatively large areas of mucosal defects regenerated quite well.

In addition to the PDT experiments, *ex vivo* light dosimetry measurements on 6 extra rats were performed to establish the actual light-dose given. These light dosimetry measurements showed significant differences in fluence due to tissue thickness and scatter of bone. The actual light dose on top of the mucosa was 3.05 times the fluence of the original incident beam (=1). Underneath mucosa of 0.4, 0.8 and 1.5 mm thick the fluence was respectively 2.85, 2.52 and 2.13 times the fluence of the original beam. Furthermore, for bone the light dose varied between 2.85-1.29 times the fluence of the incident beam. These results clearly indicate that even in tissue of 1-2 mm thick large variations in the fluence can occur which can be important in the interpretation of experimental data.

III Photodynamic therapy of experimental oral squamous cell carcinoma

After having established the optimal time interval and a relatively safe dose combination of ALPcS₂ and light, we could plan the actual PDT experiments. Forty tumour and dysplasia bearing rats were subjected to PDT using the dose combination of 1 µmol/kg ALPcS₂ and 40 J/cm² 6 h after injection (chapter 3.2). The tumours and various degrees of dysplasia were induced by 4NQO. The rats were sacrificed 48 h and 2 months after irradiation. The PDT damage as well as the dysplasia were histologically graded. The results showed that the rats which had a higher degree of dysplasia showed less damage 48 h after PDT than rats with a low grade of dysplasia. In contrast, the fluorescence measurements showed that rats with a higher grade of dysplasia had a higher fluorescence signal, indicating more ALPcS₂ in the palatal mucosa of rats with highly dysplastic tissue. This inverse relationship between damage and dysplasia (correlation -0.8) was not anticipated and could only be explained by the increased thickness of the epithelial and keratin layers in dysplastic mucosa. Histological investigation of rats treated with 4NQO showed that the thickness of the epithelial and keratin layer can increase from approximately 200 µm (normal rats) to 1 mm (4NQO treated for 26 weeks), a factor 5. This fact lead us to interpret that the inverse relationship between damage and dysplasia was caused by the significantly reduced light penetration in thickened mucosa (as was measured with light dosimetry experiments presented in chapter 3.1). Apparently the applied light dose on the tissue is the most prominent factor for a succesful

treatment, and more important than a higher AlPcS₂ concentration in tumours. After PDT, the fluorescence of the irradiated palatal mucosa was measured and still 83% of the original fluorescence signal was present. This indicates that a higher PDT effect can be obtained by simply increasing the light dose.

In chapter 3.3 a peculiar phenomenon is described which occurred during PDT. During irradiation the photosensitizer slowly degrades resulting in an inactive and altered molecule. This loss of activity can be observed as a decrease in the fluorescence intensity (photodegradation) during PDT. Photodegradation of AlPcS₂ was assessed by measuring the fluorescence before and after or during irradiation. During the experiments of PDT of normal tissue (chapter 3.1) and dysplasia and tumours (chapter 3.2), an initial increase of fluorescence was seen, indicating an increase of active AlPcS₂ molecules instead of a decline. This phenomenon of increase of fluorescence was first described in single cells in culture and was explained as an release of aggregated phthalocyanine molecules from small intra cellularly located vesicles. In our experiments we could not confirm this mechanism. However, an indication was found that the effects of PDT on the vasculature may have caused this initial increase of fluorescence.

Conclusions

It was possible to localise tumours of the oral mucosa by fluorescence localisation. The accumulation of AlPcS₂ in tumours can be expected within the first 10 h after injection. AlPcS₂ did not only accumulate in tumours but also in areas of inflammation, which makes the technique less tumour specific. Biopsies of suspect areas remain necessary.

A dose of 1 $\mu\text{mol/kg}$ AlPcS₂ and 40 J/cm² 672 nm light was relatively safe for normal tissues. Damage to teeth occurred at all dose combinations. Therefore teeth should be kept outside the PDT irradiation area. The efficacy of the treatment with PDT of the experimental oral squamous cell carcinomas could not be established. As a result of the 4NQO treatment, the mucosal layer thickened which reduced the light penetration. Remarkably, the light penetration was of greater influence on the efficacy of PDT than the amount of AlPcS₂ present in the cancerous mucosa. As often in research, experiments provide answers which raise new questions. Those new questions were formulated in chapter 4.1 and will be subject of further studies.

4.3 SAMENVATTING

Kanker ontstaat door ongecontroleerde groei van zieke cellen die zich buiten normale proporties vermenigvuldigen in het normale weefsel. Een ophoping van deze cellen vormt uiteindelijk een gezwel (Lat.= tumor). Een eigenschap van kwaadaardige tumorcellen is dat ze kunnen ingroeien in de omringende weefsels, waar die cellen normaliter niet voorkomen. Dit fenomeen wordt invasieve groei genoemd. Nadat tumorcellen invasief zijn gaan groeien kunnen deze zich via de bloed- en/of lymfevaten door het lichaam verspreiden en op andere plaatsen ver van hun oorspronkelijke lokatie uitgroeien. Dit proces wordt uitzaaiing of metastasering genoemd. Kleine, niet uitgebreide tumoren, zonder uitzaaiing zijn over het algemeen goed te behandelen en hebben, in tegenstelling tot grote en/of uitgezaaide gezwellen, een goede prognose. Wanneer kanker metastaseert naar belangrijke organen (lever of hersenen) wordt het functioneren van deze organen belemmerd en kan iemand daardoor overlijden. Vroege opsporing en behandeling van kanker is dus belangrijk.

In de slijmvliezen van het hoofd-halsgebied ontstaan tumoren mede onder invloed van langdurige inwerking van schadelijke stoffen uit tabak en alcohol. De tumoren die hierbij ontstaan worden plaveiselcelcarcinomen genoemd. Bij de behandeling van deze vorm van kanker wordt genezing beoogd door de tumor chirurgisch te verwijderen en/of de tumorcellen te doden met radiotherapie of (soms) chemotherapie. Bij deze behandelingen worden de gezonde weefsels ook beschadigd; bij chirurgie ontstaat een defect terwijl bij radiotherapie deels ook gezonde weefsels bestraald worden die beschadigd raken. Daarom is het nog steeds gewenst dat andere therapieën worden gevonden, die meer tumor selectief zijn en minder schade berokkenen aan gezonde weefsels. In de wetenschappelijke literatuur wordt photodynamische therapie genoemd als zo'n selectieve therapie. Tevens biedt photodynamische therapie (PDT) ook de mogelijkheid van detectie van kanker. Daarom zijn in dit onderzoek de mogelijkheden van detectie en behandeling van tumoren in de mondholte met deze behandeling bestudeerd.

De basis van PDT is het bestaan van stoffen die licht kunnen opnemen (absorberen). Wanneer dit gebeurt kan de energie worden doorgegeven aan andere moleculen. Bijvoorbeeld zuurstofmoleculen kunnen die energie overnemen en daarna reacties aangaan met andere stoffen van een levende cel. Het uiteindelijke resultaat van dergelijke reacties is dat de cel onherstelbaar beschadigd raakt en sterft. Sommige van deze lichtgevoelige stoffen (ook wel fotosensitizers genoemd) accumuleren meer in tumorweefsel dan in gezond weefsel. Indien na inspuiten van de fotosensitizer de tumor belicht wordt treden er reacties op waardoor de tumor kan afsterven. Na het absorberen van licht kunnen de fotosensitizers de opgenomen energie ook uitzenden in de vorm van licht. Dit wordt fluorescentie

genoemd. Deze fluorescentie kan met behulp van gevoelige apparatuur worden gemeten. De hoeveelheid fluorescentie is een maat voor de hoeveelheid fotosensitizer die aanwezig is, en als deze stof zich ophoopt in een tumor dan kan hiermee diagnostiek bedreven worden. Een interessante fotosensitizer om te gebruiken voor fluorescentie diagnostiek en PDT lijkt gedisulfoneerd aluminiumphthalocyanine, afgekort als AlPcS₂ en is daarom onderzocht in dit proefschrift

De vraagstellingen in dit onderzoek betreffende de toepassing van fluorescentie lokalisatie en PDT op tumoren van de mondholte waren: 1) kan AlPcS₂ fluorescentie worden gebruikt als middel voor detectie van tumoren; 2) is er een licht/fotosensitizer dosis die veilig is voor de normale weefsels tijdens PDT met AlPcS₂; 3) kunnen experimentele tumoren behandeld worden met PDT en AlPcS₂ als fotosensitizer. Voor dit onderzoek werd gebruik gemaakt van een eerder ontwikkeld tumor model, het 4NQO rat palatummodel (hoofdstuk 1.4). Plaveiselcelcarcinomen en verschillende graden van dysplasie (een voorstadium van kanker) kunnen in het slijmvlies van het gehemelte (palatum) van de rat worden geïnduceerd met de kankerverwekkende stof 4 nitroquinoline 1-oxide (4NQO). Een belangrijk voordeel van het palatum tumormodel is het gegeven dat de mate van dysplasie gekwantificeerd kan worden en afhankelijk is van de duur van de 4NQO behandeling. Hierdoor is het een voorspelbaar en reproduceerbaar model en geschikt voor onderzoek.

I Fluorescentie lokalisatie van AlPcS₂ in dysplasie en plaveiselcelcarcinomen

Met de fluorescentie experimenten werd de mogelijkheid van tumor detectie met AlPcS₂ bestudeerd. In hoofdstuk 2.1 wordt een methode beschreven waarmee AlPcS₂ fluorescentie in het palatum-slijmvlies van de Wistar albino rat kan worden gedetecteerd. Deze AlPcS₂ fluorescentie kan worden gebruikt om een fluorescentie-beeld te krijgen van het palatum van de rat. Op dit fluorescentiebeeld kan de verdeling van de AlPcS₂ fluorescentie worden bestudeerd. De intensiteit van de fluorescentie geeft een indicatie van de concentratie van AlPcS₂ ter plaatse. Om te voorkomen dat de fluorescentie van de rat zelf (autofluorescentie) de metingen verstoort is er een techniek gebruikt die bekend staat als de "dual wavelength excitation". Licht met een golflengte van 460 nm (blauw licht) exciteert AlPcS₂ niet terwijl de autofluorescentie wel wordt geëxciteerd. Daarentegen wordt bij licht van 610 nm (oranjerood) zowel AlPcS₂- als autofluorescentie opgewekt. Als de fluorescentie beelden opgewekt met 460 en 610 nm met behulp van een computer van elkaar worden afgetrokken blijft alleen de AlPcS₂ fluorescentie over. Dit is toegestaan omdat de autofluorescentie opgewekt met 460 en 610 nm nagenoeg identiek aan elkaar is.

Met deze techniek werd de lokalisatie van AlPcS₂ bestudeerd in twee experimenten. Allereerst werden in een groep van 20 ratten dysplasie en tumoren geïnduceerd met 4NQO.

Fluorescentie beelden opgewekt met 460 ± 20 nm (autofluorescentie) en met 610 ± 15 nm (AlPcS₂ fluorescentie) werden opgenomen via een speciaal gebouwde endoscoop (palatoscoop). Hiermee kunnen de fluorescentie-beelden van het palatum van de rat worden afgebeeld. De fluorescentie werd gedetecteerd bij een golflengte gebied van 675 ± 15 nm. In deze studie vonden we dat de fluorescentie significant toenam met de ernst van de dysplasie ($P < 0.04$). Tevens werden er "hot spots" waargenomen. Dit zijn sterk fluorescerende plekken op het beeld veroorzaakt door hoge concentraties van AlPcS₂. Histologische analyse toonde aan dat in 67% de spots invasieve tumor groei (29%) dan wel een ontstekingsproces (38%) vertegenwoordigen. Deze resultaten tonen aan dat er verscheidene mechanismen zijn voor lokalisatie van AlPcS₂ in weefsel, namelijk, een mechanisme wat een verhoogde opname in dysplastisch weefsel veroorzaakt en een ander geassocieerd met lokale veranderingen in het weefsel niet specifiek voor tumoren. Het tijdsinterval waarin deze verhoogde opname plaatsvond was binnen de eerste 10 uur na injectie van AlPcS₂. Dit gegeven is erg belangrijk omdat de concentratie van een fotosensitizer in een tumor maar voor een korte periode optimaal is. Deze experimenten lieten zien dat met AlPcS₂ detectie en PDT van tumoren kan plaatsvinden binnen 10 uur na inspuiten.

In de literatuur bestaan grote variaties in de beschreven tijdsintervallen tussen inspuiten en maximale tumoraccumulatie. Het gebruik van verschillende technieken kan hiervan een van de redenen zijn. Daarom hebben we de lokalisatie van AlPcS₂ in het 4NQO-tumor model onderzocht met de vier meest gebruikte technieken (hoofdstuk 2.2). Vergeleken werden de volgende: 1) in vivo fluorescentie (zoals hierboven beschreven); 2) fluorescentie microscopie; 3) conventionele fluorimetrie; 4) high performance liquid chromatography (HPLC) in combinatie met diode laser geïnduceerde fluorescentie (Dio-LIF). Het voert te ver om alle technieken hier in detail te bespreken, vandaar een korte beschrijving. Met fluorescentie microscopie kan op histologische coupes de lokalisatie van AlPcS₂ in de verschillende lagen van het palatum slijmvlies worden bestudeerd. Conventionele fluorimetrie meet de hoeveelheid AlPcS₂ fluorescentie van een stukje weefsel opgelost in natronloog. Een tekortkoming van deze techniek is dat er ook fluorescentie van andere stoffen in de oplossing wordt gemeten (autofluorescentie). Met HPLC-Dio-LIF wordt ook aan natronloog-oplossingen gemeten. Echter, bij deze techniek worden de stoffen eerst gescheiden met HPLC, zodat specifiek de AlPcS₂ fluorescentie gemeten kan worden. Het is dus een zeer nauwkeurige methode (detectie grens is 10^{-12} mol/L.).

Dysplasie en plaveiselcelcarcinomen werden geïnduceerd met 4NQO bij 24 ratten. Een groep van 28 onbehandelde ratten vormde de controle groep. Alle ratten kregen een injectie met $1.5 \mu\text{mol/kg}$ AlPcS₂. In vivo fluorescentie beelden toonden aan dat 4NQO

behandeld palatumslimvlies sterker fluoresceerde dan normaal slijmvlies. Ook in dit experiment werden de hot spots gevonden in de eerste 10 uur na injectie. De hot spots waren niet meer waarneembaar 24 uur na injectie. Na het opnemen van de fluorescentie beelden werden de ratten opgeofferd op verschillende tijden na injectie (2-48 uur). Stukjes van verschillende organen en weefsel uit de mondholte werden verzameld en geanalyseerd met de drie andere technieken. Fluorescentie microscopie toonde aan dat AlPcS₂ alleen waarneembaar was in het slijmvlies-epitheel tussen 2 en 8 uur na injectie. In gebieden van hot spots was de concentratie in het epitheel vaak erg hoog. Het onderliggende bindweefsel bevatte veel langer na injectie AlPcS₂, waarbij op plaatsen van hot spots zeer hoge concentraties werden gezien, ook na 24 en 48 uur. Met de HPLC-Dio-LIF werden hoge concentraties op 24 en 48 uur na injectie gemeten. Uit deze gegevens kon worden geconcludeerd dat in vivo fluorescentie metingen voornamelijk fluorescentie vanuit de slijmvlieslaag meet terwijl de conventionele en HPLC-Dio-LIF de concentraties in de onderliggende bindweefsellaag meten. Dit effect zou mede kunnen verklaren dat de resultaten van verschillende meettechnieken variëren. Duidelijk is dat AlPcS₂ zich in de eerste 10 uur na injectie localiseert in het slijmvlies. Daarnaast werden met conventionele fluorimetrie hogere concentraties AlPcS₂ gevonden in macroscopisch normale nier en huid stukjes van 4NQO behandelde ratten dan in samples van normale ratten. Dit effect blijft onverklaarbaar.

II Weefsel schade experimenten van het normale palatumslimvlies

Vóórdat PDT van dysplasie en tumoren kon worden onderzocht moest eerst een goede fotosensitizer/licht dosis combinatie worden gevonden. Dit werd gedaan door de effecten van PDT op normaal palatumslimvlies te bestuderen (hoofdstuk 3.1). Het doel van dit onderzoek was het vinden van een dosis combinatie waarbij behandeling van het slijmvlies mogelijk is zonder dat ernstige bijwerkingen optreden. Het tijdsinterval tussen injectie en PDT werd op basis van de fluorescentie localisatie experimenten gesteld op 6 uur. Zo kan op één dag geïnjecteerd, fluorescentie gemeten en therapeutisch belicht worden. Een golflengte van 672 nm (diep rood) werd gebruikt voor de therapeutische belichting omdat AlPcS₂ hier een maximale absorptie laat zien.

Veertig normale ratten werden geïnjecteerd met een dosis die kon variëren van 0.5-4 µmol/kg AlPcS₂ en werden 6 uur later belicht met een licht dosis die kon variëren van 20-160 joules/cm². De ratten werden 2 dagen en 2 maanden na therapeutische belichting opgeofferd. Voor het bestuderen van de schade werden scorelijsten ontwikkeld waarmee de schade kon worden gemeten. Op 2 dagen na PDT werd voornamelijk oedeem (vochtophoping) en necrose (weefselsterfte) gezien. Er was een duidelijk verschil in de

gevoeligheid van de verschillende weefsels voor PDT die niet correleerde met de gemeten ALPcS₂-concentraties, zoals gevonden in hoofdstuk 2.2. De tandzenuw was erg gevoelig voor PDT terwijl de traanklier volledig ongevoelig was, hoewel de gemeten ALPcS₂ concentraties vergelijkbaar waren. Permanente schade, gemeten op 2 maanden na PDT, bestond voornamelijk uit proliferatie van zenuwen en vaten, tandwortelresorptie en ankylose (vergroeiing van de tand met het bot) en botresorptie. Het slijmvlies herstelde zich goed na PDT. In geval van ernstige schade was het palatumbot zover geresorbeerd dat een doorgang (fistel) naar de neus was ontstaan. Dit kan als een extreme vorm van schade worden gezien. Echter, een dosis combinatie van 1 µmol/kg ALPcS₂ en 40 J/cm² licht gaf weinig permanente schade en kan als een veilige dosis worden beschouwd. Bij deze dosering kunnen de ongewenste tandwortelresorptie en ankylose niet worden voorkomen omdat de gebitselementen bij de rat niet buiten het belichtingsveld gehouden kunnen worden. Wanneer PDT zou worden toegepast bij mensen dan dienen op basis van deze bevindingen de tanden en kiezen buiten het belichtingsveld te blijven.

Naast deze weefselschade-experimenten werden ook lichtmetingen (dosimetrie) verricht aan het palatum-slijmvlies van 6 extra ratten om nauwkeuriger te bepalen hoe groot de lichtdosis was geweest. Uit deze metingen werd duidelijk dat door verstrooiing en reflectie van licht vooral van het onderliggende bot de lichtdosis aan het oppervlak van het slijmvlies in werkelijkheid 3 maal de opvallende lichtdosis is. Wanneer de weefseldikte toeneemt neemt de lichtsterkte af in het weefsel. Onder slijmvlies van 0,4, 0,8 en 1,5 mm dik was de lichtsterkte respectievelijk 2,85, 2,52 en 2,13 maal de opvallende lichtbundel. Tevens varieerde de lichtdosis in bot tussen 2,85-1,29 maal de opvallende lichtdosis. Deze resultaten geven aan dat zelfs in relatief dun slijmvlies de variaties in lichtdosis sterk uiteen kunnen lopen. Dit is belangrijk voor de interpretatie van de gegevens.

III Photodynamische therapie van experimentele dysplasie en plaveiselcelcarcinomen

Na het bekend worden van een optimaal tijdsinterval tussen inspuiten en belichten en nadat tevens een relatief veilige dosis combinatie was gevonden, kon worden begonnen aan de eigenlijke PDT experimenten (hoofdstuk 3.2). Veertig ratten werden voorbehandeld met 4NQO en hadden een dysplasiegraad die varieerde van mild tot ernstig. Tevens had een aantal van deze groep een plaveiselcelcarcinoom. Alle ratten kregen 1 µmol/kg ALPcS₂ ingespoten en 6 uur later een dosis van 40 joules/cm² licht met een golflengte van 672 nm. Zowel de dysplasie en de weefselschade werden gemeten op histologische coupes. De resultaten lieten zien dat het slijmvlies met een milde dysplasie meer PDT weefselschade had dan slijmvlies met een ernstige dysplasie of carcinoom. Dit was in tegenstelling met de gevonden fluorescentiewaarden, die significant hoger waren bij ratten met een ernstige

afwijking, wat op meer AlPcS₂ ter plaatse wijst. Deze omgekeerd evenredige relatie tussen PDT-schade en ernst van dysplasie (correlatie -0.8) werd niet verwacht. Een mogelijke verklaring hiervoor is dat de dikte van het slijmvlies toeneemt van $\pm 200 \mu\text{m}$ (normale ratten) tot $\pm 1 \text{ mm}$ (26 weken 4NQO behandeld), en hierdoor de lichtdosis sterk afneemt in het weefsel. Zoals gemeten in de dosimetrie-experimenten kan de lichtsterkte fors afnemen in dikker weefsel. Het duidt erop dat de lichtdosering de belangrijkste factor is voor een succesvolle behandeling, en belangrijker dan een hogere concentratie AlPcS₂ in het weefsel. Na de therapeutische belichting was nog 83% van de AlPcS₂ fluorescentie over. Er kan dus een sterkere PDT schade geïnduceerd worden door in geval van dik weefsel de lichtdosis te verhogen.

In hoofdstuk 3.3 wordt een opmerkelijk fenomeen beschreven dat optrad tijdens therapeutische belichting. Tijdens belichten degraderen fotosensitizer moleculen langzaam, wat resulteert in inactieve moleculen. Dit proces van fotodegradatie kan worden waargenomen door een afname van fluorescentie tijdens belichten. Tijdens de hier beschreven experimenten (hoofdstuk 3.2 en 3.2) werden de fluorescentie veranderingen ook gemeten. Echter, tijdens deze belichtingen werd een initiële toename van fluorescentie gemeten. Pas later tijdens de belichting werd de verwachte afname gemeten. Dit fenomeen van initiële toename is wel eerder beschreven tijdens PDT van cellen in een kweekmedium maar nog niet bij dieren. Het werd uitgelegd als een toename doordat er geaggregeerde AlPcS-moleculen los kwamen tijdens belichting. Geaggregeerde moleculen fluoresceren niet en ge-deaggregeerde moleculen wel. In onze experimenten konden we dit mechanisme niet bevestigen. Er werden aanwijzingen gevonden dat effecten op de bloedvaten mede de toename veroorzaakten. Onze hypothese is dat tijdens belichten de bloedvaten in eerste instantie verwijden en de toename van bloedstroom een toename van fluorescentie veroorzaakt. Welk mechanisme hieraan ten grondslag ligt blijft voorlopig onduidelijk.

Conclusies

Door middel van fluorescentie lokalisatie was het mogelijk tumoren te lokaliseren. AlPcS₂ accumuleert in dysplasie en tumoren binnen 10 uur na injectie. Tevens accumuleert AlPcS₂ in ontstoken weefsel. Hierdoor blijft weefselonderzoek (biopsie) van suspecte gebieden in het slijmvlies noodzakelijk.

Een dosis van $1 \mu\text{mol/kg}$ AlPcS₂ en 40 joules/cm^2 licht van 672 nm bleek een relatief veilige dosis. Dit wil zeggen dat de meeste schade aangericht door PDT zich goed herstelde zonder permanente ongewenste bijwerkingen. Echter, ernstige schade aan de tanden kon bij geen enkele dosis combinatie worden voorkomen. Het is dus belangrijk dat tanden en kiezen buiten het belichtingsveld blijven. Het was niet geheel mogelijk om de

effectiviteit van PDT op dysplasie en plaveiselcel carcinomen vast te stellen. Door de 4NQO behandeling nam de dikte van het slijmvlies toe wat resulteerde in een lagere lichtdosis. Opmerkelijk was dat de lichtdosis een belangrijkere parameter was voor succesvolle behandeling dan de hogere concentratie van ALPcS₂ in tumoren. Zoals vaak het geval in onderzoek worden door deze experimenten nieuwe vragen opgeworpen. Die zijn geformuleerd in hoofdstuk 4.1 en zullen het onderwerp zijn van verdere studie.

4.4 BIBLIOGRAPHY

- ALI H, LANGLOIS R, WAGNER JR, BRASSEUR N, PAQUETTE B AND VAN LIER JE.** (1988). Biological activities of Phthalocyanines-X synthesis and analyses of sulphonated phthalocyanines. *Photochem.Photobiol.* **47**, 713-717.
- AMBROZ M, BEEBY A, MACROBERT AJ, SIMPSON MSC, SVENSEN RK AND PHILLIPS D.** (1991). Preparative, analytical and fluorescence spectroscopic studies of sulphonated aluminum phthalocyanine photosensitizers. *J.Photochem.Photobiol.B: Biol.* **9**, 87-95.
- AMBROZ M, MACROBERT AJ, MORGAN J, RUMBLES G, FOLEY MSC AND PHILLIPS D.** (1994). Time-resolved fluorescence spectroscopy and intracellular imaging of disulphonated aluminum phthalocyanine. *J.Photochem.Photobiol.B.* **22**, 105-117.
- ANDERSSON PS, MONTAN S, PERSSON T, SVANBERG S AND TAPPER S.** (1987). Fluorescence endoscopy instrumentation for improved tissue characterization. *Med.Phys.* **14**, 633-636.
- BARR H, TRALAU CJ, BOULOS PB, MACROBERT AJ, KRASNER N, PHILLIPS D AND BOWN SG.** (1990). Selective necrosis in dimethylhydrazine induced rat colon tumors using phthalocyanine photodynamic therapy. *Gastroenterology* **98**, 1532-1153.
- BARR H, CHATLANI PT, TRALAU CJ, MACROBERT AJ, BOULOS PB AND BOWN SG.** (1991). Local eradication of rat colon cancer with photodynamic therapy: correlation of distribution of photosensitiser with biological effects in normal and tumour tissue. *Gut* **32**, 517-523.
- BAUMGARTNER R, FISSLINGER H, JOCHAM D, LENZ H, RUPRECHT L, STEPP H AND UNSOLD E.** (1987). A fluorescence imaging device for endoscopic detection of early stage cancer, instrumental and experimental studies. *Photochem.Photobiol.* **46**, 759-763.
- BEN-HUR E, SIWECKI JA, NEWMAN HC, CRANE SW AND ROSENTHAL I.** (1987a). Mechanism of uptake of sulfonated metallophthalocyanines by cultured mammalian cells. *Cancer Lett.* **38**, 215-222.
- BEN-HUR E, FUJIHARA T, SUZUKI F AND ELKIND MM.** (1987b). Genetic toxicology of the photosensitization of Chinese hamster cells by phthalocyanines. *Photochem.Photobiol.* **45**, 227-230.

- BEN-HUR E.** (1988). Release of clotting factors from photosensitized endothelial cells: a possible trigger for blood vessel occlusion by photodynamic therapy. *FEBS Lett.* **236**, 105-108.
- BERG K, BOMMER JC AND MOAN J.** (1989a). Evaluation of sulfonated aluminum phthalocyanines for use in photochemotherapy. A study on the relative efficiencies of photoinactivation. *Photochem.Photobiol.* **49**, 587-594.
- BERG K, BOMMER JC AND MOAN J.** (1989b). Evaluation of sulphonated aluminum phthalocyanines for use in photochemotherapy. Cellular uptake studies. *Cancer Lett.* **44**, 7-15.
- BERG K, MADSLIEN K, BOMMER JC, OFTEBRO R, WINKELMAN JW AND MOAN J.** (1991). Light induced relocation of sulfonated meso-tetraphenylporphines in NHIK 3025 cells and effects of dose fractionation. *Photochem.Photobiol.* **53**, 203-210.
- BIEL MA** (1995). Photodynamic therapy of head and neck cancers. *Semin-Surg-Oncol.* **11**, 355-359
- BIOLO R, JORI G, KENNEDY JC, NADEAU P, POTTIER R, REDDI E AND WEAGLE G.** (1991). A comparison of fluorescence methods used in the pharmacokinetic studies of Zn(II)phthalocyanine in mice. *Photochem.Photobiol.* **53**, 113-118.
- BOEGHEIM JP, DUBBELMAN TMAR, MULLENDERS LH AND VAN STEVENINCK J.** (1987). Photodynamic effects of haematoporphyrin derivative on DNA repair in murine L929 fibroblasts. *Biochem.J.* **244**, 711-715.
- BOWN SG, TRALAU CJ, COLERIDGE-SMITH PD, AKDEMIR D AND WIEMAN TJ.** (1986). Photodynamic therapy with porphyrin and phthalocyanine sensitization: Quantitative studies in normal rat liver. *Br.J.Cancer* **54**, 43-52.
- BOWN SG.** (1993). Photodynamic therapy in gastroenterology - current status and future prospects. *Endoscopy* **25**, 683-786.
- BOYD NM AND READE PC.** (1991). Temporal alterations in cytokeratin expression during experimental during experimental oral mucosal carcinogenesis. *Carcinogenesis* **12**, 1767-1771.
- BOYLE P, MACFARLANE GJ, BLOT WJ, CHIESA F, LEVEBVRE JL, MANO AZUL A, DE VRIES N AND SCULLY C.** (1995). European school of oncology advisory report to the European

Commission for the Europe Against Cancer programme: Oral carcinogenesis in Europe. *Oral Oncol., Eur. J. Cancer* **31B**, 75-85.

- BOYLE RW, PAQUETTE B AND VAN LIER JE.** (1992). Biological activities of phthalocyanines XIV. Effect of hydrophobic phthalimidomethyl groups on the in vivo phototoxicity and mechanism of photodynamic action of sulphonated aluminium phthalocyanines. *Br. J. Cancer* **65**, 813-817.
- BRASSEUR N, ALI H, LANGLOIS R, WAGNER JR, ROUSSEAU J AND VAN LIER JE.** (1987). Biological activities of Phthalocyanines-V. Photodynamic therapy of EMT-6 mammary tumors in mice with sulphonated phthalocyanines. *Photochem. Photobiol.* **45**, 581-586.
- BRODBECK KJ, PROFIO AE, FREWIN T AND BALCHUM OJ.** (1987). A system for real time fluorescence imaging in color for tumor diagnosis. *Med. Phys.* **14**, 637-639.
- BUETTNER GR AND REED MJ.** (1985). Hydrogen peroxide and hydroxyl free radical production by hematoporphyrin derivative ascorbate and light. *Cancer Lett.* **25**, 297-304.
- CHAN WS, MARSHALL JF, SVENSEN RK, PHILLIPS D AND HART IR.** (1987). Photosensitising activity of phthalocyanine dyes screened against tissue culture cells. *Photochem. Photobiol.* **45**, 757-761.
- CHAN WS, MARSHALL JF, LAM GY AND HART IR.** (1988). Tissue uptake distribution and potency of the photoactivatable dye chloraluminium sulphonated phthalocyanine in mice bearing transplantable tumors. *Cancer Res.* **48**, 3040-3044.
- CHAN WS, MARSHALL JF AND HART IR.** (1989). Effect of tumour location on selective uptake and retention of phthalocyanines. *Cancer Lett.* **44**, 73-77.
- CHAN WS, MARSHALL JF, SVENSEN R, BEDWELL J AND HART IR.** (1990). Effect of sulfonation on the cell and tissue distribution of the photosensitizer aluminum phthalocyanine. *Cancer Res.* **50**, 4533-4538.
- CHAN WS, WEST CML, MOORE JV AND HART IR.** (1991). Photocytotoxic efficacy of sulphonated species of aluminium phthalocyanine against cell monolayers, multicellular spheroids and in vivo tumours. *Br. J. Cancer* **64**, 827-832.

- CHAPLIN DJ.** (1991). The effect of therapy on tumour vascular function. *Int.J.Radiat.Biol.* **60**, 311-325.
- CHATLANI PT, BEDWELL J, MACROBERT AJ, BARR H, BOULOS PB, KRASNER N, PHILLIPS D AND BOWN SG.** (1991). Comparison of distribution and photodynamic effects of di- and tetra sulphonated aluminium phthalocyanines in normal rat colon. *Photochem.Photobiol.* **53**, 745-751.
- CHEN JY, CHEN W, CAI HX AND DONG RC.** (1993). Studies on pharmacokinetics of sulfonated aluminum phthalocyanine in a transplantable mouse tumor by in vivo fluorescence. *J.Photochem.Photobiol.B* **18**, 233-237.
- CRANE IJ, LUKER J, STONE A, SCULLY C AND PRIME SS.** (1986). Characterization of malignant rat keratinocytes in culture following the induction of oral squamous cell carcinomas in vivo. *Carcinogenesis* **7**, 1723-1727.
- CRANE IJ, PATEL V, SCULLY C AND PRIME SS.** (1989). Development of aneuploidy in experimental oral carcinogenesis (short communication). *Carcinogenesis* **10**, 2375-2377.
- CREAN DH, LIEBOW C, PENETRANTE RB AND MANG TS.** (1993). Evaluation of porfimer sodium fluorescence for measuring tissue transformation. *Cancer* **72**, 3068-3077.
- CUZICK J.** (1985). A Wilcoxon-type test for trend. *Statistics in Medicine* **4**, 87-90.
- DAUBERSIES P, GALIEGUE-ZOUITINA S, KOFFEL-SCHWARTZ N, FUCHS RPP, LOUCHEUX-LEFEBVRE MH AND BAILLEUL B.** (1992). Mutation spectra of the two guanine adducts of the carcinogen 4-Nitroquinolin 1-oxide in Escherichia Coli. Influence of neighbouring base sequence on mutagenesis. *Carcinogenesis* **13**, 349-354.
- DOUGHERTY TJ, GRINDLEY GB AND FIEL R.** (1975). Photoradiation therapy. Cure of animal tumors with haematoporphyrin and light. *J.Natl.Cancer Inst.* **55**, 115
- DOUGHERTY TJ.** (1987). Photosensitizers: Therapy and detection of malignant tumors. *Photochem.Photobiol.* **45**, 879-884.
- DREIZEN S, BROWN LR, HANDLER S AND LEVY BM.** (1976). Radiation induced xerostomia in cancer patients. Effect on salivary and serum electrolytes. *Cancer* **38**, 273-278.

- DUBBELMAN TMAR, PRINSZE C, PENNING LC AND VAN STEVENINCK J** (1991). Photodynamic therapy : Membrane and enzyme photobiology. In: *Photodynamic therapy basic principles and clinical applications*, Henderson BW and Dougherty TJ (eds.). pp 15-27. Marcel Dekker Inc. New York.
- FEIX JB AND KALYANARAMAN B.** (1991). An electron spin resonance study of merocyanine 540-mediated type I reactions in liposomes. *Photochem.Photobiol.* **53**, 39-45.
- FERRAUDI G, ARGUELLO GA, ALI H AND VAN LIER JE.** (1988). Types I and II sensitized photo-oxidation of aminoacid by phthalocyanines: a flash photochemical study. *Photochem.Photobiol.* **47**, 657-660.
- FEYH J, GOETZ A, MULLER W, KONIGSBERGER R AND KASTENBAUER E.** (1990). Photodynamic therapy in head and neck surgery. *J.Photochem.Photobiol.B.* **7**, 353-358.
- FINGAR VH, WIEMAN TJ AND DOAK KW.** (1990). Role of thromboxane and prostacyclin release on photodynamic therapy induced tumor destruction. *Cancer Res.* **50**, 2599-2603.
- FINGAR VH, WIEMAN TJ, WIEKLE SA AND CERRITO P.** (1992). The role of microvascular damage in photodynamic therapy: The effect of treatment on vessel constriction, permeability and leukocyte adhesion. *Cancer Res.* **52**, 4919-4921.
- FINGAR VH, WIEMAN TJ, KARAVOLOS PS, DOAK KW, OUELLET R AND VAN LIER JE.** (1993). The effects of photodynamic therapy using differently substituted zinc phthalocyanines on vessel constriction, vessel leakage and tumor response. *Photochem.Photobiol.* **58**, 251-258.
- FISKER AV.** (1978). Chemically induced experimental oral carcinogenesis. Establishment of an experimental model based on application of the carcinogen 4-nitroquinoline n-oxide on the palatal mucosa of rats. Thesis, University of Copenhagen.
- FODSTAT O.** (1988). Representivity of xenografts for clinical cancer. Tumour and host characteristics as variables of tumour take rate. In: *Human tumour xenografts in anticancer drug development*, Winograd B, Peckham MJ and Pinedo HM (eds.). pp 15-21. Springer-Verlag: Berlin.
- FOSTER TH, HARTLEY DF, NICHOLS MG AND HILF R.** (1993). Fluence rate effects in photodynamic therapy of multicell tumor spheroids. *Cancer Res.* **53**, 1249-1254.

- FRISOLI JK, TUDOR EG, FLOTTE TJ, HASAN T, DEUTSCH TF AND SCHOMACKER KT.** (1993). Pharmacokinetics of a fluorescent drug using laser-induced fluorescence. *Cancer Res.* **53**, 5954-5961.
- GOMER CJ AND RAZUM NJ.** (1984). Acute skin response in albino mice following porphyrin photosensitization under oxic and anoxic conditions. *Photochem.Photobiol.* **40**, 435-439.
- GRANT WE, SPEIGHT PM, MACROBERT AJ, HOPPER C AND BOWN SG.** (1994). Photodynamic therapy of normal rat arteries after photosensitisation using disulphonated aluminium phthalocyanine and 5-aminolaevulinic acid. *Br.J.Cancer* **70**, 72-78.
- GRIFFITHS J, CRUSE-SAWYER J, WOOD SR, SCHOFIELD J, BROWN SB AND DIXON B.** (1994). On the photodynamic action spectrum of zinc phthalocyanine tetrasulphonic acid in vivo. *J.Photochem.Photobiol.B: Biol.* **24**, 195-199.
- GROSSWEINER LI.** (1987). Photodynamic therapy of head and neck squamous cell carcinoma optical dosimetry and clinical trial. *Photochem.Photobiol.* **46**, 911-917.
- HAMBLIN MR AND NEWMAN EL.** (1994). On the mechanism of the tumour-localising effect in photodynamic therapy (review). *J.Photochem.Photobiol.B.* **23**, 3-8.
- HARRIMAN A.** (1995). Photosensitization in photodynamic therapy. In: *Organic photochemistry and photobiology*, Horspool WM, Song PS (eds.). pp 1374-1378. CRC press: Boca Raton.
- HENDERSON BW, WALDOW SM, MANG TS, POTTER WR, MALONE PB AND DOUGHERTY TJ.** (1985). Tumor destruction and kinetics of tumor cell death in two experimental mouse tumors following photodynamic therapy. *Cancer Res.* **45**, 572-576.
- HENDERSON BW AND DOUGHERTY TJ.** (1992). How does photodynamic therapy work ? *Photochem.Photobiol.* **55**, 145-157.
- HERMANEK P AND SOBIN LH** (1992). TNM classification of malignant tumours. UICC. 4th edition 2nd rev. pp 18-21. Springer Verlag, Berlin.
- JORI G.** (1993). The role of lipoproteins in the delivery of tumour-targeting photosensitizers. *Int.J.Biochem.* **25**, 1369-1375.

- KATO H, SAKAI H, KONAKA C, OKUNA T, FURUKAWA K, AIZAWA K, SAITO Y AND HAYATA, Y.** (1992). Fluorescence photodiagnosis of early stage lung cancer. In: *Photodynamic therapy and biomedical lasers*, Spinnelli P, Dal Fante M and Marchesini R (eds.). pp 876-882. Elseviers Science Publishers: Amsterdam.
- KEIJZER M, JACQUES SLJ, PRAHL SA AND WELCH AJ.** (1989). Light distribution in artery tissue: Monte Carlo simulations for finite-diameter laser beams. *Lasers Surg.Med.* **9**, 148-154.
- KESSEL D.** (1982). Components of hematoporphyrin derivatives and their tumor-localizing capacity. *Cancer Res.* **42**, 1703-1706.
- KONDO S.** (1981). Molecular biology of 4-nitroquinoline 1-oxide in the prokaryotic system. In: *The nitroquinolines*, Sugimura T (ed.). pp 47-64. Raven Press: New York.
- KORBELIK M, KROSL G AND CHAPLIN DJ.** (1991). Photofrin uptake by murine macrophages. *Cancer Res.* **51**, 2251-2255.
- LAMURAGLIA GM, ORTU P, FLOTTE TJ, ROBERTS WG, SCHOMACHER KT, CHANDRASEKAR NR AND HASAN T.** (1993). Chloroaluminum Sulfonated phthalocyanine partitioning in normal and intimal hyperplastic artery in the rat. *Am.J.Pathol.* **142**, 1898-1905.
- LANGLOIS R, ALI H, BRASSEUR N, WAGNER JR AND VAN LIER JE.** (1986). Biological activities of phthalocyanines-IV. Type II sensitized photooxidation of L-tryptophan and cholesterol by sulfonated metallo phthalocyanines. *Photochem.Photobiol.* **44**, 117-125.
- LEENGOED, VAN HLLM.** (1993a). Photosensitizers for tumour fluorescence and photodynamic therapy of cancer. Thesis, ERASMUS University, Rotterdam
- LEENGOED, VAN HLLM, VAN DER VEEN N, VERSTEEG AAC, OUELLET R, VAN LIER JE AND STAR WM.** (1993b). In vivo fluorescence kinetics of phthalocyanines in a skin-fold chamber model: role of central metal ion and degree of sulfonation. *Photochem.Photobiol.* **58**, 233-237.
- LEENGOED, VAN HLLM, VAN DER VEEN N, VERSTEEG AAC, QUELLET R, VAN LIER JE AND STAR WM.** (1993c). In vivo photodynamic effects of phthalocyanines in a skin fold observation chamber model: role of central metal ion and degree of sulphonation. *Photochem.Photobiol.* **58**, 575-580.

- LIER, VAN JE AND SPIKES JD.** (1989). The chemistry, photophysics and photosensitizing properties of phthalocyanines. *Ciba.Found.Symp.* **146**, 17-26.
- LIPSON R, ALDES E AND OLSEN A.** (1961). The use of a derivative of hematoporphyrin in tumor detection. *J.Natl.Cancer Inst.* **1**, 1-11.
- LOH CS, BEDWELL J, MACROBERT AJ, KRASNER N, PHILLIPS D AND BOWN SG.** (1992). Photodynamic Therapy of the normal rat stomach: A comparative study between di-sulphonated aluminium phthalocyanine and 5-aminolevulinic acid. *Br.J.Cancer* **66**, 452-462.
- MANG TS, DOUGHERTY TJ, POTTER WR, BOYLE DG, SOMER S AND MOAN J.** (1987). Photobleaching of porphyrins used in photodynamic therapy and implications for therapy. *Photochem.Photobiol.* **45**, 501-506.
- MANG TS, MCGINNIS C, LIEBOW C, NSEYO UO, CREAM DH AND DOUGHERTY TJ.** (1993). Fluorescence detection of tumors. Early diagnosis of microscopic lesions in preclinical studies. *Cancer* **71**, 269-276.
- MANK AGJ, GOOIJER C, LINGEMAN H, VELTHORST NH AND BRINKMAN UAT.** (1993). Selective and sensitive in vitro detection method for aluminium phthalocyanine photosensitizers, using liquid chromatography and diode-laser induced fluorescence. *Anal.Chim.Acta* **290**, 103-120.
- MARIJNISSEN JPA, STAR WM, VERSTEEG AAC AND VAN PUTTEN WLJ.** (1992). Tumor and normal tissue response to interstitial photodynamic therapy of the rat R-1 rhabdomyosarcoma. *Int.J.Radial.Oncol.Biol.Phys.* **22**, 963-972.
- MENEZES DA, SILVA FA AND NEWMAN EL.** (1995). Time-dependent photodynamic damage to blood vessels: correlation with serum photosensitizer levels. *Photochem.Photobiol.* **61**, 414-416.
- MEYER M, SPEIGHT P AND BOWN SG.** (1991). A study of the effects of photodynamic therapy on the normal tissues of the rabbit jaw. *Br.J.Cancer* **64**, 1093-1097.
- MOAN J, JOHANNESSEN JV, CHRISTENSEN T, ESPEVIK T AND MCGHIE JB.** (1982). Porphyrin-sensitized photoinactivation of human cells in vitro. *Am.J.Pathol.* **109**, 184-192.

- MOAN J.** (1986). Effect of bleaching of porphyrin sensitizers during photodynamic therapy. *Cancer Lett.* **33**, 45-53.
- MOAN J, BERG K, STEEN HB, WARLOE T AND MADSLIEN K** (1992). Fluorescence and photodynamic effects of phthalocyanines and porphyrins in cells. In: *Photodynamic Therapy. Basic principles and clinical applications*, Henderson BW and Dougherty TJ (eds.). pp 19-36. Marcel Dekker, Inc. New York.
- MOAN J, IANI V, MA LW AND PENG Q.** (1996). Photodegradation of sensitizers in mouse skin during PCT. In : *Photochemotherapy: photodynamic therapy and other modalities*. Ehrenberg B, Jori G and Moan J (eds.) pp 187-193. SPIE proceedings **2625**.
- MONNIER P, SAVARY M, FONTOLLIET C, WAGNIERES G, CHATELAIN A, CORNAZ P, DEPEURSINGE C AND VAN DEN BERGH H.** (1990). Photodetection and photodynamic therapy of early squamous cell carcinomas of the pharynx, oesophagus and tracheo-bronchial tree. *Lasers Med.Sci.* **5**, 149-168.
- MOORE JV, WEST CML AND HAYLETT AK.** (1992). Vascular function and tissue injury in murine skin following hyperthermia and photodynamic therapy, alone and in combination. *Br.J.Cancer* **66**, 1037-1043.
- NAGAO M AND SUGIMURA T.** (1976). Molecular biology of the carcinogen, 4-nitroquinoline 1-oxide. *Adv.Cancer Res.* **23**, 131-169.
- NAUTA JM, ROODENBURG JLN, NIKKELS PGJ, WITJES MJH AND VERMEY A.** (1995). Comparison of epithelial dysplasia. The 4NQO rat palatal model versus human oral mucosa. *Int.J.Oral Maxillofac.Surg.* **24**, 53-58.
- NAUTA JM, ROODENBURG JLN, NIKKELS PGJ, WITJES MJH AND VERMEY A.** (1996a). Epithelial dysplasia and squamous cell carcinoma of the Wistar rat palatal mucosa. The 4NQO model. *Head and Neck* accepted for publication
- NAUTA JM, ROODENBURG JLN, VERMEY A AND NIKKELS PGJ.** (1996b). Experimental carcinogenesis in the rat palatal mucosa. A review of the 4NQO model. *Submitted*.

- NAUTA JM, VAN LEENGOED HLLM, WITJES MJH, ROODENBURG JLN, NIKKELS PGJ, THOMSEN SL, MARIJNISSEN JPA AND STAR WM. (1996c).** Photodynamic therapy of rat palatal mucosa. Normal tissue effects and light dosimetry. *Submitted*.
- NUUTINEN PJO, CHATLANI PT, BEDWELL J, MACROBERT AJ, PHILLIPS D AND BOWN SG. (1991).** Distribution and photodynamic effect of disulphonated aluminium phthalocyanine in the pancreas and adjacent tissues in the Syrian golden hamster. *Br.J.Cancer* **64**, 1108-1115.
- OTTER R AND SCHOUTEN L W (eds.)(1995).** Head and neck tumours in the Netherlands (Conference edition). pp 9-12. Association of comprehensive cancer centres: Utrecht
- PATEL V, POULOPOULOS AK, LEVAN G, GAME SM, EVESON JW AND PRIME SS (1995).** Loss of expression of basement membrane proteins reflects anomalies of chromosomes 3 and 12 in the rat 4-nitroquinoline n-oxide model of oral carcinogenesis. *Carcinogenesis* **16**, 17-23.
- PAQUETTE B, ALI H, LANGLOIS R AND VAN LIER JE. (1988).** Biological activities of phthalocyanines--VIII. Cellular distribution in V-79 Chinese hamster cells and phototoxicity of selectively sulfonated aluminum phthalocyanines. *Photochem.Photobiol.* **47**, 215-220.
- PAQUETTE B. AND VAN LIER J.E. (1992).** Phthalocyanines and related compounds:Structure-activity relationships. In: *Photodynamic therapy. Basic principles and clinical applications*, Henderson BW and Dougherty TJ (eds.). pp 145-156. Marcel Dekker: New York.
- PENG Q, MOAN J, NESLAND JM AND RIMINGTON C. (1990).** Aluminum phthalocyanines with asymmetrical lower sulphonation and with symmetrical higher sulphonation: a comparison of localizing and photosensitizing mechanism in human tumor LOX xenografts. *Int.J.Cancer* **46**, 719-726.
- PENG Q, FARRANTS GW, MADSLIEN K, BOMMER JC, MOAN J, DANIELSEN HE AND NESLAND JM. (1991a).** Subcellular localization, redistribution and photobleaching of sulfonated aluminum phthalocyanines in a human melanoma cell line. *Int.J.Cancer* **49**, 290-295.
- PENG Q, MOAN J, FARRANTS G, DANIELSEN HE AND RIMINGTON C. (1991b).** Localization of potent photosensitizers in human tumor LOX by means of laser scanning microscopy. *Cancer Lett.* **58**, 17-27.

- PENG Q AND MOAN J.** (1995). Correlation of distribution of sulphonated aluminium phthalocyanines with their photodynamic effect in tumour and skin of mice bearing CaD2 mammary carcinoma. *Br.J.Cancer* **72**, 565-574.
- PENNING LC, TIJSSEN K, BOEGHEIM JP, VAN STEVENINCK J AND DUBBELMAN TMAR.** (1994). Relationship between photodynamically induced damage to various cellular parameters and loss of clonogenicity in 3 different cell types with hematoporphyrin derivative as sensitizer. *Biochim.Biophys.Acta* **1221**, 250-258.
- POON WS, SCHOMACHER KT, DEUTSCH TF AND MARTUZA RL.** (1992). Laser-induced fluorescence: experimental intraoperative delineation of tumor resection margins. *J.Neurosurg.* **76**, 697-686.
- POPE AJ, MACROBERT AJ, PHILLIPS D AND BOWN SG.** (1991). The detection of phthalocyanine fluorescence in normal rat bladder wall using sensitive digital imaging microscopy. *Br.J.Cancer* **64**, 875-879.
- PRAHL SA.** (1988). Light transport in tissue. Thesis, University of Texas at Austin.
- PRIME SS, MALAMOS D, ROSSER TJ AND SCULLY CM.** (1986). Oral epithelial atypia and acantholytic dyskeratosis in rats painted with 4-nitroquinoline N-oxide. *J.Oral Pathol.* **15**, 280-283.
- PROFIO AE, DOIRON DR, BALCHUM OJ AND HUTH G.** (1983). Fluorescence bronchoscopy for localisation of carcinoma in situ. *Med.Phys.* **10**, 35-39.
- RAMANUJAM N, MITCHELL MF, MAHADEVAN A, THOMSEN S, MALPICA A, WRIGHT TC, ATKINSON N AND RICHARDS-KORTUM RR.** (1994). In vivo diagnosis of cervical intraepithelial neoplasia using 337 nm excitation. *Proc. Natl. Acad.Sci USA* **91**, 10193-10197.
- RICCHELLI F, JORI G, GOBBO S AND TRONCHIN M.** (1991). Liposomes as models to study the distribution of porphyrins in cell membranes. *Biochim.Biophys.Acta* **1065**, 42-48.
- RICHARDS-KORTUM RR, RAVA RP, PETRAS RE, FITZMAURICE M, SIVAK MV AND FELD MS.** (1991). Spectroscopic diagnosis of colonic dysplasia. *Photochem Photobiol.* **53**, 777-786.

- ROBERTS WG AND HASAN T.** (1993). Tumor-secreted vascular permeability factor/vascular endothelial growth factor influences photosensitizer uptake. *Cancer Res.* **53**, 153-157.
- ROGERS DW, LANZAFAME RJ, BLACKMAN JR, NAIM JO, HERRERA HR AND HINSHAW JR.** (1990). Methods for the endoscopic photographic and visual detection of helium cadmium laser-induced fluorescence of Photofrin II. *Lasers Surg. Med.* **10**, 45-51.
- RONN AM, LOFGREN LA, WESTERBORN A AND NILSSON E.** (1995). Interspecies pharmacokinetics as applied to the "hard drug" photosensitizing agent meta(tetrahydroxyphenyl)chlorin. In: *European Biomedical Optics Week*, pp 79, Abstract book **2625** (Abstract no. 50)
- ROSENTHAL I, KRISHNA CM, RIESZ P AND BEN-HUR E.** (1986). The role of molecular oxygen in the photodynamic effect of phthalocyanines. *Radiat. Res.* **107**, 136-142.
- ROSENTHAL I, BEN-HUR E, GREENBERG S, CONCEPCION-LAM A, DREW DM AND LEZNOFF CC.** (1987). The effect of substituents on phthalocyanine photocytotoxicity. *Photochem. Photobiol.* **46**, 959-963.
- ROSENTHAL I.** (1991). Phthalocyanines as photodynamic sensitizers. *Photochem. Photobiol.* **53**, 859-870.
- RÜCK A, HILDEBRANDT C, KOLLNER T, SCHNECKENBURGER H AND STEINER R.** (1990). Competition between photobleaching and fluorescence increase of photosensitizing porphyrins and tetrasulphonated chloroaluminiumphthalocyanine. *J. Photochem. Photobiol. B.* **5**, 311-319.
- RÜCK A, BECK G, AKGÜN N, GSCHWEND MH AND STEINER R.** (1996). Dynamic fluorescence changes of hydrophilic and lipophilic phthalocyanines during PDT in vivo and in vitro. In: *Photochemotherapy: photodynamic therapy and other modalities*. Ehrenberg B, Jori G and Moan J (eds.) pp 124-137. SPIE proceedings **2625**.
- SALET C AND MORENO G.** (1990). New trends in photobiology (Invited review). Photosensitization of mitochondria. Molecular and cellular aspects. *J. Photochem. Photobiol. B: Biol.* **5**, 133-150.
- SMITH CJ AND PINDBORG JJ** (1969). *Histological grading of oral epithelial atypia by the use of photographic standards*. C.Hamburger, Copenhagen.

- SPIKE RC, PAYNE AP, THOMPSON GG AND MOORE MR.** (1990). High-performance liquid chromatographic analyses of porphyrins in hamster Harderian glands. *Biochim.Biophys.Acta* **1034**, 1-3.
- SPIKES JD.** (1986). Phthalocyanines as photosensitizers in biological systems and for the photodynamic therapy of tumors (yearly review). *Photochem.Photobiol.* **43**, 691-699.
- SPIKES JD.** (1992). Quantum yields and kinetics of the photobleaching of hematoporphyrin, photofrin II, tetra(4-sulphonatophenyl)-porphine and uroporphyrin. *Photochem.Photobiol.* **55**, 797-808.
- STAR WM, MARIJNISSEN JPA, VAN DER BERG-BLOK AE, VERSTEEG AAC, FRANKEN KAP AND REINHOLD HS.** (1986). Destruction of rat mammary tumour and normal tissue microcirculation by hematoporphyrin derivative photoradiation observed in vivo in sandwich observation chambers. *Cancer Res.* **46**, 2532-2540.
- STAR WM AND MARIJNISSEN JPA.** (1989). Calculating the response of isotropic light dosimetry probes as a function of the tissue refractive index. *Appl.Opt.* **12**, 2288-2291.
- STAR WM AND MARIJNISSEN JPA.** (1995). Calibration of isotropic light dosimetry probes on scattering bulbs in clear media (submitted). *Phys.Med.Biol.*
- STENMAN G.** (1981). Malignancy of 4NQO-induced oral squamous cell carcinomas in the rat. *Acta Otolaryngol.(Stockh)* **92**, 557-561.
- STEPNIEWSKA KA AND ALTMAN DG.** (1992). Non-parametric test for trend across ordered groups. *Stata Technical Bulletin*, **9**, 21-22.
- STEVENINCK J, DUBBELMAN TMAR AND VERWEIJ H.** (1983). Photodynamic membrane damage. *Adv.Exp.Med.Biol.* **160**, 227-240.
- STRAIGHT RC AND SPIKES JD.** (1985). Preliminary studies with implanted polyvinyl alcohol sponges as a model for studying the role of neointerstitial and neovascular compartments of tumors in the localization, retention and photodynamic effects of photosensitizers. *Adv.Exp.Med.Biol.* **193**, 77-89.
- SUEN JY** (1989) Cancer of the neck. In: *Cancer of the head and neck* . Myers EN and Suen JY (eds.). pp 221-254. Churchill Livingstone 2nd ed.

- SUTOU S.** (1973). Endoreduplication in cultured mammalian cells treated with 4-nitroquinoline I-oxide. *Mutat.Res.* **18**, 171-178.
- TRALAU CJ, BARR H, SANDEMAN DR, BARTON T, LEWIN MR AND BOWN SG.** (1987). Aluminum sulfonated phthalocyanine distribution in rodent tumors of the colon, brain and pancreas. *Photochem.Photobiol.* **46**, 777-781.
- TRALAU CJ, YOUNG A, WALKER N, VERNON DI, MACROBERT AJ AND BROWN SB.** (1989). Mouse skin photosensitivity with dihaematoporphyrin ether (DHE) and aluminium sulphonated phthalocyanine (AISPc): a comparative study. *Photochem.Photobiol.* **49**, 305-312.
- VERMEY A, OLDHOFF J, PANDERS AK, ROBINSON PH AND VAN OORT RP** (1991). Hoofd hals tumoren (head and neck tumours). In: *Oncologie (oncology)*. Zwaveling A, Bosman FT, Schaberg A, Van De Velde CJH and Wagner DJT (eds.). pp 185-243. Bohn Stafleu Van Loghum: Houten (NL).
- VISSER O, COEBERG JWW AND SCHOUTEN LW** (eds.)(1995). *Incidence of cancer in the Netherlands 1992*. Forth report of the Netherlands Cancer Registry. pp 38-41. Association of comprehensive cancer centres: Utrecht.
- WAGNER JR, ALI H, LANGLOIS R, BRASSEUR N AND VAN LIER JE.** (1987). Biological activities of phthalocyanines-VI. Photooxidation of L-tryptophan by selectively sulphonated phthalocyanines: Singlet oxygen yields and effect of aggregation. *Photochem.Photobiol.* **45**, 587-594.
- WALLENIUS K, LEKHOLM U** (1973). Oral cancer in rats induced by the water soluble carcinogen 4-nitroquinoline I-oxide. *Odontol Rev.* **24**, 39-48
- WEISHAUPT KR, GOMER CJ AND DOUGHERTY TJ.** (1976). Identification of singlet oxygen as the cytotoxic agent in photoactivation of a murine tumor. *Cancer Res.* **36**, 2326-2329.
- WENIG BL, KURTZMAN DM, GROSSWEINER LI, MAFEE MF, HARRIS DM, LOBRACIO RV, PRYCZ RA AND APPELBAUM EL.** (1990). Photodynamic therapy in the treatment of squamous cell carcinoma of the head and neck. *Arch.Otolaryngol.Head Neck Surg.* **116**, 1267-1270.
- WEST CML.** (1989a). Size-dependent resistance of human tumour spheroids to photodynamic treatment. *Br.J.Cancer* **59**, 510-514.

WEST CML AND MOORE JV. (1989*b*). Flow cytometric analysis of intracellular hematoporphyrin derivative in human tumor cells and multicellular spheroids. *Photochem.Photobiol.* **50**, 665-669.

WITJES MJH, SCHOLMA J, VAN DRUNEN E, ROODENBURG JLN, MESANDER G, HAGEMEIJER A AND TOMSON AM. (1995*a*). Characterization of a rat oral squamous cell carcinoma cell line UHG-RaC '93 induced by 4-nitroquinoline-1-oxide in vivo. *Carcinogenesis* **16**, 2825-2832.

WITJES MJH, SPEELMAN OC, NAUTA JM, ROODENBURG JLN AND STAR WM. (1995*b*). Photobleaching of disulphonate aluminium phthalocyanine in vivo. Observation of an initial increase of fluorescence during illumination. In: *European Biomedical Optics Week*. pp 71-72, Abstract book **2625** (Abstract no. 27).

WITJES MJH, SPEELMAN OC, NIKKELS PGJ, NOOREN CAAM, NAUTA JM, VAN DER HOLT B, VAN LEENGOED HLLM, STAR WM AND ROODENBURG JLN. (1996*a*). In vivo fluorescence kinetics and localisation of aluminium phthalocyanine disulphonate in an autologous tumour model. *Br.J.Cancer* **73**, 573-580.

WITJES MJH, MANK AJG, SPEELMAN OC, POSTHUMUS R, NOOREN CAAM, NAUTA JM, ROODENBURG JLN AND STAR WM. (1996*b*). Distribution of aluminium phthalocyanine disulphonate in an oral squamous cell carcinoma model. *In vivo* fluorescence imaging compared with *ex vivo* analytical methods. *Photochem.Photobiol*, *accepted*

WITJES MJH, NIKKELS PGJ, SPEELMAN OC, NOOREN CAAM, MARIJNISSEN JPA, NAUTA JM, VERMEY A, THOMSEN SL, STAR WM AND ROODENBURG JLN. (1996*c*). Photodynamic therapy of normal rat oral mucosa using aluminium phthalocyanine disulphonate. Analysis of the nature and recovery of injury. *Submitted*.

WU S, ZHANG H, CUI G, XU D AND XU H. (1985). A study on the ability of some phthalocyanine compounds for photogenerating singlet oxygen. *Acta Chim. Sinica* **43**, 21-25.

ZAGARS G.K., NORANTE J.D, SMITH J.L. AND MCDONALD S. (1993). Tumors of the head and neck. In: *Clinical oncology*, Rubin P, McDonald S and Quazi R. pp 319-362. W.B.Saunders Company: Philadelphia.

ADDENDUM A

HISTOLOGICAL INDEX OF ORAL EPITHELIAL ATYPIA (EAI)

adapted from "Smith and Pindborg (1969), Histological grading of oral atypia by the use of photographic standards. C. Hamburger, Copenhagen"

ITEM :	GRADES :	GRADE & REMARKS:
1 DROP SHAPED RETE RIDGES	NONE	0
	SLIGHT	2
	MARKED	4
2 IRREGULAR STRATIFICATION	NONE	0
	SLIGHT	2
	MARKED	5
3 KERATINISATION OF CELLS BELOW THE KERATINISED LAYER	NONE	0
	FEW/SHALLOW	1
	MANY/DEEP	3
4 BASAL CELL HYPERPLASIA	NONE	0
	SLIGHT	1
	MARKED	4
5 LOSS OF INTERCELLULAR ADHERANCE	NONE	0
	SLIGHT	1
	MARKED	5
6 LOSS OF POLARITY	NONE	0
	SLIGHT	2
	MARKED	6
7 HYPERCHROMATIC NUCLEI	NONE	0
	SLIGHT	2
	MARKED	5
8 INCREASED NUCLEO-CYTOPLASMATIC RATIO (INCREASED DENSITY) IN BASAL AND PRICKLE CELL LAYER	NO INCREASE	0
	SLIGHT INCREASE	2
	MARKED INCREASE	6
9 ANISOCYTOSIS AND ANISONUCLEOSIS	NONE	0
	SLIGHT	2
	MARKED	6
10 PLEOMORPHIC CELLS AND NUCLEI	NONE	0
	SLIGHT	2
	MARKED	6
11 MITOTIC ACTIVITY	NORMAL	0
	SLIGHT INCREASE	1
	MARKED INCREASE	5
12 LEVEL OF MITOTIC ACTIVITY	NORMAL	0
	LOWER ½ ONLY	3
	ALSO UPPER ½	10
13 PRESCENCE OF BIZARRE MITOSIS	NONE	0
	SINGLE	6
	MULTIPLE	10

ADDENDUM B

HISTOLOGICAL GRADING SYSTEM OF DAMAGE TO RAT PALATE 2 DAYS AFTER PDT

ITEM :	GRADES :	GRADE & REMARKS
1 EDEMA IN MUCOSA	-NOT PRESENT	0
	-SLIGHT	1
	-MARKED	2
2 EDEMA BEYOND PALATAL BONE	-NOT PRESENT	0
	-SLIGHT	1
	-MARKED	2
3 HEMORRHAGE IN MUCOSA	-NOT PRESENT	0
	-SLIGHT	1
	-MARKED	2
4 HEMORRHAGE BEYOND PALATAL BONE	-NOT PRESENT	0
	-SLIGHT	1
	-MARKED	2
5 PARAKERATOSIS OF EPITHELIUM	-NOT PRESENT	0
	-PRESENT	1
6 PARTIAL NECROSIS OF EPITHELIAL LAYER	-NOT PRESENT	0
	-SLIGHT	2
	-MARKED	3
7 TOTAL NECROSIS OR ABSENCE OF EPITHELIAL LAYER	-NOT PRESENT	0
	-PRESENT	5
8 VASCULAR EDEMA OF VESSELS IN MUCOSA	-NOT PRESENT	0
	-SLIGHT	1
	-MARKED	2
9 VASCULAR EDEMA OF VESSELS BEYOND PALATAL BONE -	-NOT PRESENT	0
	-SLIGHT	1
	-MARKED	2
10 CONGESTION/HEMOSTASIS OF VESSELS	-NOT PRESENT	0
	-MUCOSA	1
	-MUCOSA & BEYOND PALATAL BONE	2
11 VASCULAR THROMBOSIS	-NOT PRESENT	0
	-MUCOSA	1
	-MUCOSA & BEYOND PALATAL BONE	2
12 VASCULAR NECROSIS OF VESSELS IN MUCOSA	-NOT PRESENT	0
	-ARTERIES	1
	-VEINS & ARTERIES	2
13 VASCULAR NECROSIS OF VESSELS BEYOND PALATAL BONE	-NOT PRESENT	0
	-ARTERIES	1
	-VEINS & ARTERIES	2
14 DISRUPTION OF LAMINA ELASTICA INTERNA OF ARTERIES	-NOT PRESENT	0
	-MUCOSA	1
	-MUCOSA & BEYOND PALATAL BONE	2

HISTOLOGICAL GRADING SYSTEM 2 DAYS AFTER PDT/ PAGE 2

ITEM :	GRADES :	GRADE & REMARKS
15 INTRA SUTURE TISSUE EDEMA PALATAL HALF -	-NOT PRESENT	0
	-SLIGHT	1
	-MARKED	2
16 INTRA SUTURE TISSUE EDEMA PALATAL HALF - & SINAL HALF	-NOT PRESENT	0
	-SLIGHT	2
	-MARKED	3
17 INTRA SUTURE TISSUE HEMORRHAGE PALATAL HALF	-NOT PRESENT	0
	-SLIGHT	1
	-MARKED	2
18 INTRA SUTURE TISSUE HEMORRHAGE PALATAL &SINAL HALF	-NOT PRESENT	0
	-SLIGHT	2
	-MARKED	3
19 INTRA SUTURE TISSUE NECROSIS PALATAL HALF	-NOT PRESENT	0
	-SLIGHT	1
	-MARKED	2
20 INTRA SUTURE TISSUE NECROSIS PALATAL & SINAL HALF	-NOT PRESENT	0
	-SLIGHT	2
	-MARKED	3
21 OSTEOCYTE NECROSIS	-NOT PRESENT	0
	-PALATAL HALF	1
	-PALATAL & SINAL HALF	2
22 PULP NECROSIS	-NOT PRESENT	0
	-SLIGHT	1
	-MARKED	2
23 BONE MARROW HEMORRHAGE	-NOT PRESENT	0
	-SLIGHT	1
	-MARKED	2
24 HEAMATOPOIETIC CELL LOSS OF MARROW	-NONE	0
	-SLIGHT	1
	-MARKED	2
25 INCREASED MUCUS SECRETION OF GOBLET CELLS OF SINAL EPITHELIUM	-NOT PRESENT	0
	-SLIGHT	1
	-MARKED	2
26 GOBLET CELL NECROSIS OF SINAL EPITHELIUM	-NOT PRESENT	0
	-SLIGHT	1
	-MARKED	2
27 NECROSIS LACRIMAL GLAND	-NOT PRESENT	0
	-SLIGHT	1
	-MARKED	2

ADDENDUM C

HISTOLOGICAL GRADING SYSTEM OF DAMAGE TO RAT PALATE 2 MONTHS AFTER PDT

ITEM :	GRADES :	GRADE & REMARKS:
1 IRREGULAR DISTRIBUTION OR IRREGULAR SHAPED RETE RIDGES	-NOT PRESENT	0
	-SLIGHT	1
	-MARKED	2
2 EPITHELIAL ISLES, INCLUSIONS & (PSEUDO) CYSTS IN STROMA	-NOT PRESENT	0
	-PRESENT	2
3 SCAR TISSUE SUBMUCOSAL	-NOT PRESENT	0
	-SLIGHT	1
	-MARKED	2
4 SCAR TISSUE BEYOND PALATAL BONE	-NOT PRESENT	0
	-SLIGHT	1
	-MARKED	2
5 FOREIGN BODY REACTION IN MUCOSA	-NOT PRESENT	0
	-PRESENT	1
		2
6 HYPERTROPHY OF VESSEL WALL	-NOT PRESENT	0
	-MUCOSA	1
	-MUCOSA & BEYOND PALATAL BONE2	
7 VASCULAR RECANALISATION	-NOT PRESENT	0
	-MUCOSA	1
	-MUCOSA & BEYOND PALATAL BONE2	
8 VASCULAR PROLIFERATION	-NOT PRESENT	0
	-MUCOSA	1
	-MUCOSA & BEYOND PALATAL BONE2	
9 NEURONAL PROLIFERATION	-NOT PRESENT	0
	-MUCOSA	1
	-MUCOSA & BEYOND PALATAL BONE	2
10 PALATAL BONE REMODELING	-NOT PRESENT	0
	-INCREASED	2
11 LOSS OF GREAT PALATAL ARTERY & VENE	-NO LOSS	0
	-LOSS	2
12 LOSS OF GREAT PALATAL NERVE	-NO LOSS	0
	-PARTIAL LOSS	1
	-TOTAL LOSS	2
13 LOSS OF PALATAL BONE	-NONE	0
	-PARTIAL	1
	-TOTAL	2

HISTOLOGICAL GRADING SYSTEM OF DAMAGE 2 MONTHS AFTER PDT/PAGE 2

ITEM :	GRADES :	GRADE & REMARKS:
14 DENTAL HARD TISSUE RESORPTION	-NOT PRESENT	0
	-SLIGHT	1
	-MARKED	2
15 ANKYLOSIS OF ROOT	-NOT PRESENT	0
	-SLIGHT	1
	-MARKED	2
16 IRREGULAR DENTIN FORMATION IN PULP CHAMBER	-NOT PRESENT	0
	-SLIGHT	1
	-MARKED	2
17 PAPILLAR HYPERPLASIA OF EPITHELIAL LINING OF SINUS & IRREGULAR DISTRIBUTION OF GOBLET CELLS	-NONE	0
	-SLIGHT	1
	-MARKED	2
18 ORAL EPITHELIUM CON - TINEOUS WITH NASAL CAVITY	-PRESENT	0
	-NOT PRESENT	10

LIST OF CO-AUTHORS

E. van Drunen	Dept. of Cell Biology and Genetics, Erasmus University, Rotterdam, The Netherlands
Prof. Dr. A. Hagemeyer	Dept. of Cell Biology and Genetics, Erasmus University, Rotterdam, The Netherlands
Drs. B. van der Holt	Dept. of Statistics, Dr. Daniel den Hoed Cancer Center, Rotterdam, The Netherlands
Dr. H.L.L.M. van Leengoed	Dept. of Clinical Physics, Dr. Daniel den Hoed Cancer Center, Rotterdam, The Netherlands
Dr. A.J.G. Mank	Dept of Analytical Chemistry, Free University, Amsterdam, The Netherlands
Dr. J.P.A. Marijnissen	Dept. of Clinical Physics, Dr. Daniel den Hoed Cancer Center, Rotterdam, The Netherlands
G. Mesander	Dept. of Internal Medicine (Flow Cytometry unit), University Hospital Groningen, The Netherlands
Dr. J.M. Nauta	Dept. of Oral & Maxillofacial Surgery, University Hospital Groningen, The Netherlands
Dr. P.G.J. Nikkels	Dept. of Pathology, University Hospital Groningen, The Netherlands
C.A.A.M. Nooren	Dept. of Oral & Maxillofacial Surgery, University Hospital Groningen, The Netherlands
R. Posthumus	Dept of Analytical Chemistry, Free University, Amsterdam, The Netherlands
Prof Dr. J.L.N. Roodenburg JLN	Dept. of Oral & Maxillofacial Surgery, University Hospital Groningen, The Netherlands

- J. Scholma
Dept. of Internal Medicine (pulmonology),
University Hospital Groningen, The Netherlands
- O.C. Speelman
Dept. of Clinical Physics, Dr. Daniel den Hoed
Cancer Center, Rotterdam, The Netherlands
- Dr. W.M. Star
Dept. of Clinical Physics, Dr. Daniel den Hoed
Cancer Center, Rotterdam, The Netherlands
- Prof Dr. S.L. Thomsen
Dept of Pathology/Laser Biology Research
Laboratory, M.D. Anderson Cancer Center,
University of Texas, Houston, USA
- Dr. A.M. Tomson
Central laboratory of Clinical Haematology,
University Hospital Groningen, The Netherlands
- Prof. Dr. A Vermey, FACS
Dept. of Surgery/Oncology, University Hospital
Groningen, The Netherlands

The chapters of this thesis were submitted or have been published in the following papers:

Chapter 1.4:

Witjes MJH, Scholma J, Drunen van E, Roodenburg JLN, Mesander G, Hagemeyer A and Tomson AM (1995). Characterisation of a rat oral squamous cell carcinoma cell line UHG-RaC '93 induced by 4-nitroquinoline-1-oxide in vivo. *Carcinogenesis*, **16**, 2825-2832

Nauta JM, Roodenburg JLN, Nikkels PGJ, Witjes MJH and Vermey A (1996). Epithelial dysplasia and squamous cell carcinoma of the Wistar rat palatal mucosa. The 4NQO model. *Head and Neck* **18**, 441-449

Chapter 2.1:

Witjes MJH, Speelman OC, Nikkels PGJ, Nooren CAAM, Nauta JM, van der Holt B, van Leengoed HLLM, Star WM and Roodenburg JLN. (1996). *In vivo* fluorescence kinetics and localisation of aluminium phthalocyanine disulphonate in an autologous tumour model. *Br.J.Cancer*, **73**, 573-580.

Chapter 2.2:

Witjes MJH, Mank AJG, Speelman OC, Posthumus R, Nooren CAAM, Nauta JM, Roodenburg JLN and Star WM. (1996). Distribution of aluminium phthalocyanine disulphonate in an oral squamous cell carcinoma model. *In vivo* fluorescence imaging compared with *ex vivo* analytical methods. *Photochem. Photobiol.*, *in press*

Chapter 3.1:

Witjes MJH, Nikkels PGJ, Speelman OC, Nooren CAAM, Marijnissen JPA, Nauta JM, Vermey A, Thomsen SL, Star WM and Roodenburg JLN (1996) Photodynamic therapy of normal rat oral mucosa using aluminium phthalocyanine disulphonate. Analysis of the nature and recovery of injury. *Submitted*

Chapter 3.2:

Witjes, MJH., Nikkels,PGJ., Speelman OC, Marijnissen JPA, Nauta JM, Nooren CAAM, Vermey A, Star WM, Roodenburg JLN. Photodynamic therapy of experimental dysplasia and squamous cell carcinoma of the rat oral mucosa using aluminium phthalocyanine disulphonate. *Submitted*

Chapter 3.3:

Witjes MJH, Speelman OC, Nauta JM, Roodenburg JLN, Star WM. Increase of aluminium phthalocyanine disulphonate mediated fluorescence during PDT. *Submitted*

DANKWOORD

Vele personen hebben bijgedragen aan dit proefschrift. Al deze personen wil ik bedanken waarvan een aantal in het bijzonder.

Carmelita, echtgenote en meest verbonden lotgenoot. Het is me duidelijk geworden dat promoveren pas lukt als het thuisfront er achterstaat. Jouw energie om het huishouden, met onze kinderen Milan en Andra, te verzorgen en tevens een praktijk draaiende te houden is indrukwekkend. Het is een hectische maar ook bijzondere tijd geweest die we intens hebben beleefd.

Prof. Dr. J.L.N. Roodenburg, eerste promotor en inspirator van het PDT onderzoek aan de afdeling Mondziekten, Kaakchirurgie en Bijzondere Tandheelkunde. Jouw initiatieven hebben geleid tot een duurzame onderzoekslijn betreffende de toepassing van lasers op ons vakgebied. Beste Jan, jouw tact en heldere geest hebben voor een belangrijk deel bijgedragen tot een duidelijke lijn in mijn proefschrift. Sommige promovendi zijn nou eenmaal niet af te remmen en kunnen het niet laten om alle loopgraven te willen bekijken. Je enthousiaste reactie op het feit dat ik als kaakchirurg in opleiding nog eens vier jaar in de buurt blijf is een hele geruststelling.

Prof Dr. Vermey, tweede promotor. Hartelijk dank voor Uw inzet en bijdrage. We zullen, naar ik hoop, nog vele discussies hebben omtrent de betekenis van onze onderzoeksresultaten voor toepassing in de kliniek. Uit Uw vermogen om taalkundig de punten op de i te zetten blijkt duidelijk dat U een stilist van voor de “mammoetwet” bent. Uw fenomenale snelheid om stukken te beoordelen nog net voordat de drukker het manuscript ophaalde was zeer welkom.

Een bijzondere plaats bij de tot standkoming van dit proefschrift wordt ingenomen door *Dr. W.M. Star*. Beste Willem, een verzameling van jouw uitspraken geuit tijdens de beoordeling van een manuscript zijn op zichzelf boekvullend en zouden gretig aftrek vinden bij de promovendi die mij voor zijn gegaan. “Wat bedoel je nou ?, schrijf dat dan ook zo op”, is er één die is blijven hangen. Je bent voor ons een belangrijk een klankbord voor nieuwe ideeën. Helaas biedt het promotie reglement geen mogelijkheid om jouw rol bij dit onderzoek beter weer te geven.

Dr. P.G.J. Nikkels, tweede referent. Peter, ook jij hebt veel meer tijd en aandacht besteed aan het onderzoek dan mag worden verwacht van een referent. Dat je niet hopeloos werd van de hoeveelheid dozen met coupes waarmee ik wekelijks je werkkamer betrad is me nog steeds een raadsel (in de loop der jaren meer dan 750 coupes). Jouw enthousiasme voor zowel de pathologie als gastronomie vormen een mix die de uren lange sessies aangenaam maakten. Ik verneem graag van je hoe het vaderschap je zal bevallen.

Dr. J.M. Nauta, ontwikkelde tezamen met Jan Roodenburg het 4NQO palatummodel, een belangrijke pijler van dit proefschrift. Beste Jan, dankzij jouw voorwerk en introductie in de PDT kon ik al snel mijn eigen weg vinden in het onderzoek. Wellicht lukt het ons nog eens om de verschillen in PDT met HpD en phthalocyanines aan de buitenwereld duidelijk te maken.

Otto Speelman, die ons onderzoek in de Daniel den Hoed kliniek coördineerde. Otto, zoals jij en Jet mij ontvangen hebben op jullie vorige kleine behuizing in Zwijndrecht getuigt van een grote tolerantie. Jouw bereidheid om voor mijn onderzoek vele overuren te draaien vind ik nog steeds geweldig.

Dr A.G.J. Mank, Beste Arjan, jouw interesse in de detectie van phthalocyanines in complexe matrices kwam goed van pas. Velen discussiëren over de noodzaak van integratie van de verschillende vakgebieden in onderzoek. Je dit ook daadwerkelijk ten uitvoer gebracht, net als andere ideeën die in je opkomen. Tezamen met *Richard Posthumus* heb je veel werk verzet voor hoofdstuk 2.2. Wie weet, misschien komt het er inderdaad nog eens van om samen in Nepal een 7000-er te bedwingen.

Prof. Dr. S.L. Thomsen, pathologist and globetrotter with a traveling schedule which must equal that of our Queen Beatrix. Dear Sharon, your experience in laser pathology was essential in the 'off the beaten track' we traveled to complete the histological grading lists. Your willingness to review our slides I greatly appreciated. Carmelita and I hope to be able to present some more of our secrets of Italian cooking.

Corina Nooren, de research analist van onze afdeling en in staat om van alles wat aangeboden wordt een coupe te vervaardigen. Je hebt mij jarenlang veel praktisch werk uit handen genomen waarvan we beide weten dat het anders onmogelijk was geweest om het onderzoek te volbrengen.

Dr H.L.L.M. van Leengoed, Beste Eric, jouw introductie in de wondere wereld van de phthalocyanine fluorescentie en de digitale beeldbewerking heeft mijn gedachtenvorming omtrent de detectie van phthalocyanines sterk beïnvloed. Je zenuwen voor tandartsen opgedaan tijdens je eigen promotie jaren zijn hopelijk gedesensibiliseerd nu je in Groningen woont en regelmatig op de afdeling komt.

Dr. A.M. Tomson en Jannie Scholma, die mij de kunst van *in vitro* celkweek hebben bij gebracht en hiermee ons een interessante cellijn hebben nagelaten. Helaas bleek de reallocatie van jullie lab onafwendbaar. Ik ben er van overtuigd dat we samen nog veel meer hadden kunnen creëren als we de kans hadden gekregen.

Dr. H. Marijnissen, beste Hans, hartelijk dank voor je input en heldere ideeën waarmee we samen tot een lichtdosimetrie-experiment zijn gekomen. Vanwege jouw vermogen om fysische fenomenen helder uit te leggen heb ik er ook nog iets van begrepen.

Drs. R. van der Holt en dhr L. van der Weele wil ik danken voor hun geduld en adviezen op het gebied van de statistiek.

Prof Dr. A. Hagemijer en *Ellen van Drunen*, met een open vizier hebben jullie een verdwaalde tandarts uit Groningen ontvingen die zo graag een karyotypering van zijn met 4NQO behandelde cellen wilde. Hartelijk dank voor jullie bijdrage.

Mijn dank gaat vanzelfsprekend uit naar de leden van de promotie commissie *Prof. Dr. J.J. ten Bosch*, *Prof. Dr. P. Slootweg* en in het bijzonder *Prof. Dr. G. Boering*. Prof. Boering, onder U ben ik aan de afdeling Mondziekten, Kaakchirurgie en Bijzondere Tandheelkunde begonnen aan mijn proefschrift en heb tijdens de beoordeling van het complete manuscript mogen ondervinden waarom anderen U roemen om Uw grondigheid en grenzeloze interesse. *Nynke van der Veen*, *Riët de Bruin*, *Lars Murrer* en *Hugo van Staveren*, medewerkers van het PDT lab aan de Daniel den Hoed kliniek in Rotterdam die altijd bereid waren een helpende hand toe te steken bij de uitvoering van onze experimenten.

Verder wil ik mijn dank uitspreken naar *Geert Mesander*, FACS-beheerder, de fotografen *Sten Sliwa* en *Hans Vuik* (Daniel den Hoed Kliniek, Rotterdam) en *Peter van de Syde* en *Dick Huizinga* (lab voor celbiologie en E.M. R.U.G.), de medewerkers van het *Centraal Dieren Lab.* in Groningen, met name *Hans Bartels* die vele dierexperimenten begeleidde.

Harrie de Jonge, *Karin Wolthuis*, *Gerda Boezerooij* en alle andere medewerkers van de afdeling Mondziekten, Kaakchirurgie en Bijzondere Tandheelkunde die in de afgelopen jaren bijgedragen hebben en geïnteresseerd waren in de ontwikkelingen van mijn onderzoek. *Pieter Duijser*, die voor mij het omslag in zeer korte tijd ontworpen heeft en pas nerveus werd toen ik zelf de kleur bij de drukker moest uitzoeken. Pieter bedankt !

Mijn paranimfen *Max Rutten* en *Jos Coops* wil ik alvast bedanken voor de morele ondersteuning die ze op 21 mei zullen verlenen en voor hun interesse in de voortgang van mijn onderzoek alsmede hun vriendschap.

‘Last but not least’ wilde ik mijn ouders bedanken die voor mij de gelegenheid hebben gecreëerd om deze weg te kunnen bewandelen.

Allen bedankt !

CURRICULUM VITAE

- April 4, 1965 Date of birth, Katwijk, The Netherlands.
- 1977-1985 High school, A-levels (HAVO/VWO).
- 1988-1990 Research assistant at the laboratory for Materia Technica
University of Groningen, The Netherlands.
Chair: Prof. Dr. J. Arends.
- 1991
(Jan.-June) Research assistant at the department of Biomaterials
University of Alabama School of Dentistry,
Birmingham, Alabama, U.S.A..
Chair: Prof. Dr. D.H. Retief.
- 1985-1991 Dentistry, Faculty of Dentistry, University of Groningen, The
Netherlands.
- 1991-1996 PhD student at the department of Oral & Maxillofacial Surgery,
University Hospital Groningen, The Netherlands.
Chair: Prof Dr. L.G.M. de Bont (Chair until Nov. 1994: Prof. Dr. G.
Boering).
- 1996-1997 Part-time clinical assistant (AGNIO), department of Oral &
Maxillofacial Surgery, University Hospital Groningen, The Netherlands.
- 1997 (March) "Doctoraal examen" Faculty of Medical Sciences, University of
Groningen, The Netherlands (comparable to a master's degree in
medicine).
- 1997 (Sept.) Start of residency, Oral & Maxillofacial Surgery, department of Oral &
Maxillofacial Surgery, University Hospital Groningen, The
Netherlands.

Address for correspondence

Max Witjes
Dept of Oral & Maxillofacial Surgery and Special Dentistry
University Hospital Groningen
P.O. Box 30.001
9700 RB Groningen
The Netherlands
phone: +31-50-3613840
fax: +31-50-3611136